AERMOD Model Formulation

EPA-454/B-24-010
November 2024

AERMOD Model Formulation

U.S. Environmental Protection Agency
Office of Air Quality Planning and Standards
Air Quality Assessment Division
Research Triangle Park, NC

Notice

The original document, AERMOD: Description of Model Formulation, was published in September 2004, with the EPA document number EPA-454/R-03-004. This document has since undergone multiple revisions, including a title change when the evaluation results were added, and the document was retitled AERMOD Model Formulation and Evaluation. With the release of AERMOD version 22112, the evaluation results were moved to a separate document, AERMOD Model Evaluation, and the title of this document also changed to AERMOD Model Formulation. This version of the document reflects additions and changes to the AERMOD Modeling System released as version 24142.

This report has been reviewed by the Office of Air Quality Planning and Standards, U.S. Environmental Protection Agency, and has been approved for publication. Mention of trade names or commercial products does not constitute endorsement or recommendation for use.

Table of Contents

Figures

Figure **Page**

1. Introduction

1.1 Background

In 1991, the American Meteorological Society (AMS) and the U.S. Environmental Protection Agency (EPA) initiated a formal collaboration with the designed goal of introducing current planetary boundary layer (PBL) concepts into regulatory dispersion models. A working group (**A**MS/**E**PA **R**egulatory **M**odel **I**mprovement **C**ommittee, **AERMIC**) comprised of AMS and EPA scientists was formed for this collaborative effort.

In most air quality applications, one is concerned with dispersion in the PBL, the turbulent air layer next to the earth's surface that is controlled by the surface heating and friction, and the overlying stratification. The PBL typically ranges from a few hundred meters in depth at night to 1 - 2 km during the day. Major developments in understanding the PBL began in the 1970s through numerical modeling, field observations, and laboratory simulations; see Wyngaard (1988) for a summary. For the convective boundary layer (CBL), a milestone was Deardorff's (1972) numerical simulations which revealed the CBL's vertical structure and important turbulence scales. Major insights into dispersion followed from laboratory experiments, numerical simulations, and field observations (e.g., see Briggs (1988), Lamb (1982) and Weil (1988a) for reviews). For the stable boundary layer (SBL), advancements occurred more slowly. However, a sound theoretical/experimental framework for surface layer dispersion and approaches for elevated sources emerged by the mid-1980s (e.g., see Briggs (1988) and Venkatram (1988)).

During the mid-1980s, researchers began to apply this information to simple dispersion models for applications. This consisted of eddy-diffusion techniques for surface releases, statistical theory and PBL scaling for dispersion parameter estimation, a new probability density function (pdf) approach for the CBL, simple techniques for obtaining meteorological variables (e.g., surface heat flux) needed for turbulence parameterizations, etc. Much of this work was

reviewed and promoted in workshops (Weil 1985), revised texts (Pasquill and Smith 1983), and in short courses and monographs (Nieuwstadt and van Dop 1982; Venkatram and Wyngaard 1988). By the mid-1980s, new applied dispersion models based on this technology had been developed including PPSP (Weil and Brower 1984), OML (Berkowicz et al. 1986), HPDM (Hanna and Paine 1989), TUPOS (Turner et al. 1986), CTDMPLUS (Perry et al. 1989); later, ADMS developed in the United Kingdom (see Carruthers et al. (1992)) was added as well as SCIPUFF (Sykes et al. 1996). AERMIC members were involved in the development of three of these models - PPSP, CTDMPLUS and HPDM.

By the mid-to-late 1980s, a substantial scientific base on the PBL and new dispersion approaches existed for revamping regulatory dispersion models. In a review of existing or proposed regulatory models developed prior to 1984, Smith (1984) reported that the techniques were many years behind the state-of-the-art and yielded predictions that did not agree well with observations. Similar findings were reported by Hayes and Moore (1986), who summarized 15 model evaluation studies. The need for a comprehensive overhaul of EPA's basic regulatory models was clearly recognized. This need, including a summary of background information and recommendations, was the focus of an AMS/EPA Workshop on Updating Applied Diffusion Models held 24-27 January 1984 in Clearwater, Florida (see Weil (1985) and other review papers in the November 1985 issue of the Journal of Climate and Applied Meteorology).

In February 1991, the U.S. EPA, in conjunction with the AMS, held a workshop for state and EPA regional meteorologists on the parameterization of PBL turbulence and state-of-the-art dispersion modeling. One of the outcomes of the workshop was the formation of AERMIC. As noted above, the expressed purpose of the AERMIC activity was to build upon the earlier model developments and to provide a state-of-the-art dispersion model for regulatory applications. The early efforts of the AERMIC group are described by Weil (1992). In going through the design process and in considering the nature of present regulatory models, AERMIC’s goal expanded from its early form. In addition to improved parameterization of PBL turbulence,

other problems such as plume interaction with terrain, surface releases, building downwash and urban dispersion were recognized as needing attention.

The model developed by AERMIC is aimed at short-range dispersion from stationary industrial sources, the same scenario handled by its predecessor, the EPA Industrial Source Complex Model, ISC3 (U.S. EPA, 1995). This work clearly has benefitted from the model development activities of the 1980s, especially in the parameterization of mean winds and PBL turbulence, dispersion in the CBL, and the treatment of plume/terrain interactions. Techniques used in this model for PBL parameterizations and CBL dispersion are like those used in earlier models. Turbulence characterization in the CBL adopts "convective scaling", as suggested by Deardorff (1972), as is included in most of the models mentioned above (e.g., PPSP, OML, and HPDM). Algorithms used in these earlier models were considered along with variants and improvements to them. In addition, the developers of OML met with AERMIC to discuss their experiences. Thus, much credit for the AERMIC model development is to be given to the pioneering efforts of the 1980s.

1.2 The AERMIC focus: a replacement for the ISC3 model

AERMIC's initial focus was on the regulatory models designed for estimating near-field impacts from a variety of industrial source types. EPA's regulatory platform for near-field modeling, with few exceptions, has remained fundamentally unchanged. ISC3 was the workhorse regulatory model (used in the construction of most State Implementation Plans, new source permits, risk assessments and exposure analysis for toxic air pollutants) with code structure that is conducive to change. Therefore, AERMIC selected the EPA's ISC3 Model for a major overhaul. AERMIC's objective was to develop a complete replacement for ISC3 by 1) adopting ISC3's input/output computer architecture; 2) updating, where practical, antiquated ISC3 model algorithms with newly developed or current state-of-the-art modeling techniques; and 3) ensuring that the source and atmospheric processes presently modeled by ISC3 will continue to be handled by the AERMIC Model (AERMOD), albeit in an improved manner.

The AERMOD modeling system consists of two pre-processors and the dispersion model. The AERMIC meteorological preprocessor (AERMET) provides AERMOD with the meteorological information it needs to characterize the PBL. The AERMIC terrain pre-processor (AERMAP) both characterizes the terrain and generates receptor grids for the dispersion model (AERMOD).

AERMET uses meteorological data and surface characteristics to calculate boundary layer parameters (e.g., mixing height, friction velocity, etc.) needed by AERMOD. This data, whether measured off-site (e.g., airport), on-site (site-specific), or forecast data from a prognostic weather model, must be representative of the meteorology in the modeling domain.

AERMAP uses gridded terrain data for the modeling area to calculate a representative terrain-influence height associated with each receptor location. AERMAP can process multiple formats of gridded elevation data to compute elevations for both discrete receptors and receptor grids.

In developing AERMOD, AERMIC adopted design criteria to yield a model with desirable regulatory attributes. It was determined that the model should: 1) provide reasonable concentration estimates under a wide variety of conditions with minimal discontinuities; 2) be user friendly and require reasonable input data and computer resources as is the case with the ISC3 model; 3) capture the essential physical processes while remaining fundamentally simple; and 4) accommodate modifications with ease as the science evolves.

Relative to ISC3, AERMOD contains new or improved algorithms for: 1) dispersion in both the convective and stable boundary layers; 2) plume rise and buoyancy; 3) plume penetration into elevated inversions; 4) computation of vertical profiles of wind, turbulence, and temperature; 5) the urban nighttime boundary layer; 6) the treatment of receptors on all types of terrain from the surface up to and above the plume height; 7) the treatment of building wake

effects; 8) an improved approach for characterizing the fundamental boundary layer parameters; and 9) the treatment of plume meander.

1.3 Model development process

A seven-step model development process, followed by AERMIC, resulted in the promulgation of AERMOD, a regulatory replacement for the ISC3 model. The process followed was: 1) initial model formulation; 2) developmental evaluation; 3) internal peer review and beta testing; 4) revised model formulation; 5) performance evaluation and sensitivity testing; 6) external peer review; and 7) submission to EPA's Office of Air Quality Planning and Standards (OAQPS) for consideration as a regulatory model.

The initial formulations of AERMOD are summarized in Perry et al. (1994) and Cimorelli et al. (1996). Once formulated, the model was tested (developmental evaluation) against a variety of field measurements to identify areas needing improvement. The developmental evaluation provided a basis for selecting formulation options.

This developmental evaluation was conducted using five databases. Three consisted of event-based tracer releases, while the other two each contain up to a full year of continuous SO_2 measurements. These databases cover elevated and surface releases, complex and simple terrain, and rural and urban boundary layers. A description of the early developmental evaluation is presented in Lee et al. (1995) and in a later report by Lee et al. (1998). Additionally, a comprehensive peer review (U.S. EPA, 2002) was conducted. Many revisions to the original formulation have resulted from this evaluation and comments received during the peer review, beta testing, and the public forum at EPA's Sixth Conference on Air Quality Modeling (in 1995). Lee et al. (1998) describe the developmental evaluation that was repeated after revisions based on the developmental evaluation and peer review.

In addition, AERMOD underwent a comprehensive performance evaluation (Brode 2002) designed to assess how well AERMOD's concentration estimates compare against a variety of independent databases and to assess the adequacy of the model for use in regulatory decision making. That is, how well does the model predict concentrations at the high end of the concentration distribution? AERMOD was evaluated against five independent databases (two in simple terrain and three in complex terrain), each containing one full year of continuous SO_2 measurements. Additionally, AERMOD's performance was compared against the performance of four other applied, regulatory models: ISC3 (U.S. EPA, 1995), CTDMPLUS (Perry 1992), RTDM (Paine and Egan 1987), and HPDM (Hanna and Paine 1989; Hanna and Chang 1993). The performance of these models against AERMOD has been compared using the procedures in EPA's "Protocol for Determining the Best Performing Model" (U.S. EPA, 1992).

On April 21, 2000, EPA proposed[1] that AERMOD be adopted as a replacement to ISC3 in Appendix A of the Guideline on Air Quality Models (Code of Federal Regulations 1997). As such, upon final action, AERMOD would become EPA's preferred regulatory model for both simple and complex terrain. Furthermore, on May 19, 2000, EPA announced[2] its intention to hold the Seventh Conference on Air Quality Modeling on 28-29 June 2000. The purpose of this conference was to receive comments on the April 2000 proposal. At the Seventh Conference, results of the performance evaluation and peer review were presented, and public comments were received. Based on these comments AERMOD was revised to incorporate the Plume Rise Model Enhancements (PRIME) algorithms for building downwash (Schulman et al., 2000), to remove the dependency on modeling domain in AERMOD's complex terrain formulation, and a variety of other less significant issues. A description of the fully revised model is presented

[1]40 CFR Part 51 pages 21506-21546

[2]Federal Register on May 19, 2000 (Volume 65, Number 98)

here and in Cimorelli et al. (2004) and Perry et al. (2003). Performance of the final version of AERMOD is documented in Perry et al. (2003) and Brode (2002).

1.4 Purpose of the document

The purpose of this document is to provide a comprehensive, detailed description of the technical formulation of AERMOD and its preprocessors. This document is intended to provide many details that are not included in the published journal articles (Cimorelli et al. 2004; Perry et al. 2003).

2. Model overview

This section provides a general overview of the most important features of AERMOD. AERMOD serves as a complete replacement for ISC3. Thus, the AERMOD model described here is applicable to rural and urban areas, flat and complex terrain, limited overwater applications, surface and elevated releases, and multiple source types (including, point, area, volume, buoyant line, and mobile sources). Every effort has been made to avoid model formulation discontinuities wherein large changes in calculated concentrations result from small changes in input parameters.

Since it was originally developed and promulgated as a preferred EPA model, the AERMOD Modeling System has been updated with added capabilities including improved characterization of certain emission sources with new source types and the ability to process offshore meteorology.

AERMET was originally designed to process land-based meteorology (i.e., meteorological data collected over land surfaces) to estimate PBL parameters influenced by land-air interactions where due to the diurnal cycle of surface heating and cooling, the atmosphere is generally convective during daytime hours and stable during the nighttime. Beginning with version 23132, AERMET was updated to include the Coupled Ocean Atmosphere Response Experiment (COARE) (Fairall, et al., 2003) to appropriately characterize the marine boundary layer using data collected offshore. This addition to AERMET is the first in a series of planned enhancements to the AERMOD Modeling system to expand AERMOD's capability to model offshore emission sources. For information on the formulation and usage of the COARE algorithm in AERMET, the reader is directed to Fairall, et al. (2003). The formulation of AERMET as described in this document continues to focus on the treatment of land-based meteorology.

The BUOYLINE source type for characterizing buoyant line sources was added beginning with version 15181. The BUOYLINE source type serves as an implementation of the Buoyant Line and Point (BLP) source dispersion model originally developed to estimate impacts from aluminum smelter potline emissions. Integration and testing of the BLP model and source type with AERMOD is described in EPA (2016). While a few functional enhancements have been made to the BUOYLINE source type beyond the capability of the BLP model, the formulation of the BUOYLINE source type has not been updated from the formulation described in the Buoyant Line and Point Source Dispersion Model User's Guide (BLP User's Guide) (Schulman and Scire, 1980). Users should refer to the BLP User's Guide for a description of the formulation of the BUOYLINE source type in AERMOD.

Similarly, the RLINE source type was added beginning with version 19191 to better characterize mobile source emissions (i.e., roadways). The RLINE source type is an adaptation of the Research Line (R-LINE) model (Snyder and Heist, 2013). For a description of the formulation of the RLINE source type in AERMOD, refer to Snyder and Heist (2013) and EPA (2023e).

AERMOD is a steady-state plume model. In the stable boundary layer (SBL), it assumes the concentration distribution to be Gaussian in both the vertical and horizontal. In the convective boundary layer (CBL), the horizontal distribution is also assumed to be Gaussian, but the vertical distribution is described with a bi-Gaussian probability density function (pdf). This behavior of the concentration distributions in the CBL was demonstrated by Willis and Deardorff (1981) and Briggs (1993). Additionally, in the CBL, AERMOD treats "plume lofting," whereby a portion of plume mass, released from a buoyant source, rises to and remains near the top of the boundary layer before becoming mixed into the CBL. AERMOD also tracks any plume mass that penetrates the elevated stable layer, and then allows it to re-enter the boundary layer when and if appropriate. For sources in both the CBL and the SBL, AERMOD treats the enhancement of lateral dispersion resulting from plume meander.

Using a relatively simple approach, AERMOD incorporates current concepts about flow and dispersion in complex terrain. Where appropriate, the plume is modeled as either impacting and/or following the terrain. This approach has been designed to be physically realistic and simple to implement, while avoiding the need to distinguish among simple, intermediate, and complex terrain, as required by other regulatory models. As a result, AERMOD removes the need for defining complex terrain regimes. All terrain is handled in a consistent and continuous manner while considering the dividing streamline concept (Snyder et al. 1985) in stable stratified conditions.

One of the major improvements that AERMOD brings to applied dispersion modeling is its ability to characterize the PBL through both surface and mixed layer scaling. AERMOD constructs vertical profiles of required meteorological variables based on measurements and extrapolations of those measurements using similarity (scaling) relationships. Vertical profiles of wind speed, wind direction, turbulence, temperature, and temperature gradient are estimated using all available meteorological observations. AERMOD is designed to run with a minimum of observed meteorological parameters. AERMOD can operate using data that are readily available from National Weather Service (NWS) stations. AERMOD requires only a single surface measurement of wind speed (measured between $7z_o$ and 100m – where z_o is the surface roughness height), wind direction and ambient temperature. AERMOD also needs observed cloud cover. However, if cloud cover is not available (e.g., from an on-site monitoring program), two vertical measurements of temperature (typically at 2 and 10 meters) and a measurement of solar radiation can be substituted. A full morning upper air sounding (rawinsonde) is required to calculate the convective mixing height throughout the day. Surface characteristics (surface roughness, Bowen ratio, and albedo) are also needed to construct similarity profiles of the relevant PBL parameters.

Unlike prior regulatory models, AERMOD accounts for the vertical inhomogeneity of the PBL in its dispersion calculations. This is accomplished by "averaging" the parameters of the actual PBL into "effective" parameters of an equivalent homogeneous PBL.

Figure 1 shows the flow and processing of information in AERMOD. The modeling system consists of one main program (AERMOD) and two pre-processors (AERMET and AERMAP). The major purpose of AERMET is to calculate boundary layer parameters for use by AERMOD. The meteorological INTERFACE, internal to AERMOD, uses these parameters to generate profiles of the needed meteorological variables. In addition, AERMET passes all meteorological observations to AERMOD.

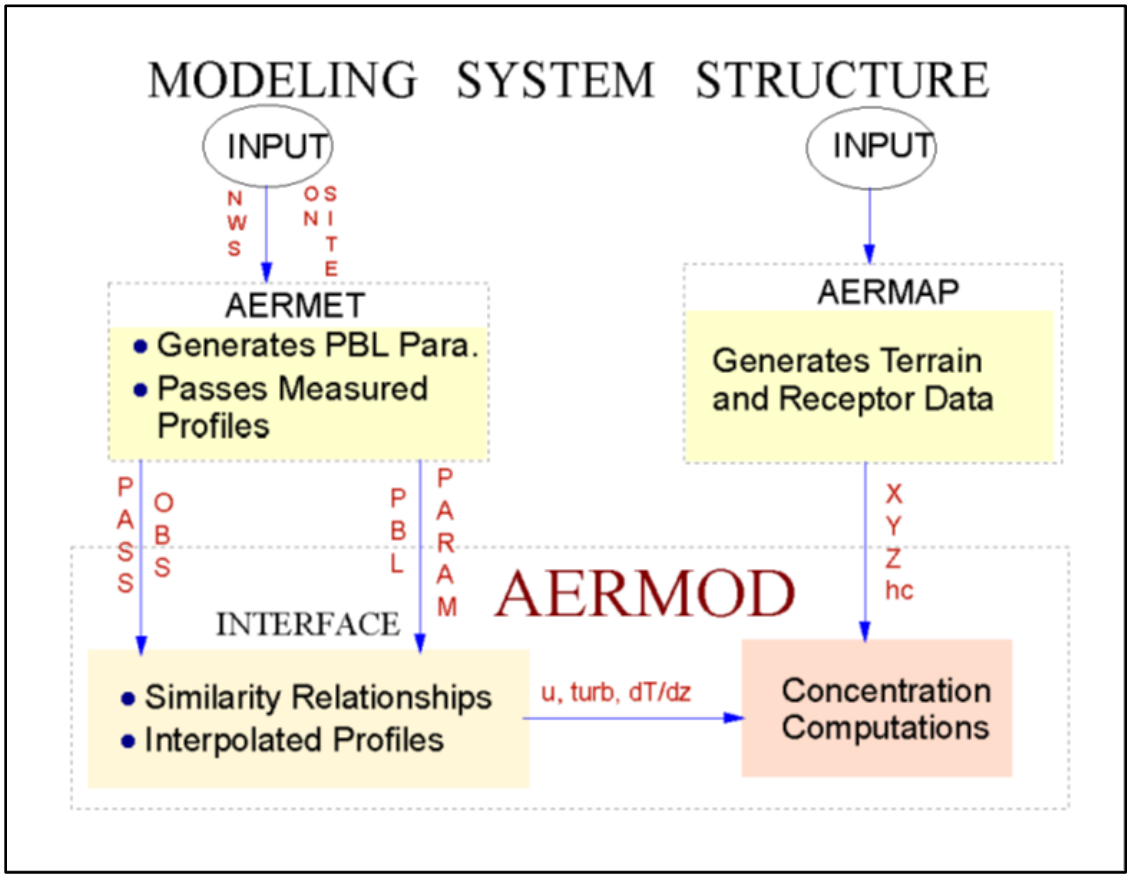

Figure 1. Data flow in the AERMOD modeling system

Surface characteristics in the form of albedo, surface roughness, and Bowen ratio, plus standard meteorological observations (wind speed, wind direction, temperature, and cloud cover), are input to AERMET. AERMET then calculates the PBL parameters: friction velocity (u_*), Monin-Obukhov length (L), convective velocity scale (w_*), temperature scale (θ_*), mixing

height (z_i), and surface heat flux (H). These parameters are then passed to the INTERFACE (which is within AERMOD) where similarity expressions (in conjunction with measurements) are used to calculate vertical profiles of wind speed (u), lateral and vertical turbulent fluctuations (σ_v, σ_w), potential temperature gradient ($d\theta/dz$), and potential temperature (θ).

The terrain pre-processor, AERMAP, uses gridded terrain data to calculate a representative terrain-influence height (h_c), also referred to as the terrain height scale. The terrain height scale h_c, which is uniquely defined for each receptor location, is used to calculate the dividing streamline height. The gridded data needed by AERMAP is selected from Digital Elevation Model (DEM) data. AERMAP can also be used to create receptor grids. The elevation for each specified receptor can be assigned through AERMAP. For each receptor, AERMAP passes the following information to AERMOD: the receptor's location (x_r, y_r), its height above mean sea level (z_r), and the receptor specific terrain height scale (h_c).

A comprehensive description of the basic formulation of the AERMOD dispersion model, including the INTERFACE, AERMET, and AERMAP, is presented in this document. Included are: 1) a complete description of the AERMET algorithms that provide quantitative hourly PBL parameters; 2) the general form of the concentration equation with adjustments for terrain; 3) plume rise and dispersion algorithms appropriate for both the convective and stable boundary layers; 4) handling of boundary layer inhomogeneity; 5) algorithms for developing vertical profiles of the necessary meteorological parameters; 6) a treatment of the nighttime urban boundary layer; 7) treatment of building downwash (incorporation of PRIME); and 8) enhancement of lateral dispersion due to plume meander. The model described here represents the 24142 version of AERMOD, AERMET, and AERMAP. In addition, all the symbols used for the many parameters and variables that are referred to in this document are defined, with their appropriate units, in Section 6 titled "List of Symbols."

3. Meteorological preprocessor (AERMET)

The basic purpose of AERMET is to use meteorological measurements, representative of the modeling domain, to compute certain boundary layer parameters used to estimate profiles of wind, turbulence, and temperature. These profiles are estimated by the AERMOD interface, which is described in Section 4.

While the structure of AERMET is based upon an existing regulatory model preprocessor, the Meteorological Processor for Regulatory Models (MPRM) (Irwin et al. 1988), the actual processing of the meteorological data is like that done for the CTDMPLUS (Perry 1992) and HPDM (Hanna and Paine 1989; Hanna and Chang 1993) models. The growth and structure of the atmospheric boundary layer is driven by the fluxes of heat and momentum which in turn depend upon surface effects. The depth of this layer and the dispersion of pollutants within it are influenced on a local scale by surface characteristics such as surface roughness, reflectivity (albedo), and the availability of surface moisture. The surface parameters provided by AERMET are the Monin-Obukhov Length (L), surface friction velocity (u_*), surface roughness length (z_o), surface heat flux (H), and the convective scaling velocity (w_*). AERMET also provides estimates of the convective and mechanical mixed layer heights, z_{ic} and z_{im}, respectively. AERMET defines the stability of the PBL by the sign of H (convective for $H > 0$ and stable for $H < 0$). Although AERMOD can estimate meteorological profiles with data from as little as one measurement height, it will use as much data as the user can provide for defining the vertical structure of the boundary layer. In addition to PBL parameters, AERMET passes all measurements of wind, temperature, and turbulence in a form necessary for AERMOD.

It should be noted as mentioned in section 1.2 of the Introduction to this document, the formulation descriptions that follow focus on the treatment of land-based observed data and the characterization of the planetary boundary layer over land. For information on the formulation

of the COARE algorithm and the treatment of offshore meteorology to characterize the marine boundary layer, refer to Fairall, et al. (2003).

3.1 Energy balance in the PBL

The fluxes of heat and momentum drive the growth and structure of the PBL. To properly characterize the PBL, one first needs a good estimate of the surface sensible heat flux (H) which depends on the net radiation (R_n) and surface characteristics such as the available surface moisture (described in the form of the Bowen ratio (B_o)). In the CBL, a simple energy balance approach, as in Oke (1978), is used to derive the expression, used in AERMET, to calculate the sensible heat flux, H. We begin with the following simple characterization of the energy balance in the PBL:

$$H + \lambda E + G = R_n \qquad \textbf{(1)}$$

where H is the sensible heat flux, λE is the latent heat flux, G is the soil heat flux, and R_n is the net radiation. To arrive at an estimate of H, simple parameterizations are made for the soil and latent heat flux terms; that is $G=0.1\ R_n$ and $\lambda E = H / B_o$, respectively. Substituting these expressions into eq. **(1)** the expression for surface heat flux becomes

$$H = \frac{0.9\ R_n}{(1 + {}^{1}/_{B_o})}. \qquad \textbf{(2)}$$

3.1.1 Net radiation

If measured values for R_n are not available, the net radiation is estimated from the insolation and the thermal radiation balance at the ground following the method of Holtslag and van Ulden (1983) as

$$R_n = \frac{(1 - r\{\varphi\})\, R + c_1\, T_{ref}^6 - \sigma_{SB}\, T_{ref}^4 - c_2 n}{1 + c_3}, \qquad \textbf{(3)}$$

where c_1 = 5.31 x 10^{-13} W m^{-2} K^{-4}, c_2 = 60 W m^{-2}, c_3 = 0.12, σ_{SB} is the Stefan Boltzman constant (5.67 x 10^{-8} W m^{-2} K^{-4}), T_{ref} is the ambient air temperature at the reference height for temperature, and R_n is the net radiation. The albedo is calculated as

$$\{\varphi\} = r' + (1 - r')\exp(a\varphi + b),$$

where a = -0.1, b = -0.5(1-r'), and $r' = r\{\varphi = 90°\}$. Note, braces, {}, are used throughout this report to denote the functional form of variables.

Solar radiation, R, corrected for cloud cover, is taken from Kasten and Czeplak (1980) as

$$R = R_o\,(1 - 0.75 n^{3.4}), \qquad \textbf{(4)}$$

where n is the fractional cloud cover and Ro is the clear sky insolation, which is calculated as R_o = 990(sin φ) - 30, and $\varphi = (\varphi\{t_p\} + \varphi\{t\})/2)$ is the solar elevation (t_p and t are the previous and present hours, respectively). Note that when observations of cloud cover are unavailable a value of 0.5 is assumed in eq. **(3)** and measurements of solar radiation are required.

3.1.2 Transition between the CBL and SBL

When the PBL transitions from convective to stable conditions the heat flux changes sign from a positive to a negative value. At the point of transition, the heat flux must therefore, vanish, implying that the net radiation is equal to zero. By setting R_o equal to zero in eq. **(3)**, and solving for sin φ, the critical solar elevation angle, φ_{crit}, corresponding to the transition point between the CBL and the SBL can be determined from

$$\sin(\varphi_{crit}) = \frac{1}{990}\left[\frac{-c_1 T^6 + \sigma_{SB} T^4 - c_2 n}{(1 - r\{\varphi\})(1 - 0.75 n^{3.4})} + 30\right]. \quad \textbf{(5)}$$

Therefore, AERMET defines the point of transition between the CBL and SBL (day to night) as the point in time when the solar elevation angle $\varphi = \varphi_{crit}$. On average, for clear and partly cloudy conditions, the transition from stable to convective conditions occurs when φ reaches approximately 13°; for overcast conditions φ_{crit} increases to about 23° (Holtslag and van Ulden 1983).

However, if solar radiation measurements are available AERMET determines φ_{crit} from an estimate of cloud cover rather than the actual observations themselves. In eq. **(5)** the cloud cover (n) is replaced with an equivalent cloud cover (n_{eq}) that is calculated from eq. **(4)** such that

$$n_{eq} = \left(1 - {R/R_o}/{0.75}\right)^{1/3.4}$$

3.2 Derived parameters in the CBL

3.2.1 Friction velocity (u_*) and Monin Obukhov length (L) in the CBL

In the CBL, AERMET computes the surface friction velocity, u_*, and the Monin-Obukhov length, L, using the value of H estimated from eq. **(2)**. Since the friction velocity and the Monin Obukhov length depend on each other, an iterative method, like that used in CTDMPLUS (Perry 1992), is used. AERMOD initializes u_*, and L by assuming neutral conditions (i.e., L=∞). The final estimate of u_* and L is made once convergence is reached through iterative calculations (i.e., there is less than a 1% change between successive iterations). The expression for u_* (e.g., Panofsky and Dutton, 1984) is,

$$u_* = \frac{k\, u_{ref}}{\ln\left(z_{ref}/z_0\right) - \Psi_m\{z_{ref}/L\} + \Psi_m\{z_0/L\}}, \qquad \textbf{(6)}$$

where k is the von Karman constant (= 0.4), u_{ref} is the wind speed at reference height, z_{ref} is the reference measurement height for wind in the surface layer, and z_o is the roughness length. The stability terms (Ψ_m's) in eq. **(6)** are computed as follows:

$$\Psi_m\left\{\frac{z_{ref}}{L}\right\} = 2\ln\left(\frac{1+\mu}{2}\right) + \ln\left(\frac{1+\mu^2}{2}\right) - 2\tan^{-1}\mu + \pi/2$$

$$\Psi_m\left\{\frac{z_0}{L}\right\} = 2\ln\left(\frac{1+\mu_0}{2}\right) + \ln\left(\frac{1+\mu_0^2}{2}\right) - 2\tan^{-1}\mu_0 + \pi/2 \qquad \textbf{(7)}$$

where $\mu = (1 - 16z_{ref}/L)^{1/4}$ and $\mu_0 = (1 - 16z_0/L)^{1/4}$.

The initial step in the iteration is to solve eq. **(6)** for u_* assuming that $\psi_m = 0$ (neutral limit) and setting $u = u_{ref}$. Having an initial estimate of u_*, L is calculated from the following definition (e.g., see Wyngaard (1988)):

$$L = -\frac{\rho\, c_p\, T_{ref} u_*^3}{k\, g\, H} \qquad \textbf{(8)}$$

where g is the acceleration of gravity, c_p is the specific heat of air at constant pressure, ρ is the density of air, and T_{ref} is the ambient temperature representative of the surface layer. Then u_* and L are iteratively recalculated using equations **(6)**, **(7),** and **(8)** until the value of L changes by less than 1%.

The reference heights for wind speed and temperature that are used in determining the friction velocity and Monin-Obukhov length are optimally chosen to be representative of the

surface layer in which the similarity theory has been formulated and tested with experimental data. Typically, a 10 m height for winds and a temperature within the range of 2 to 10 m is chosen. However, for excessively rough sites (such as urban areas where z_o can be in excess of 1 m), AERMET has a safeguard to accept wind speed reference data that range vertically between $7z_o$ and 100 m. Below $7z_o$ (roughly, the height of obstacles or vegetation), measurements are unlikely to be representative of the general area. A similar restriction for temperature measurements is imposed, except that temperature measurements as low as z_o are permitted. Above 100 m, the wind and temperature measurements are likely to be above the surface layer, especially during stable conditions. Therefore, AERMET imposes an upper limit of 100 meters for reference wind speed and temperature measurements for the purpose of computing the similarity theory friction velocity and Monin-Obukhov length each hour. Of course, other US EPA guidance for acceptable meteorological siting should be consulted in addition to keeping the AERMET restrictions in mind.

3.2.2 Convective velocity scale (w_*)

AERMOD utilizes the convective velocity scale to characterize the convective portion of the turbulence in the CBL. Field observations, laboratory experiments, and numerical modeling studies show that the large turbulent eddies in the CBL have velocities proportional to the convective velocity scale (w_*) (Wyngaard 1988). Thus, to estimate turbulence in the CBL, an estimate of w_* is needed. AERMET calculates the convective velocity scale from its definition as:

$$w_* = \left(\frac{g\ H\ z_{ic}}{\rho\ c_p\ T_{ref}} \right)^{1/3}, \qquad \textbf{(9)}$$

where z_{ic} is the convective mixing height (see Section 3.4).

3.3 Derived parameters in the SBL

In this section the parameters used to characterize the SBL are discussed along with their estimation methods. During stable conditions the energy budget term associated with the ground heating component is highly site-specific. During the day, this component is only about 10% of the total net radiation, while at night its value is comparable to that of the net radiation (Oke, 1978). Therefore, errors in the ground heating term can generally be tolerated during the daytime, but not at night. To avoid using a nocturnal energy balance approach that relies upon an accurate estimate of ground heating, AERMIC has adopted a much simpler semi-empirical approach for computing u_* and L.

3.3.1 Original friction velocity (u_*) in the SBL

The computation of u_* depends on the empirical observation that the temperature scale, θ_* defined as

$$\theta_* = -H/\rho\, c_p\, u_*\,, \qquad \textbf{(10)}$$

varies little during the night. Following the logic of Venkatram (1980), we combine the definition of L eq. **(8)** with eq. **(10)** to express the Monin-Obukhov length in the SBL as

$$L = \frac{T_{ref}}{k\, g\, \theta_*}\, u_*^2 \qquad \textbf{(11)}$$

From (Panofsky and Dutton 1984) the wind speed profile in stable conditions takes the form

$$u = \frac{u_*}{k}\left[\ln\left(\frac{z}{z_0}\right) + \frac{\beta_m z_{ref}}{L}\right], \qquad \textbf{(12)}$$

where $\beta_m = 5$ and z_{ref} is the wind speed reference measurement height. Substituting eq. **(11)** into eq. **(12)** and defining the drag coefficient, C_D, as $k / ln(z_{ref}/z_0)$ (Garratt 1992), results in

$$\frac{u}{u_*} = \frac{1}{C_D} + \frac{\beta_m z_{ref} g\, \theta_*}{T_{ref}\, u_*^2}. \qquad \textbf{(13)}$$

Multiplying eq. **(13)** by $C_D\, u_*^2$ and rearranging yields a quadratic of the form

$$u_*^2 - C_D u\, u_* + C_D u_0^2 = 0 \qquad \textbf{(14)}$$

where $u_0^2 = \beta_m\, z_{ref}\, g\, \theta_* / T_{ref}$. As is used in HPDM (Hanna and Chang 1993) and CTDMPLUS (Perry 1992) this quadratic has a real solution of the form

$$u_* = \frac{C_D\, u_{ref}}{2}\left[1 + \left(1 - \left(\frac{2\, u_0}{C_D^{\frac{1}{2}}\, u_{ref}}\right)^2\right)^{1/2}\right] \qquad \textbf{(15)}$$

Equation **(15)** produces real-valued solutions only when the wind speed is greater than or equal to the critical value $u_{cr} = \left[4\, \beta_m\, z_{ref} g\, \theta_* / T_{ref} C_D\right]^{1/2}$. For the wind speed less than the critical value, u_* and θ_* are parameterized using the following linear expression:

$$u_* = u_*\{u = u_{cr}\}\left(\frac{u}{u_{cr}}\right) \qquad for\ u < u_{cr}$$

$$\theta_* = \theta_*\left(\frac{u}{u_{cr}}\right) \qquad for\ u < u_{cr}$$

These expressions approximate the u_* versus θ_* dependence found by van Ulden and Holtslag (1983).

To calculate u_* from eq. **(15),** an estimate of θ_* is needed. If representative cloud cover observations are available, the temperature scale in the SBL is taken from the empirical form of van Ulden and Holtslag (1985) as

$$\theta_* = 0.09\,(1 - 0.5\,n^2)\,, \qquad \textbf{(16)}$$

where n is the fractional cloud cover.

If cloud cover measurements are not available, AERMET can estimate θ_* from measurements of temperature at two levels and wind speed at one level. This technique, known as the Bulk Richardson approach, starts with the similarity expression for potential temperature (Panofsky and Dutton 1984), that is,

$$\theta\{z\} - \theta_0 = \frac{\theta_*}{k}\left(ln\frac{z}{z_0} + \beta_m\frac{z}{L}\right), \qquad \textbf{(17)}$$

where $\beta_m \approx 5$ and k (= 0.4) is the von Karman constant. Applying eq. **(17)** to the two levels of temperature measurements and rearranging terms yields

$$\theta_* = \frac{k(\theta_2 - \theta_{1)}}{\left[\left(ln\frac{z_2}{z_1}\right) + \beta_m\frac{(z_2 - z_1)}{L}\right]}. \qquad \textbf{(18)}$$

Since both u_* (eq. **(12)**) and θ_* (eq. **(18)**) depend on L, and L (eq. **(11)**) in turn depends on $u*$ and $\theta*$, an iterative approach is needed to estimate u_*. First u_* and θ_* are found by assuming an initial value for L and iterating among the expressions for u_*, θ_* (eq. **(18)**) and L (eq. **(11)**) until convergence is reached. The expression used for u_*, in the iteration, is taken from (Holtslag 1984) and depends on atmospheric stability. For situations in which $z/L < 0.5$ is estimated using eq. **(12)**, otherwise (for more stable cases) $u*$ is calculated as follows:

$$u_* = \frac{ku}{\left[\ln\frac{z}{z_o} + 7\ln\frac{z}{L} + \frac{4.25}{(z/L)} - \frac{0.5}{(z/L)^2} + \frac{\beta_m}{2} - 1.648\right]}. \quad \textbf{(19)}$$

3.3.2 Adjusted friction velocity (u_*) in the SBL

Beginning with the 2017 updated regulatory version of the model (version 16216), a second approach for calculating the u_* value based on Qian and Venkatram (2011) was added. Under this formulation, u_* is computed as a function of the drag coefficient for neutral conditions (C_{DN}),

$$C_{DN} = \frac{k^2}{\left(\ln\left(\frac{z_r - d_h}{z_0}\right)\right)^2}$$

where z_r is the measurement height and d_h the zero-plane displacement (see Eq. 20 in Qian and Venkatram (2011)). Using CDN, u_* can be calculated based on eq. 26 from Qian and Venkatram (2011),

$$u_* = \frac{C_{DN}U}{2}\left(\frac{1 + \exp\left(-\frac{r^2}{2}\right)}{1 - \exp\left(-\frac{2}{r}\right)}\right),$$

with

$$r = \frac{2u_0}{U(C_{DN})^{1/4}}$$

and

$$u_0 = \left[\left(\frac{\beta_g(z_r - d_h - z_0)\,T_0}{T_0}\right)^{1/2}\right]$$

The minimum limit of the u_* value here can be computed as

$$u_{*,min} = \frac{U_{Cr}\, C_{DN}^{1/2}}{4}$$

with

$$U_{Cr} = \frac{2u_0}{C_{DN}^{1/4}}.$$

The final u$_*$ value is then the maximum of $u_{*,min}$ and the u_*. Using this value of u_*, θ_* is computed based on eq. **(18).**

As with the original method, if cloud cover measurements are not available, AERMET can estimate θ_* from measurements of temperature at two levels and wind speed at one level. This technique, known as the Bulk Richardson approach; however, when using the adjusted u_* formulation, the computation is based on Luhar and Rayner (2009). When the z_{ref} (reference height for the wind speed) is greater than *0.7*L* (the Monin-Obukhov Length), then u_* is calculated based on the initial estimate of *L* derived from the two-level temperature measurements,

$$u_* = \frac{ku}{\alpha\left[\zeta^{\beta}(1+\gamma\zeta^{(1-\beta)}) - \zeta_0^{\beta}(1+\gamma{\zeta_0}^{(1-\beta)})\right]}$$

where $\alpha = 4$, $\beta = 0.5$and $\gamma = 0.3$ and

$$\zeta = \frac{z_0}{L}.$$

Using this value of u_*, θ_* is computed based on eq. **(18).**

3.3.3 Sensible heat flux (*H*) in the SBL

Having computed u_* and θ_* for stable conditions, AERMET calculates the surface heat flux from eq. **(10)** as

$$H = -\rho\, c_p u_* \theta_* . \qquad \textbf{(20)}$$

AERMET limits the amount of heat that can be lost by the underlying surface to 64 W m^{-2}. This value is based on a restriction that Hanna (1986) placed on the product of θ_* and u_*. That is, for typical conditions, Hanna found that

$$[\theta_* u_*]_{max} = 0.05 ms^{-1}\, K\,. \qquad \textbf{(21)}$$

When the heat flux, calculated from eq. **(20)**, is such that $\theta_* u_* > 0.05$ m s^{-1} K, AERMET recalculates u_* by substituting $0.05/u_*$ into eq. **(15)** for θ_* (u_o in eq. **(15)** is a function of θ_*).

3.3.4 Monin-Obukhov length (L) in the SBL

Using the sensible heat flux of eq. **(20)** and u_* from eq. **(15)**, the Monin-Obukhov Length, for the SBL, is calculated from eq. **(8)**.

3.4 Mixing height

The mixing height (z_i) in the CBL depends on both mechanical and convective processes and is assumed to be the larger of a mechanical mixing height (z_{im}) and a convective mixing height (z_{ic}). Whereas, in the SBL, the mixing height results exclusively from mechanical (or shear induced) turbulence and therefore is identically equal to z_{im}. The same expression for calculating z_{im} is used in both the CBL and the SBL. The following two sections describe the procedures used to estimate z_{ic} and z_{im}, respectively.

3.4.1 Convective mixing height (z_{ic})

The height of the CBL is needed to estimate the profiles of important PBL variables and to calculate pollutant concentrations. If measurements of the convective boundary layer height are available, they are selected and used by the model. If measurements are not available, z_{ic} is calculated with a simple one-dimensional energy balance model (Carson 1973), as modified by

Weil and Brower (1983). This model uses the early morning potential temperature sounding (prior to sunrise), and the time varying surface heat flux to calculate the time evolution of the convective boundary layer as

$$z_{ic}\theta\{z_{ic}\} - \int_0^{z_{ic}} \theta\{z\}dz = (1 + 2A)\int_0^t \frac{H\{t'\}}{\rho\, c_p}dt, \qquad \textbf{(22)}$$

where θ is the potential temperature, A is set equal to 0.2 from Deardorff (1980), and t is the hour after sunrise. Weil and Brower found good agreement between predictions and observations of z_{ic}, using this approach.

3.4.2 Mechanical mixing height (z_{im})

In the early morning when the convective mixed layer is small, the full depth of the PBL may be controlled by mechanical turbulence. AERMET estimates the heights of the PBL during convective conditions as the maximum of the estimated (or measured if available) convective boundary layer height (z_{ic}) and the estimated (or measured) mechanical mixing height. AERMET uses this procedure to ensure that in the early morning, when z_{ic} is very small, but considerable mechanical mixing may exist, the height of the PBL is not underestimated. When measurements of the mechanical mixed layer are not available, z_{im} is calculated by assuming that it approaches the equilibrium height given by Zilitinkevich (1972) as

$$z_{ie} = 0.4\left(u_* L/f\right)^{0.5}, \qquad \textbf{(23)}$$

where z_{ie} is the equilibrium mechanical mixing height and f is the Coriolis parameter.

Venkatram (1980) has shown that, in mid-latitudes, eq. **(23)** can be empirically represented as

$$z_{ie} = 2400\, u_*^{3/2}, \qquad \textbf{(24)}$$

where z_{ie} (calculated from eq. **(24)**) is the unsmoothed mechanical mixed layer height. When measurements of the mechanical mixed layer height are available, they are used in lieu of z_{ie}.

To avoid estimating sudden and unrealistic drops in the depth of the shear-induced, turbulent layer, the time evolution of the mechanical mixed layer height (whether measured or estimated) is computed by relaxing the solution toward the equilibrium value appropriate for the current hour. Following the approach of Venkatram (1982)

$$\frac{dz_{im}}{dt} = \frac{(z_{ie} - z_{im})}{\tau}. \qquad \textbf{(25)}$$

The time scale, τ, governs the rate of change in height of the layer and is taken to be proportional to the ratio of the turbulent mixed layer depth and the surface friction velocity (i.e. $\tau = z_{im} / \beta_\tau\, u_*$). AERMOD uses a constant β_τ value of 2. For example, if u_* is of order 0.2 m s^{-1}, and z_{im} is of order 500 m, the time scale is of the order of 1250 s, which is related to the time it takes for the mechanical mixed layer height to approach its equilibrium value. Notice that when $z_{im} < z_{ie}$, the mechanical mixed layer height increases to approach its current equilibrium value; conversely, when $z_{im} > z_{ie}$, the mechanical mixed layer height decreases towards its equilibrium value.

Because the friction velocity changes with time, the current smoothed value of $z_{im}\{t+\Delta t\}$ is obtained by numerically integrating eq. **(25)** such that

$$z_{im}\{t + \Delta t\} = z_{im}\{t\}\left(e^{-\Delta t/\tau}\right) + z_{ie}\{t + \Delta t\}\left[1 - \left(e^{-\Delta t/\tau}\right)\right] . \qquad \textbf{(26)}$$

where $z_{im}\{t\}$ is the previous hour's smoothed value. For computing the time scale in eq. **(26)**, z_{im} is taken from the previous hour's estimate and u_* from the current hour. In this way, the time

scale (and thus relaxation time) will be short if the equilibrium mixing height grows rapidly but will be long if it decreases rapidly.

Although equations **(24)** and **(26)** are designed for application in the SBL, they are used in the CBL to ensure a proper estimate of the PBL height during the short transitional period at the beginning of the day when mechanical turbulence generally dominates. The procedure, used by AERMET, guarantees the use of the convective mixing height once adequate convection has been established even though the mechanical mixing height is calculated during all convective conditions. Since AERMET uses eq. **(26)** to estimate the height of the mixed layer in the SBL, discontinuities in z_i from nighttime to daytime are avoided.

In AERMOD, the mixing height z_i, has an expanded role in comparison to how it is used in ISC3. In AERMOD, the mixing height is used as an elevated reflecting/penetrating surface, an important scaling height, and enters in the w_* determination found in eq. **(9)**. The mixing height z_i for the convective and stable boundary layers is therefore defined as follows:

$$\begin{aligned} z_i &= \text{MAX}[z_{ic} \,;\, z_{im}] \qquad \text{for } L < 0 \text{ (CBL)} \\ z_i &= z_{im} \qquad\qquad\qquad\quad \text{For } L > 0 \text{ (SBL)} \end{aligned} \tag{27}$$

The sign of L is used by AERMET; if $L < 0$ then the PBL is considered to be convective (CBL) otherwise it is stable (SBL). then the PBL is considered to be convective (CBL) otherwise it is stable (SBL).

3.5 Adjustment for the low wind speed/stable conditions in AERMET

An option has been incorporated in AERMET to address issues associated with model overpredictions under low wind/stable conditions. The ADJ_U* option is available in AERMET by specifying ADJ_U* on the METHOD STABLEBL keyword in the Stage 3 AERMET control file for versions of AERMET prior to 22112 and the Stage 2 control file beginning with version 22112.

The ADJ_U* option can be specified with or without the Bulk Richardson Number option in AERMET, which utilizes delta-T measurements. The Bulk Richardson Number option in AERMET is selected by specifying BULKRN on a separate METHOD STABLEBL keyword in the Stage 3 AERMET input file. The formulation for the ADJ_U* option without the BULKRN option is based on Equation 26 of Qian and Venkatram (2011). The formulation for the ADJ_U* option with the BULKRN option is based on Equations 22, 23, and 25 of Luhar and Rayner (2009), with a critical value of z/L of 0.7.

4. Vertical structure of the PBL - AERMOD'S meteorological interface

The AERMOD interface, a set of routines within AERMOD, uses similarity relationships with the boundary layer parameters, the measured meteorological data, and other site-specific information provided by AERMET to compute vertical profiles of: 1) wind direction, 2) wind speed, 3) temperature, 4) vertical potential temperature gradient, 5) vertical turbulence (σ_w), and 6) lateral turbulence (σ_v).

For any one of these six variables (or parameters), the interface (in constructing the profile) compares each height at which a meteorological variable must be calculated with the heights at which observations were made, and if it is below the lowest measurement or above the highest measurement (or in some cases data is available at only one height), the interface computes an appropriate value from selected PBL similarity profiling relationships. If data are available both above and below a given height, an interpolation is performed which is based on both the measured data and the shape of the computed profile (see Section A.1). Thus, the approach used for profiling simultaneously takes advantage of the information contained in both the measurements and similarity parameterizations. As will be discussed, at least one level of measured wind speed, wind direction, and temperature is required. However, turbulence profiles can be parameterized without any direct turbulence measurements.

The following sub-sections in Section 4.1 provide a comprehensive description of AERMOD's profiling equations and how these estimated profiles are used to extract pertinent layer-averaged meteorology for AERMOD's transport and dispersion calculations. Also, example profiles (one typical of the CBL and one typical of the SBL) for the various parameters have been constructed for illustration. The CBL case assumes that z_i = 1000 m, L = -10 m and z_o = 0.1 m (i.e., $z_o = 0.0001 z_i$ and $L = -0.01 z_i$). The SBL case assumes that z_i = 100 m, L = 10 m and z_o = 0.1 m (i.e., $z_o = 0.001\ z_i$ and $L = 0.1\ z_i$).

4.1 General profiling equations

4.1.1 Wind speed profiling

The AERMOD profile equation for wind speed, has the familiar logarithmic form:

$$\begin{aligned} u &= u\{7z_o\}\left[\frac{z}{7z_o}\right] && \text{for} \quad z < 7z_o \\ u &= \frac{u_*}{k}\left[\ln\left(\frac{z}{z_o}\right) - \Psi_m\left\{\frac{z}{L}\right\} + \Psi_m\left\{\frac{z_o}{L}\right\}\right] && \text{for} \quad 7z_o \le z \le z_i \\ u &= u\{z_i\} && \text{for} \quad z > z_i \end{aligned} \qquad \textbf{(28)}$$

At least one wind speed measurement, that is representative of the surface layer, is required for each simulation with AERMOD. Since the logarithmic form does not adequately describe the profile below the height of obstacles or vegetation, eq. **(28)** allows for a linear decrease in wind speed from its value at $7z_o$.

For the CBL, the $\Psi_m s$ are evaluated using eq. **(7)** with z_{ref} replaced by z, and during stable conditions they are calculated from van Ulden & Holtslag (1985) as

$$\begin{aligned} \Psi_m\left\{\frac{z}{L}\right\} &= -17\left[1 - \exp\left(-0.29\frac{z}{L}\right)\right] \\ \Psi_m\left\{\frac{z_o}{L}\right\} &= -17\left[1 - \exp\left(-0.29\frac{z_o}{L}\right)\right]. \end{aligned} \qquad \textbf{(29)}$$

For small z/L ($<<1$), and with a series expansion of the exponential term, the first equation in (29) reduces to the form given in eq. **(12)**, i.e., $\psi_m = \beta_m z/L$ with $\beta_m = 5$. However, for large z/L (>1) and heights as great as 200 m in the SBL, the ψ_m given by eq. **(29)** is found to fit wind observations much better than the ψ_m given by eq. **(12)** (van Ulden and Holtslag 1985). Using the example case parameter values, Figure 2 and Figure 3 were constructed to illustrate the form of the wind profiles used by AERMOD in the layers above and below $7z_o$.

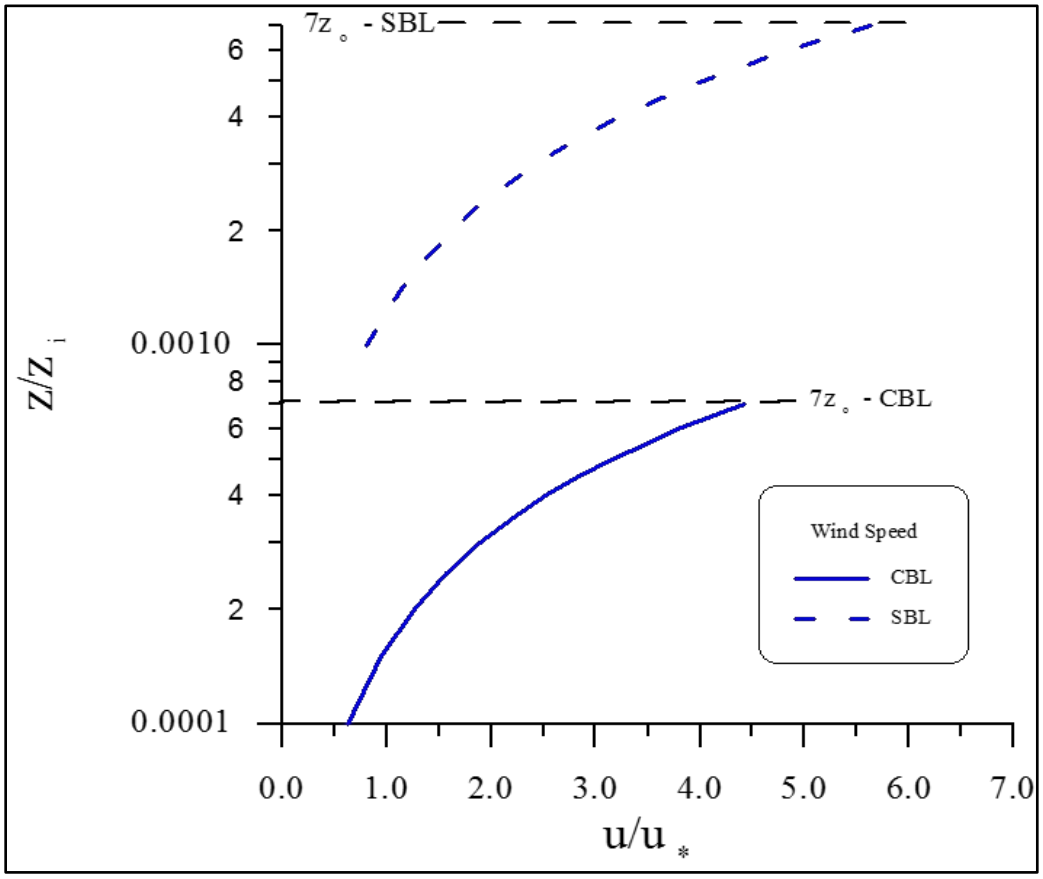

Figure 2. Wind speed profile, for both the CBL and SBL, in the region below 7z0

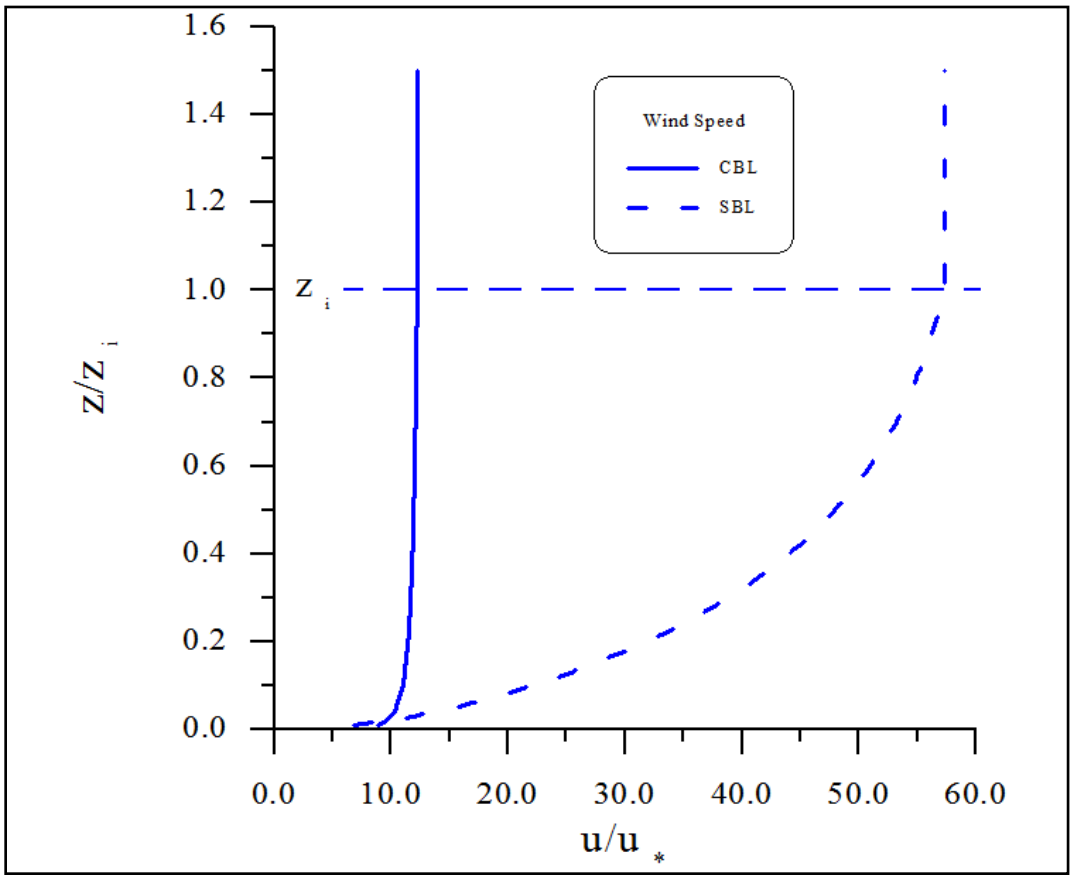

Figure 3. Wind speed profiling, for both the CBL and SBL, in the region above 7z0

4.1.2 Wind direction profiles

For both the CBL and SBL, wind direction is assumed to be constant with height both above the highest and below the lowest measurements. For intermediate heights, AERMOD linearly interpolates between measurements. At least one wind direction measurement is required for each AERMOD simulation.

4.1.3 Profiles of the potential temperature gradient

Above the relatively shallow super adiabatic surface layer, the potential temperature gradient in the well mixed CBL is taken to be zero. The gradient in the stable interfacial layer just above the mixed layer is taken from the morning temperature sounding. This gradient is an important factor in determining the potential for buoyant plume penetration into and above that layer. Above the interfacial layer, the gradient is typically constant and slightly stable. Although the interfacial layer depth varies with time, for the purposes of determining the strength of the stable stratification aloft, AERMET uses a fixed layer of 500 m to ensure that a sufficient layer of the morning sounding is sampled. A 500 m layer is also used by the CTDMPLUS model (Perry 1992) for this same calculation. This avoids strong gradients (unrealistic kinks) often present in these data. For a typical mixed layer depth of 1000 m, an interfacial layer depth of 500 m is consistent with that indicated by Deardorff (1979). A constant value of 0.005 K m^{-1} above the interfacial layer is used, as suggested by Hanna and Chang (1991). Using the morning sounding to compute the interfacial temperature gradient assumes that as the mixed layer grows throughout the day, the temperature profile in the layer above z_i changes little from that of the morning sounding. Of course, this assumes that there is neither significant subsidence nor cold or warm air advection occurring in that layer. Field measurements (e.g., Clarke et al. (1971)) of observed profiles throughout the day lend support to this approach. These data point out the relative invariance of upper-level temperature profiles even during periods of intense surface heating.

Below 100 m, in the SBL, AERMOD uses the definition of the potential temperature gradient suggested by Dyer (1974), as well as Panofsky and Dutton (1984). That is,

$$\frac{\partial\theta}{\partial z} = \frac{\theta_*}{k(2)}\left[1 + 5\frac{(2)}{L}\right] \qquad for \;\; z \le 2m$$
$$\frac{\partial\theta}{\partial z} = \frac{\theta_*}{k\,z}\left[1 + 5\frac{z}{L}\right] \qquad for \;\; 2m < z \le 100m. \qquad \textbf{(30)}$$

Eq. **(30)** is similar to that of Businger et al. (1971). Above 100 m the form of the potential temperature gradient, taken from Stull (1983) and van Ulden & Holtslag (1985) is

$$\frac{\partial\theta}{\partial z} = \frac{\partial\theta\{z_{mx}\}}{\partial z}\exp\left[-\frac{(z - z_{mx})}{0.44 z_{i\theta}}\right] \qquad \textbf{(31)}$$

where z_{mx} = 100 m, $z_{i\theta}$ = max[z_{im}; *100m*], and the constant 0.44 within the exponential term of eq. **(31)** is inferred from typical profiles taken during the Wangara experiment (Andre and Mahrt 1982). For all z, $\partial\theta/\partial z$ is limited to a minimum of 0.002 K m^{-1} (Paine and Kendall 1993).

In the SBL, if $d\theta/dz$ measurements are available below 100 m and above z_o, then θ_* is calculated from eq. **(30)** using the value of $\partial\theta/\partial z$ at the lowest measurement level and z_{Tref} replaced by the height of the $\partial\theta/\partial z$ measurements. The upper limit of 100 m for the vertical temperature gradient measurements is consistent with that imposed by AERMET for wind speed and temperature reference data used to determine similarity theory parameters such as the friction velocity and the Monin-Obukhov length. Similarly, the lower limit of z_o for the vertical temperature gradient measurements is consistent with that imposed for reference temperature data. If no measurements of $\partial\theta/\partial z$ are available, in that height range, then θ_* is calculated by combining equations **(8)** and **(20)**. θ_* is not used in the CBL.

Figure 4 shows the inverse height dependency of $\partial\theta/\partial z$ in the SBL. To create this curve we assumed that: Z_{im}=100 m; and therefore, $Z_{i\,\theta}$ = 100 m; L = 10 m; u_* = .124, which is consistent with a mixing height of 100 m; T_{ref} = 293 K; and therefore based on eq. **(11)** θ_* =

0.115 K. These parameter values were chosen to represent a strongly stable boundary layer. Below 2 m, $\partial\theta/\partial z$ is persisted downward from its value of 0.228 K m^{-1} at 2m. Above 100 m, $\partial\theta/\partial z$ is allowed to decay exponentially with height.

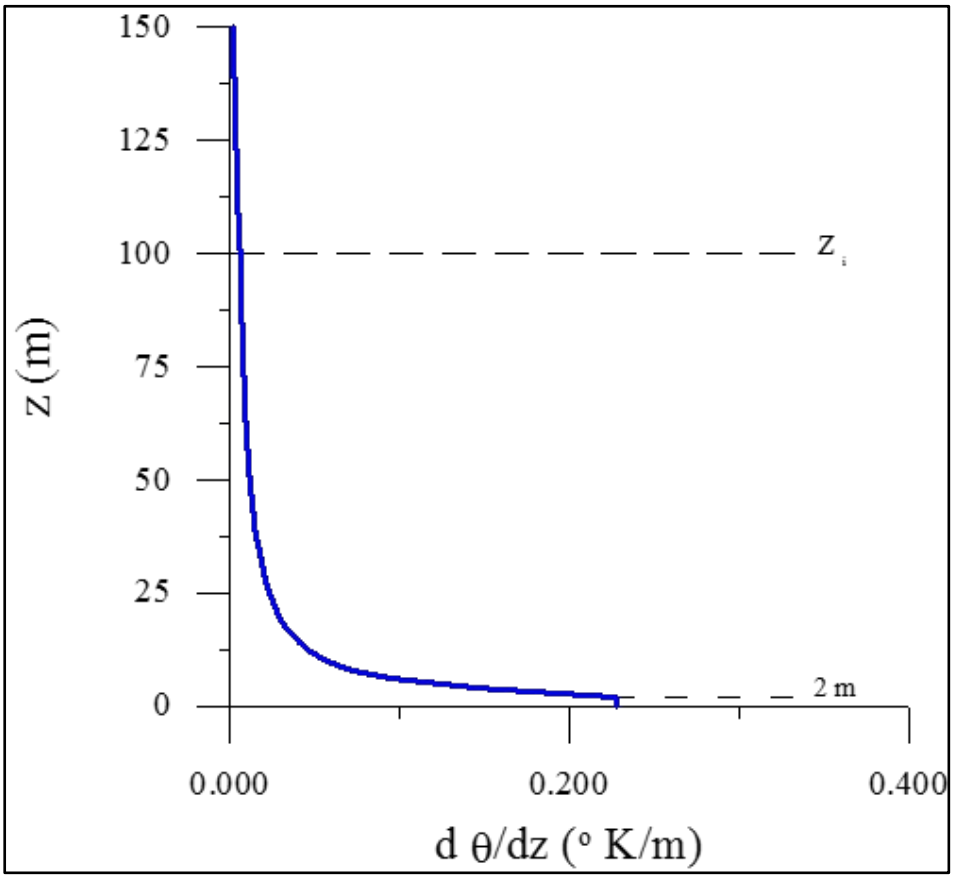

Figure 4. Profile of potential temperature gradient for the SBL

4.1.4 Potential temperature profiling

For use in plume rise calculations, AERMOD develops the vertical profile of potential temperature from its estimate of the temperature gradient profile. First, the model computes the potential temperature at the reference height for temperature (i.e., z_{Tref}) as

$$\theta\{z_{Tref}\} = T_{ref} + \frac{g\, z_{msl}}{c_P}, \qquad \textbf{(32)}$$

where $z_{msl} = z_{ref} + z_{base}$ is the user specified elevation for the base of the temperature profile (i.e., meteorological tower). Then for both the CBL and SBL the potential temperature is calculated as follows:

$$\theta\{z + \Delta z\} = \theta\{z\} + \left.\frac{\partial\theta}{\partial z}\right|_{\bar{z}} \Delta z \qquad \textbf{(33)}$$

where $\overline{\partial\theta}/_{\partial z}$ is the average potential temperature gradient over the layer Δz. Note that for $z < z_{Tref}$, Δz is negative.

4.1.5 Vertical turbulence calculated

In the CBL, the vertical velocity variance or turbulence (σ_{wT}^2) is profiled using an expression based on a mechanical or neutral stability limit ($\sigma_{wm} \propto u_*$) and a strongly convective limit ($\sigma_{wc} \propto w_*$). The total vertical turbulence is given as:

$$\sigma_{wT}^2 = \sigma_{wc}^2 + \sigma_{wm}^2. \qquad \textbf{(34)}$$

This form is similar to one introduced by Panofsky et al. (1977) and included in other dispersion models (e.g., Berkowicz et al. (1986), Hanna and Paine (1989), and Weil (1988a)).

The convective portion ($\sigma^2{}_{wc}$) of the total variance is calculated as:

$$\sigma_{wc}^2 = 1.6\left(\frac{z}{z_{ic}}\right)^{2/3} \cdot w_*^2 \qquad for \;\; z \le 0.1 z_{ic}$$

$$\sigma_{wc}^2 = 0.35 w_*^2 \qquad for \;\; 0.1 z_{ic} < z \le z_{ic} \qquad \textbf{(35)}$$

$$\sigma_{wc}^2 = 0.35 w_*^2 \exp\left[-\frac{6\left(z - z_{ic}\right)}{z_{ic}}\right] \qquad for \;\; z > z_{ic}$$

where the expression for $z \le 0.1\ z_{ic}$ is the free convection limit (Panofsky et al. 1977), for $0.1 z_i < z \le z_{ic}$ is the mixed-layer value (Hicks 1985), and for $z > z_{ic}$ is a parameterization to connect the mixed layer σ^2_{wc} to the assumed near-zero value well above the CBL. An example profile of convective vertical turbulence described in eq. **(35)** is presented in Figure 5.

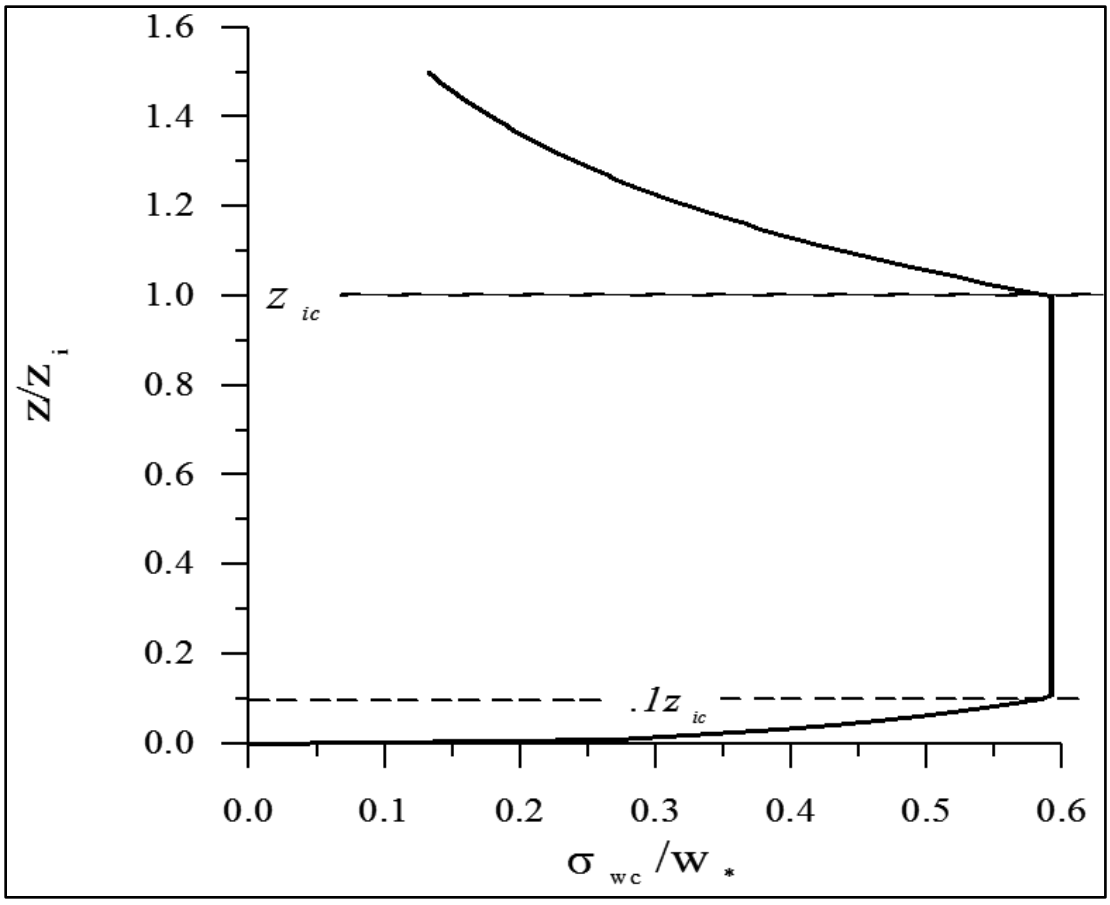

Figure 5. Convective portion of the vertical turbulence in the CBL

The mechanical turbulence (σ_{wm}) is assumed to consist of a contribution from the boundary layer (σ_{wml}) and from a "residual layer" (σ_{wmr}) above the boundary layer ($z > z_i$) such that,

$$\sigma_{wm}^2 = \sigma_{wml}^2 + \sigma_{wmr}^2. \qquad \textbf{(36)}$$

This is done to satisfy the assumed decoupling between the turbulence aloft ($z > z_i$) and that at the surface in the CBL shear layer, and to maintain a continuous variation of σ^2_{wm} with z near $z = z_i$. The expression for σ_{wml} following the form of Brost et al. (1982) is

$$\sigma_{wml} = 1.3u_* \left(1 - \frac{z}{z_i}\right)^{1/2} \qquad for \;\; z < z_i \tag{37}$$

$$\sigma_{wml} = 0.0 \qquad for \;\; z \geq z_i$$

where the $\sigma_{wml} = 1.3u_*$ at $z = 0$ is consistent with Panofsky et al. (1977).

Above the mixing height, σ_{wmr} is set equal to the average of measured values in the residual layer above z_i. If measurements are not available, then σ_{wmr} is taken as the default value of 0.02 $u\{z_i\}$. The constant 0.02 is an assumed turbulence intensity i_z (= σ_{wm} / u) for the very stable conditions presumed to exist above z_i (Briggs 1973). Within the mixed layer the residual turbulence (σ_{wmr}) is reduced linearly from its value at z_i to zero at the surface. Figure 6 presents the profile of the mechanical portion of the vertical turbulence in the CBL. The effect of combining the residual and boundary layer mechanical turbulence (eq. **(36)**) can be seen in this figure.

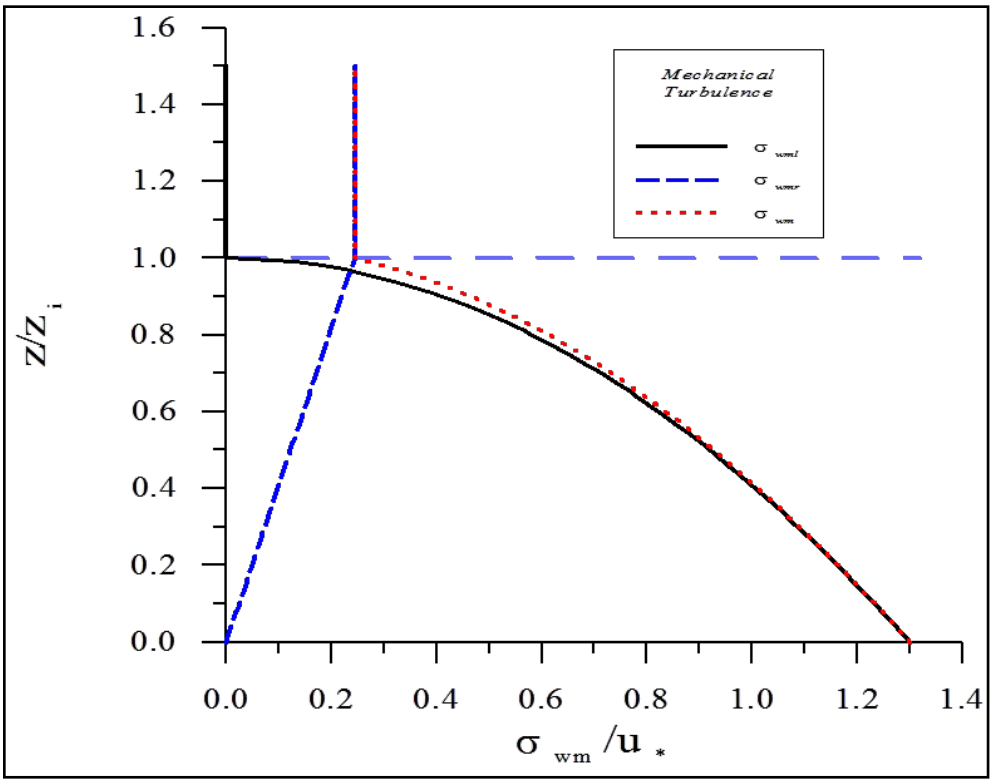

Figure 6. Mechanical portion of the vertical turbulence in the CBL

In the SBL the vertical turbulence contains only a mechanical portion which is given by eq. **(36)**. The use of the same σ^2_{wm} expressions for the SBL and CBL is done to ensure continuity of turbulence in the limit of neutral stability. Figure 7 illustrates AERMOD's assumed vertical turbulence profile for the SBL. This is similar to the profile for the CBL except for a notable increase in the value of σ_{wmr}. Since values for σ_{wmr} are based on the magnitude of the wind speed at z_i, the differences in the two figures stem from setting $z_o = 0.0001z_i$ in the CBL example case, while for the SBL case $z_o = 0.001z_i$.

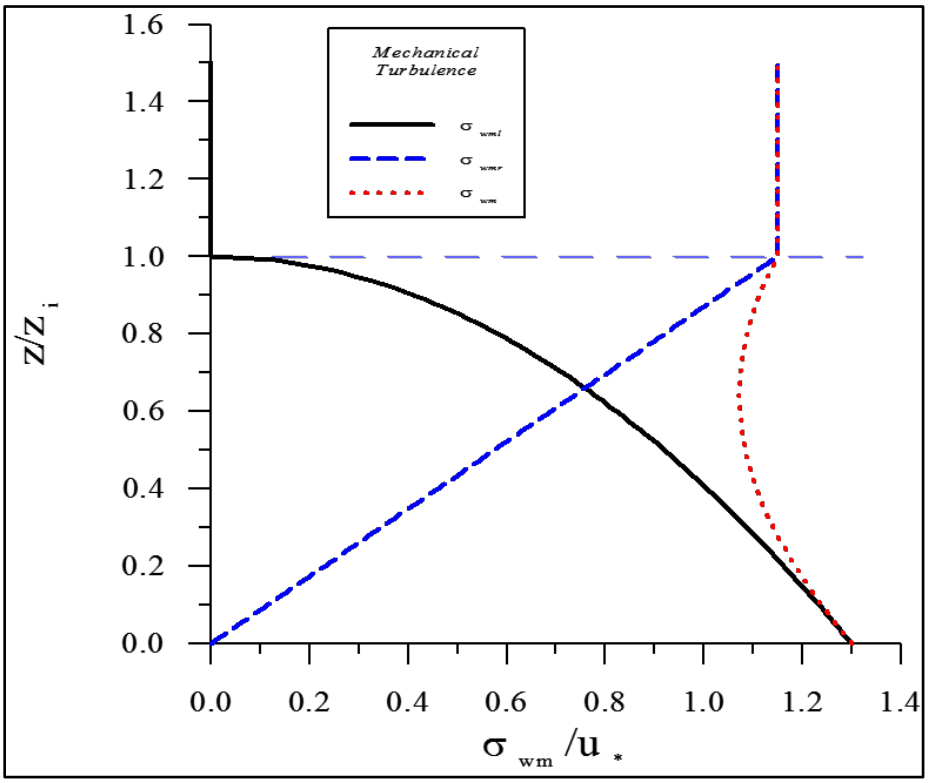

Figure 7. Profile of vertical turbulence in the SBL

4.1.6 Lateral turbulence calculated by the interface

In the CBL the total lateral turbulence, σ^2_{vT}, is computed as a combination of a mechanical (σ_{vm}) and convective (σ_{vc}) portions such that

$$\sigma_{vT}^2 = \sigma_{vc}^2 + \sigma_{vm}^2. \qquad \textbf{(38)}$$

In the SBL the total lateral turbulence contains only a mechanical portion. AERMOD, uses the same σ_{vm} expression in the CBL and SBL. This is done to maintain continuity of σ_{vm} in the limit of neutral stability. A description of mechanical and convective profiles of lateral turbulence follows.

4.1.6.1 Mechanical portion of the lateral turbulence

The variation with height of the mechanical portion of the lateral turbulence is bounded by its value at the surface and an assumed residual value at the top of the mechanical mixed layer. The variation between these two limits is assumed to be linear. Based on observations from numerous field studies, Panofsky and Dutton (1984) report that, in purely mechanical turbulence, the lateral variance near the surface has the form

$$\sigma_{v0}{}^2 = Cu_*{}^2, \qquad \textbf{(39)}$$

where the constant, C, ranges between 3 and 5. Based on an analysis of the Kansas data, Izumi (1971) and Hicks (1985) support the form of eq. **(39)** with a value of 3.6 for C.

Between the surface and the top of the mechanically mixed layer, σ^2_{vm} is assumed to vary linearly as

$$\begin{aligned} \sigma_{vm}^2 &= \left[\frac{\sigma_{vm}^2\{z_{im}\} - \sigma_{vo}^2}{z_{im}} \right] z + \sigma_{vo}^2 \qquad for \;\; z \le z_{im} \\ \sigma_{vm}^2 &= \sigma_{vm}^2\{z_{im}\} \qquad\qquad\qquad for \;\; z > z_{im}, \end{aligned} \qquad \textbf{(40)}$$

where $\sigma_{vm}^2\{z_m\} = \min[\sigma_{vo}^2; 0.25\ m^2 s^{-2}]$ and σ_{vo}^2, the surface value of the lateral turbulence, is equal to 3.6 u_*^2. This linear variation of σ^2_{vm} with z is consistent with field observations (e.g., Brost et al. (1982)). In the SBL the total lateral turbulence contains only a mechanical portion and it is given by eq. **(40)**.

Above the mixed layer, lateral turbulence is expected to maintain a modest residual level. Hanna (1983) analyzed ambient measurements of lateral turbulence in stable conditions. He found that even in the lightest wind conditions, the measurements of σ_{vc} were typically 0.5 m s^{-1} but were observed to be as low as 0.2 m s^{-1}. AERMOD adopts the lower limit of 0.2 m s^{-1} for σ_{vc} in near-surface conditions, as discussed below, but uses the more typical value of 0.5 m s^{-1} for the residual lateral turbulence above the mixed layer. Above the height of the CBL, the model linearly decreases σ_{vc}^2 from $\sigma_{vc}^2\{ z_{ic} \}$ to 0.25 at 1.2 z_{ic} and holds σ_{vc}^2 constant above 1.2 z_{ic}. However, if $\sigma_{vc}^2\{ z_{ic} \} < 0.25$ m^2 s^{-2}, then $\sigma_{vc}^2\{ z_{ic} \}$ is persisted upward from z_{ic}. Furthermore, it was found that a value of the order $\sigma_{vc}^2 = 0.25$ m^2 s^{-2} provided consistently good model performance (for plumes commonly above z_{im}) during the developmental evaluation (Perry et al. 2005) supporting the presence of residual lateral turbulence in this layer.

Figure 8 shows how the vertical profile of lateral mechanical turbulence changes over a range of mechanical mixing heights, and related friction velocities. The values of u_* used to produce these curves are consistent with the relationship between z_{im} and u_* which is found in eq. **(24)**. For the SBL Figure 8 represents profiles of the total lateral turbulence. In the CBL these curves depict only the mechanical portion of the total lateral variance. Note that for z_{im} = 300 m and 100 m the values σ_{vo}^2 are less than 0.25 m^2 s^{-2}. Therefore, the profiles are constant with height.

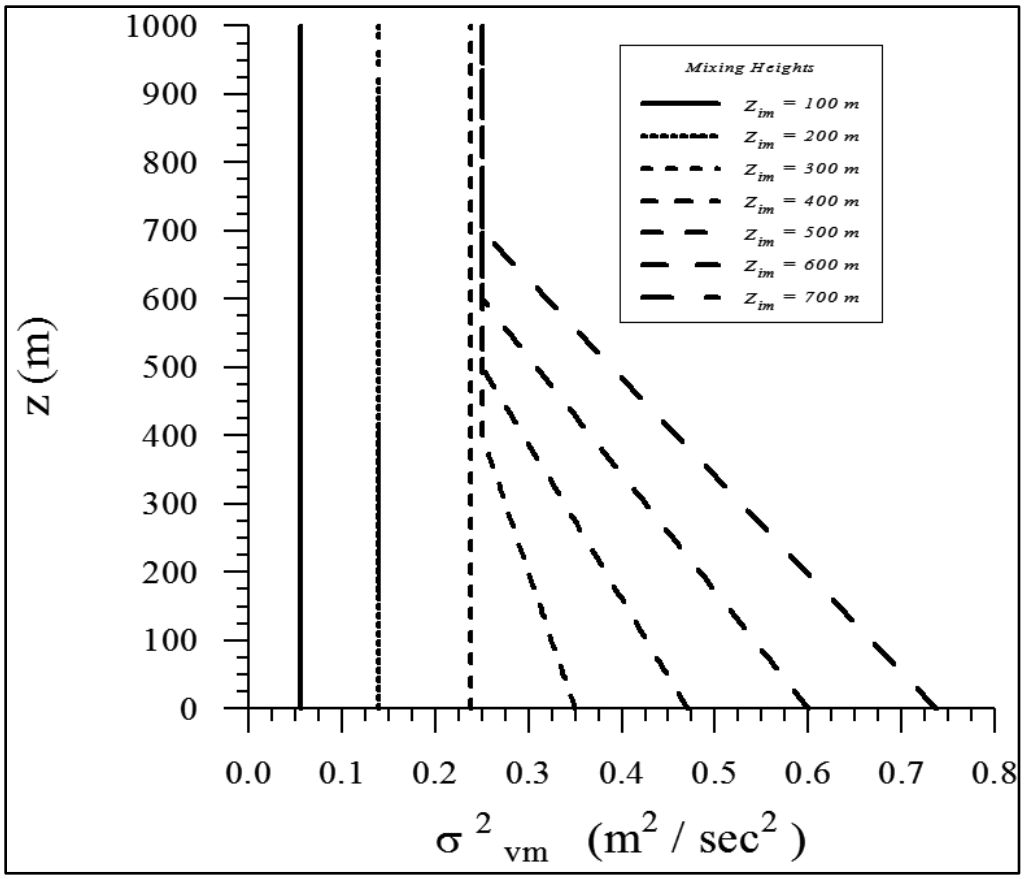

Figure 8. Family of lateral mechanical turbulence profiles over a range of mechanical mixing heights

4.1.6.2 Convective portion of the lateral turbulence

The convective portion of the lateral turbulence within the mixed layer is constant and calculated as:

$$\sigma_{vc}^2 = 0.35 w_*^2 \quad \textbf{(41)}$$

This constant value of $\sigma_v^2 / w_*^2 = 0.35$ is supported by the Minnesota data (Readings et al. 1974; Kaimal et al. 1976) and by data collected at Ashchurch, England (Caughey and Palmer

1979).

For $z > z_{ic}$, the model linearly decreases σ_{vc}^2 from $\sigma_{vc}^2\{ z_{ic} \}$ to 0.25 at 1.2 z_{ic} and holds σ_{vc}^2 constant above 1.2 z_{ic}. However, if $\sigma_{vc}^2\{ z_{ic} \} < .25$ m^2 s^{-2}, then $\sigma_{vc}^2\{ z_{ic} \}$ is persisted upward from z_{ic}.

4.2 Vertical inhomogeneity in the boundary layer as treated by the interface

AERMOD is designed to treat the effects on dispersion from vertical variations in wind and turbulence. Consideration of the vertical variation in meteorology is important for properly modeling releases in layers with strong gradients, for capturing the effects of meteorology in layers into which the plume may be vertically dispersing, and to provide a mechanism (in the CBL) by which sources that are released into, or penetrate into, an elevated stable layer can eventually re-enter the mixed layer. However, AERMOD is a steady-state plume model and therefore can use only a single value of each meteorological parameter to represent the layer through which these parameters are varying. Thus, the model "converts" the inhomogeneous values into equivalent effective or homogeneous values. This technique is applied to u, σ_{vT}, σ_{wT}, $\partial\theta/\partial z$, and the Lagrangian time scale. The effective parameters are denoted by a tilde throughout the document (e.g., effective wind speed is denoted by $\tilde{u}$).

Fundamental to this approach is the concept that the primary layer of importance, relative to receptor concentration, is the one through which plume material travels directly from source to receptor. Figure 9 presents a schematic illustration of the approach AERMOD uses to determine these effective parameters (α is used to generically represent these parameters). The effective parameters are determined by averaging their values over that portion of the layer that contains plume material between the plume centroid height, $H_p\ \{x\}$, (a simplified surrogate for the height of the plume's center of mass) and the receptor height (z_r). In other words, the averaging layer is determined by the vertical half-depth of the plume (defined as 2.15 $\sigma_z\ \{x_r\}$ where x_r is the distance from source to receptor) but is bounded by $H_p\ \{x_r\}$ and z_r. The values

used in the averaging process are taken from AERMOD's vertical profiles. This technique is best illustrated with examples.

Consider the two receptors depicted in Figure 9. Both receptors are located at the same distance x_r from the source but at different heights above ground, i.e., z_{r1} and z_{r2}. An example profile of some parameter α is shown at the far left of the Figure 9. The value of the effective parameter used by AERMOD to represent transport and diffusion from source to receptor depends on the location of the receptor. For receptor 1 the effective parameter value $\tilde{\alpha}_1$ (shown in the figure as α_{eff1}) is determined by averaging the values of $\alpha\ \{z\}$ between $H_p\ \{x_r\}$ and z_{r1}. Therefore, the layer over which this average is taken is smaller than the plume's half-depth, whereas, $\tilde{\alpha}_2$ (shown in the figure as α_{eff2}) is determined by averaging $\alpha\ \{z\}$ over the full layer from $H_p\ \{x_r\}$ down through a depth of $2.15\sigma_z\ \{x_r\}$ since the receptor is located below the defined lower extent of the plume.

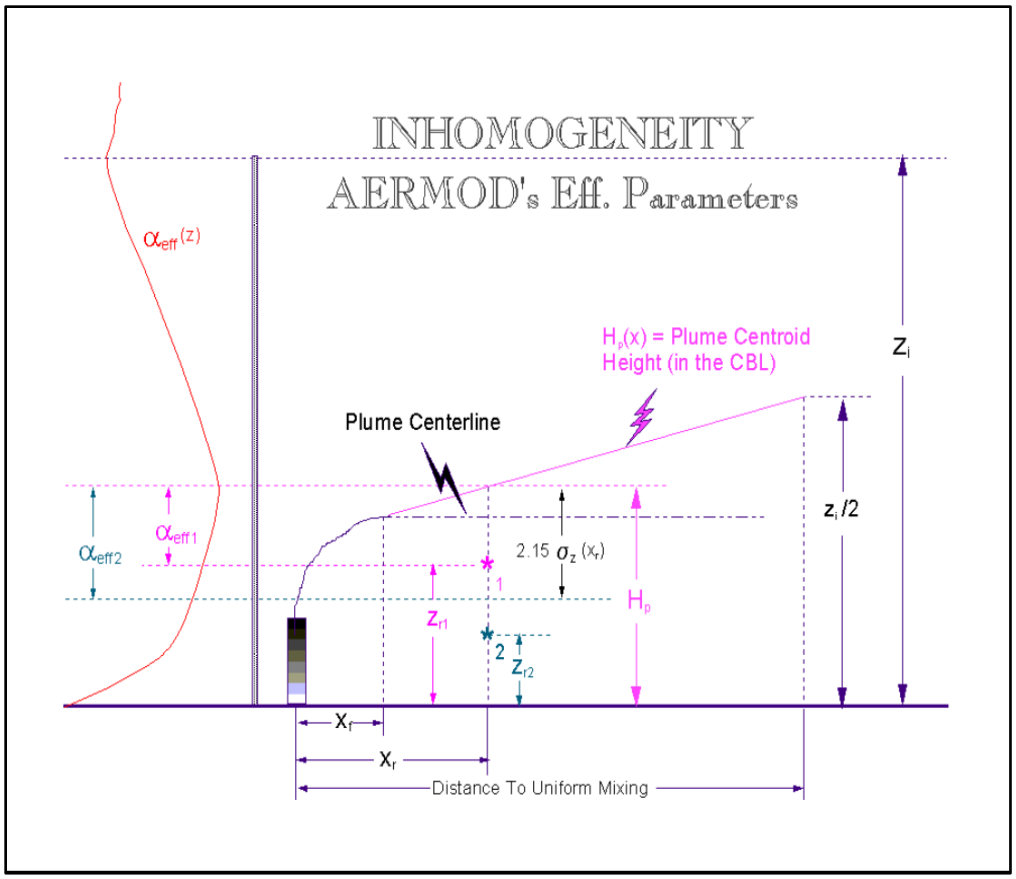

Figure 9. AERMOD's Treatment of the Inhomogeneous Boundary Layer

Since $\sigma_z\ \{x_r\}$ depends on the effective values of σ_{wT} and u, the plume size is estimated by first using the plume height values of $\sigma_{wT}\ \{H_p\}$ and $u\ \{H_p\}$ to calculate $\sigma_z\ \{x_r\}$. As illustrated in **Error! Reference source not found.**, $\sigma_z\{x_r\}$ is then used to determine the layer over which $\tilde{\sigma}_{wT}\{x_r\}$ and $\tilde{u}\{x_r\}$ are calculated. Once the averaging layer for a given plume and receptor is established the effective values, $\tilde{\alpha}$, are computed as simple averages:

$$\tilde{\alpha} = \frac{1}{(h_t - h_b)} \int_{h_b}^{h_t} \alpha\{z\}\, dz \quad , \qquad \textbf{(42)}$$

where h_b and h_t are the bottom and top, respectively, of the layer of importance such that:

$$h_b = \begin{Bmatrix} H_p\{x_r, y_r\}, & if \quad H_p\{x_r, y_r\} \le z_r \\ MAX\left\{\left[H_p\{x_r, y_r\} - 2.15\sigma_z\{x_{sr}\}\right], z_r\right\}, & if \quad H_p\{x_r, y_r\} > z_r \end{Bmatrix}$$

$$h_t = \begin{Bmatrix} MIN\left\{\left[H_p\{x_r, y_r\} + 2.15\sigma_z\{x_{sr}\}\right], z_r\right\}, & if \quad H_p\{x_r, y_r\} \le z_r \\ H_p\{x_r, y_r\}, & if \quad H_p\{x_r, y_r\} > z_r \end{Bmatrix} \qquad \textbf{(43)}$$

For all plumes, both limits are bounded by either the z_r or H_p. For both the direct and indirect sources h_t, in eq. **(43)** is not allowed to exceed z_i and if $h_b \geq z_i$ then $\tilde{\alpha} = \alpha\{z_i\}$.

For plumes in stable conditions and for the penetrated source in the CBL, H_p is always set equal to the plume centerline height ($\Delta h_s + h_s$) where h_s is the stack height corrected for stack tip downwash and Δh_s is the stable source plume rise. The stable source plume rise Δh_s is calculated from expressions found in Section 5.6.2.

In the CBL, the specification of H_p is somewhat more complicated. Because of limited mixing in the CBL the center of mass of the plume will be the plume height close to the source and the mid-point of the PBL at the distance where it becomes well mixed. Beyond final plume rise, H_p is varied linearly between these limits.

Prior to plume stabilization, i.e., $x < x_f$ (distance to plume stabilization),

$$H_p = h_s + \Delta h_{d,p},$$

where Δh_d is the plume rise for the direct source (estimated from eq. **(91)**), and Δh_p (= h_{ep} - h_s) is the plume rise for the penetrated source, where h_{ep} (penetrated source plume height) is calculated from eq. **(94)**.

The distance to plume stabilization, x_f, is determined following Briggs (Briggs 1975; Briggs 1971) as

$$\begin{aligned} x_f &= 49\, F_b^{5/8} \qquad for \quad F_b < 55 \\ x_f &= 119\, F_b^{2/5} \qquad for \quad F_b \geq 55 \end{aligned}, \tag{44}$$

where the buoyancy flux (F_b) is calculated from eq. **(57)**.

For $F_b = 0$ the distance to final rise is calculated from the ISCST3 ((U.S. EPA, 1995)) expression

$$x_f = {8 r_s \left(w_s + 3 u_p \right)^2} \Big/ {w_s u_p}, \tag{45}$$

where u_p is the wind speed at source height, r_s is the stack radius, and w_s is the stack exit gas velocity.

Beyond plume stabilization ($x > x_f$), H_p varies linearly between the stabilized plume height ($H\{x_f\}$) and the mid-point of the mixed layer ($z_i/2$). This interpolation is performed over the distance range x_f to x_m, where x_m is the distance at which pollutants first become uniformity mixed throughout the boundary layer.

The distance x_m is taken to be the product of the average mixed layer wind speed and the mixing time scale, $z_i/\overline{\sigma}_{wT}$. That is,

$$x_m = \frac{\overline{u}\, z_i}{\overline{\sigma}_{wT}}, \tag{46}$$

where the averaging of u and σ_{wT} are taken over the depth of the boundary layer.

For distances beyond x_f, H_p is assumed to vary linearly between the plume's stabilized height, $H\{x_f\}$, and $z_i/2$ such that:

$$H_p = H\{x_f\} + \left(\frac{z_i}{2} - H\{x_f\}\right) \cdot \frac{\left(x - x_f\right)}{\left(x_m - x_f\right)} \quad \textbf{(47)}$$

Note that in the CBL, both the direct and indirect source will have the same α (effective parameter) values. In eq. **(43)** σ_z is the average of the updraft σ_z and the downdraft σ_z, the maximum value of h_t is z_i, and when $h_b \geq z_i$, $\alpha = \alpha\{z_i\}$.

As discussed previously, when multiple vertical measurements of wind direction are available a profile is constructed by linearly interpolating between measurements and persisting the highest and lowest measurements up and down, respectively. The approach taken for selecting a transport wind direction from the profile is different from the above. The transport wind direction is selected as the mid-point of the range between stack height and the stabilized plume height.

5. The AMS/EPA Regulatory Model: AERMOD

AERMOD is a steady-state plume model in that it assumes that concentrations at all distances during a modeled hour are governed by the temporally averaged meteorology of the hour. The steady state assumption yields useful results since the statistics of the concentration distribution are of primary concern rather than specific concentrations at particular times and locations. AERMOD has been designed to handle the computation of pollutant impacts in both flat and complex terrain within the same modeling framework. In fact, with the AERMOD structure, there is no need for the specification of terrain type (flat, simple, or complex) relative to stack height since receptors at all elevations are handled with the same general methodology. To define the form of the AERMOD concentration equations, it is necessary to simultaneously discuss the handling of terrain.

In the stable boundary layer (SBL), the concentration distribution is assumed to be Gaussian in both the vertical and horizontal. In the convective boundary layer (CBL), the horizontal distribution is assumed to be Gaussian, but the vertical distribution is described with a bi-Gaussian Probability Density Function (PDF). This behavior of the concentration distributions in the CBL was demonstrated by Willis and Deardorff (1981) and Briggs (1993). Additionally, in the CBL, AERMOD treats "plume lofting," whereby a portion of plume mass, released from a buoyant source, rises to and remains near the top of the boundary layer before becoming vertically mixed throughout the CBL. The model also tracks any plume mass that penetrates into an elevated stable layer, and then allows it to re-enter the boundary layer when and if appropriate.

In urban areas, AERMOD accounts for the dispersive nature of the "convective-like" boundary layer that forms during nighttime conditions by enhancing the turbulence over that which is expected in the adjacent rural, stable boundary layer. The enhanced turbulence is the result of the urban heat flux and associated mixed layer which are estimated from the urban-rural temperature difference as suggested by Oke (1978; 1982).

In complex terrain, AERMOD incorporates the concept of the dividing streamline (Snyder et al., 1985) for stably stratified conditions. Where appropriate, the plume is modeled as a combination of two limiting cases: a horizontal plume (terrain impacting) and a terrain-following (terrain responding) plume. That is, AERMOD handles the computation of pollutant impacts in both flat and complex terrain within the same modeling framework. Generally, in stable flows, a two-layer structure develops in which the lower layer remains horizontal while the upper layer tends to rise over the terrain. The concept of a two-layer flow, distinguished at the dividing streamline height (H_c), was first suggested by theoretical arguments of Sheppard (1956) and demonstrated through laboratory experiments, particularly those of Snyder et al. (1985). In neutral and unstable conditions $H_c = 0$.

A plume embedded in the flow below H_c tends to remain horizontal; it might go around the hill or impact on it. A plume above H_c will ride over the hill. Associated with this is a tendency for the plume to be depressed toward the terrain surface, for the flow to speed up, and for vertical turbulent intensities to increase. These effects in the vertical structure of the flow are accounted for in models such as the Complex Terrain Dispersion Model (CTDMPLUS) (Perry 1992). However, because of the model complexity, input data demands for CTDMPLUS are considerable. EPA policy (Code of Federal Regulations 1997) requires the collection of wind and turbulence data at plume height when applying CTDMPLUS in a regulatory application. As previously stated, the model development goals for AERMOD include having methods that capture the essential physics, provide plausible concentration estimates, and demand reasonable model inputs while remaining as simple as possible. Therefore, AERMIC arrived at a terrain formulation in AERMOD that considers vertical flow distortion effects in the plume, while avoiding much of the complexity of the CTDMPLUS modeling approach. Lateral flow channeling effects on the plume are not considered by AERMOD.

AERMOD captures the effect of flow above and below the dividing streamline by weighting the plume concentration associated with two possible extreme states of the boundary layer (horizontal plume and terrain-following). As is discussed below, the relative weighting of

the two states depends on: 1) the degree of atmospheric stability; 2) the wind speed; and 3) the plume height relative to terrain. In stable conditions, the horizontal plume "dominates" and is given greater weight while in neutral and unstable conditions, the plume traveling over the terrain is more heavily weighted.

5.1 General structure of AERMOD including terrain

In general, AERMOD models a plume as a combination of two limiting cases: a horizontal plume (terrain impacting) and a terrain-following plume. Therefore, for all situations, the total concentration, at a receptor, is bounded by the concentration predictions from these states. In flat terrain the two states are equivalent. By incorporating the concept of the dividing streamline height, in elevated terrain, AERMOD's total concentration is calculated as a weighted sum of the concentrations associated with these two limiting cases or plume states (Venkatram et al. 2001).

The AERMOD terrain pre-processor (AERMAP) uses gridded terrain data to calculate a representative terrain-influence height (h_c) for each receptor with which AERMOD computes receptor specific H_c values. Through this approach, AERMOD handles the computation of pollutant impacts in both flat and elevated terrain within the same modeling framework, thereby removing the need to differentiate between the formulations for simple and complex terrain (as required with previous regulatory models).

The general concentration equation, which applies in stable or convective conditions is given by

$$C_T\{x_r, y_r, z_r\} = f \cdot C_{c,s}\{x_r, y_r, z_r\} + \left(1 - f\right) C_{c,s}\{x_r, y_r, z_p\}, \qquad \textbf{(48)}$$

where $C_T\{x_r,y_r,z_r\}$ is the total concentration $C_{c,s}\{z_r,y_r,z^r\}$ is the contribution from the horizontal plume state (subscripts *c* and *s* refer to convective and stable conditions, respectively),

$C_{c,s}\{z_r,y_r,z'\}$ is the contribution from terrain-following state, f is the plume state weighting function, $\{x_r, y_r, z_r\}$ is the coordinate representation of a receptor (with z_r defined relative to stack base elevation) $z_p = z_r - z_t$ is the height of a receptor above local ground, and z_t is the terrain height at a receptor. Note that in flat terrain, $z_t = 0$, $z_p = z_r$ and the concentration (eq. **(48)**) reduces to the form for a single horizontal plume. It is important to note that for any concentration calculation all heights (z) are referenced to stack base elevation. Figure 10 illustrates the relationship between the actual plume and AERMOD's characterization of it.

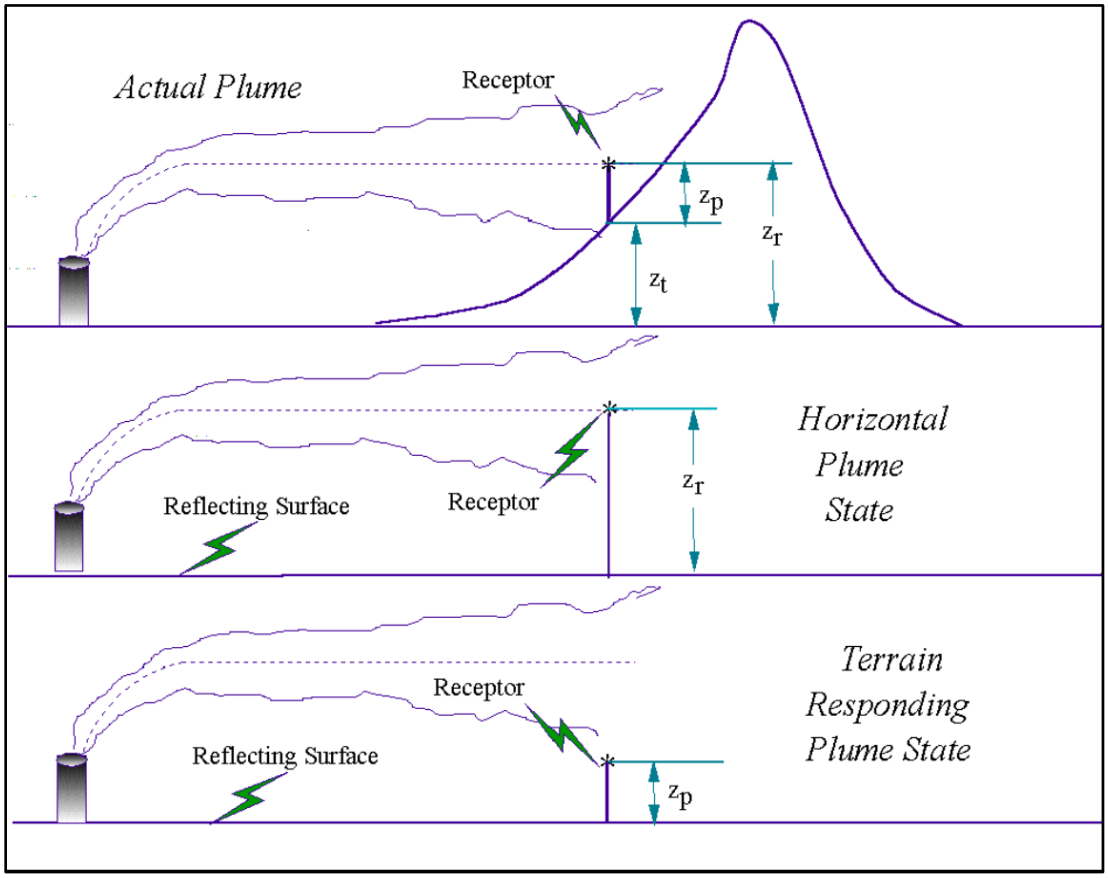

Figure 10. AERMOD two state approach. The total concentration predicted by AERMOD is the weighted sum of the two extreme possible plume states.

The formulation of the weighting factor requires the computation of H_c. Using the

receptor specific terrain height scale (h_c) from AERMAP, H_c is calculated from the same algorithms found in CTDMPLUS as:

$$1/2 \cdot u^2\{H_c\} = \int_{H_c}^{h_c} N^2\left(h_c - z\right) dz. \qquad \textbf{(49)}$$

where $u\ \{H_c\}$ is the wind speed at height H_c, and $N = \left[\frac{g}{\theta}\frac{\partial\theta}{\partial z}\right]^{1/2}$ is the Brunt-Vaisala frequency. The height scale, h_c, characterizes the height of the surrounding terrain that most dominates the flow in the vicinity of the receptor.

The weighting between the two states of the plume depends on the relationship between H_c and the vertical concentration distribution at the receptor location. Assuming that the wind speed increases with height, H_c can be thought of as the level in the stable atmosphere where the flow has sufficient kinetic energy to overcome the stratification and rise to the height of the terrain. However, in determining the amount of plume material in the terrain-following state at a receptor, it is only important to know the lowest height in the flow where the kinetic energy is sufficient for a streamline to just maintain its height above the surface, i.e. terrain-following. Whether it will be deflected further and reach the top of some specified hill is not important for determining the amount of plume material in the terrain-following state for this receptor. Venkatram et al. (2001) first proposed the idea that for real terrain, often characterized by a number of irregularly shaped hills, H_c should be defined in relation to a terrain-following height at each receptor location. This contrasts with the more classical definition where H_c is defined in relation to the top of a single representative hill upon which may reside many receptor locations.

In the AERMOD approach, plume height, receptor elevation, and H_c will determine how much plume material resides in each plume state. For a receptor at elevation z_t and an effective plume at height h_e, the height that the streamlines must reach to be in the terrain-following state

is z_t+h_e. Therefore, the terrain height of importance, h_c, in determining H_c is simply equal to this local terrain-following height. Any actual terrain above $h_c = z_t + h_e$ is of no consequence to the concentration at the receptor. This receptor and plume dependent approach to computing H_c assumes that there is sufficient terrain affecting the flow near the receptor to vertically force the streamlines to the terrain-following level. If the actual surrounding terrain does not reach the height of the terrain-following state, h_c is calculated from the highest actual terrain height in the vicinity of the receptor. Therefore, for any receptor, h_c is defined as the minimum of the highest actual terrain and the local terrain-following height. Given h_c, the dividing streamline height is computed with the same integral formula found in the CTDMPLUS model.

The fraction of the plume mass below H_c (i.e., ϕ_p) is computed as:

$$\varphi_p = \frac{\int_0^{H_c} C_s\{x_r, y_r, z_r\}\, dz}{\int_0^{\infty} C_s\{x_r, y_r, z_r\}\, dz}, \qquad \textbf{(50)}$$

where $C_s\{x_r.y_r,z_r\}$ is the concentration in the absence of the hill for stable conditions. In convective conditions $H_c = 0$ and $\varphi_p = 0$. As described by Venkatram et al. (2001), the plume state weighting factor f is given by $f = 0.5(1 + \varphi_p)$. When the plume is entirely below H_c ($\varphi_p = 1.0$ and f =1.0) the concentration is determined only by the horizontal plume. When the plume is entirely above the critical dividing streamline height or when the atmosphere is either neutral or convective, ($\varphi_p = 0$ and f =0.5). Therefore, during convective conditions the concentration at an elevated receptor is simply the average of the contributions from the two states. As plumes above H_c encounter terrain and are deflected vertically, there is also a tendency for plume material to approach the terrain surface and to spread out around the sides of the terrain. To simulate this the estimated concentration is constrained to always contain a component from the horizontal state. Therefore, under no conditions is the plume allowed to completely approach the terrain-following state. For flat terrain, the contributions from the two states are equal, and are equally weighted.

Figure 11 illustrates how the weighting factor is constructed and its relationship to the estimate of concentration as a weighted sum of two limiting plume states.

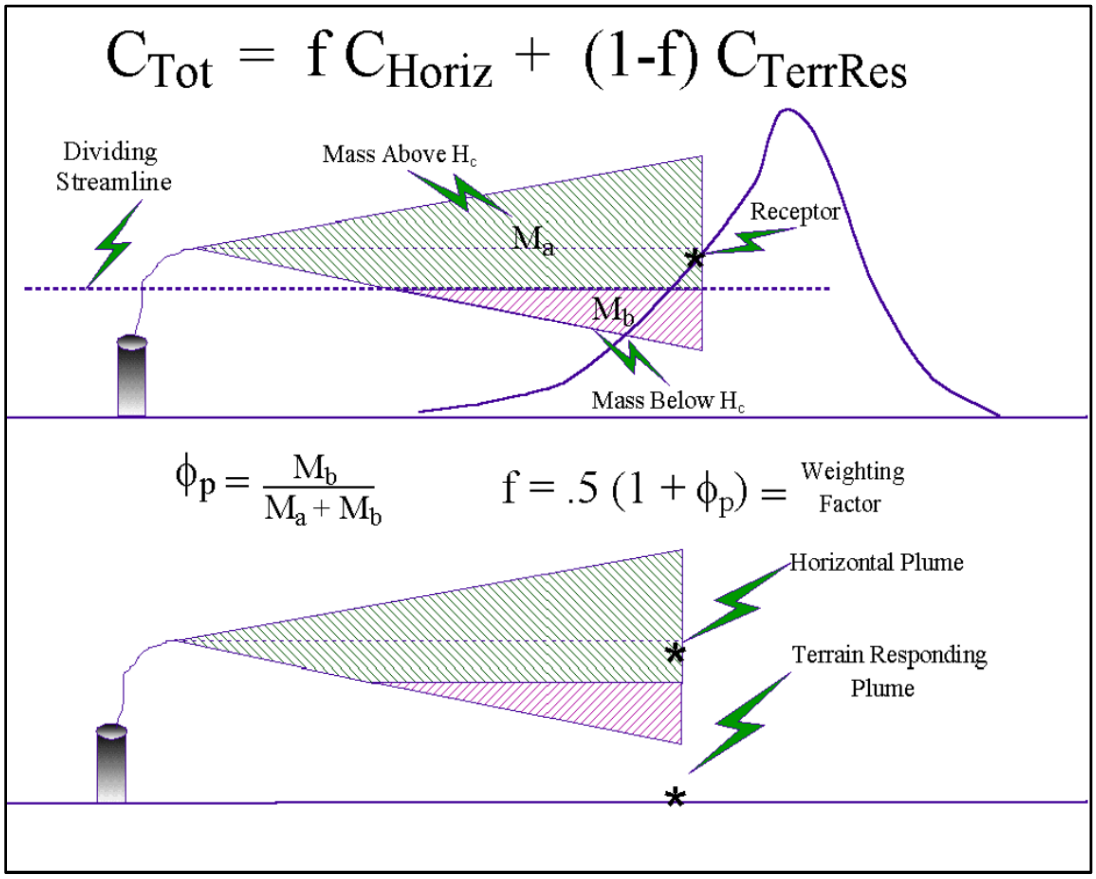

Figure 11. Treatment of Terrain in AERMOD. Construction of the weighting factor used in calculating total concentration.

The general form of the expressions for concentration in each term of eq. **(48)** for both the CBL and the SBL can be written as follows:

$$C\{x,y,z\} = \left(Q/\tilde{u}\right) P_y\{y;x\}\, P_z\{z;x\}, \qquad \textbf{(51)}$$

where Q is the source emission rate, $\tilde{u}$ is the effective wind speed, and p_y and p_z are probability density functions (pdf) which describe the lateral and vertical concentration distributions,

respectively. AERMOD assumes a traditional Gaussian PDF for both the lateral and vertical distributions in the SBL and for the lateral distribution in the CBL. The CBL's vertical distribution of plume material reflects the distinctly non-Gaussian nature of the vertical velocity distribution in convectively mixed layers. The specific form for the concentration distribution in the CBL is found in eq. **(54)** which uses the notation $C_c\ \{x_r, y_r, z_r\}$. Similarly, in the SBL, the concentration takes the form of eq. **(67)** and used the notation $C_s\ \{x_r, y_r, z_r\}$.

AERMOD simulates five different plume types depending on the atmospheric stability and on the location in and above the boundary layer: 1) direct, 2) indirect, 3) penetrated, 4) injected and 5) stable. All of these plumes will be discussed, in detail, throughout the remainder of this document. During stable conditions, plumes are modeled with the familiar horizontal and vertical Gaussian formulations. During convective conditions ($L<0$), the horizontal distribution is still Gaussian; the vertical concentration distribution results from a combination of three plume types: 1) the direct plume material within the mixed layer that initially does not interact with the mixed layer lid; 2) the indirect plume material within the mixed layer that rises up and tends to initially loft near the mixed layer top; and 3) the penetrated plume material that is released in the mixed layer but, due to its buoyancy, penetrates into the elevated stable layer.

During convective conditions, AERMOD also handles a special case referred to as an injected source where the stack top (or release height) is greater than the mixing height. Injected sources are modeled as plumes in stable conditions, however the influence of the turbulence and the winds within the mixed layer are considered in the inhomogeneity calculations as the plume material passes through the mixed layer to reach receptors.

As described above, AERMOD accounts for the vertical variation of meteorology through the use of effective values of wind speed, turbulence, and the Lagrangian time scale. Being a steady state plume model, AERMOD uses a single value of each meteorological variable to represent the state of the dispersive layer for each modeling period (typically one hour). Specifically, the effective parameters are determined by averaging values from the

meteorological profile within the layer between the plume's center of mass and the receptor. Effective variables or parameters are denoted by an overbar tilde (e.g., $\tilde{u}$).

5.2 Concentration predictions in the CBL

In AERMOD, the dispersion formulation for the convective boundary layer (CBL) represents one of the more significant model advances by comparison with existing regulatory models. One assumes that plume sections are emitted into a traveling train of convective elements - updrafts and downdrafts - that move with the mean wind. The vertical and lateral velocities in each element are assumed to be random variables and characterized by their probability density functions (PDF). The mean concentration is found from the PDF of the position of source-emitted "particles"; this position PDF in turn is derived from the PDF of the lateral and vertical velocities as described by Weil et al. (1997); also see Misra (1982), Venkatram (1983), and Weil (1988a).

In the CBL, the PDF of the vertical velocity (w) is positively skewed and results in a non-Gaussian vertical concentration distribution, F_z (Lamb 1982). The positive skewness is consistent with the higher frequency of occurrence of downdrafts than updrafts; for an elevated non-buoyant source the skewness also leads to the decent of the plume centerline, as defined by the locus of maximum concentration (Lamb 1982; Weil 1988a). Figure 12 presents a schematic representation of an instantaneous plume in a convective boundary layer and its corresponding ensemble average. The base concentration prediction in AERMOD is representative of a one-hour average. Notice that since a larger percentage of the instantaneous plume is affected by downdrafts, the ensemble average has a general downward trend. Since downdrafts are more prevalent the average velocity of the downdrafts is correspondingly weaker than the average updraft velocity to ensure that mass is conserved. In AERMOD, a skewed vertical velocity pdf is modeled using a bi-Gaussian distribution, which has been shown to be a good approximation to laboratory convection tank data (Baerentsen and Berkowicz 1984). In contrast to the vertical component, the lateral velocity pdf is approximately Gaussian (Lamb 1982), and this pdf and the resulting concentration distribution, F_y, are assumed to be Gaussian.

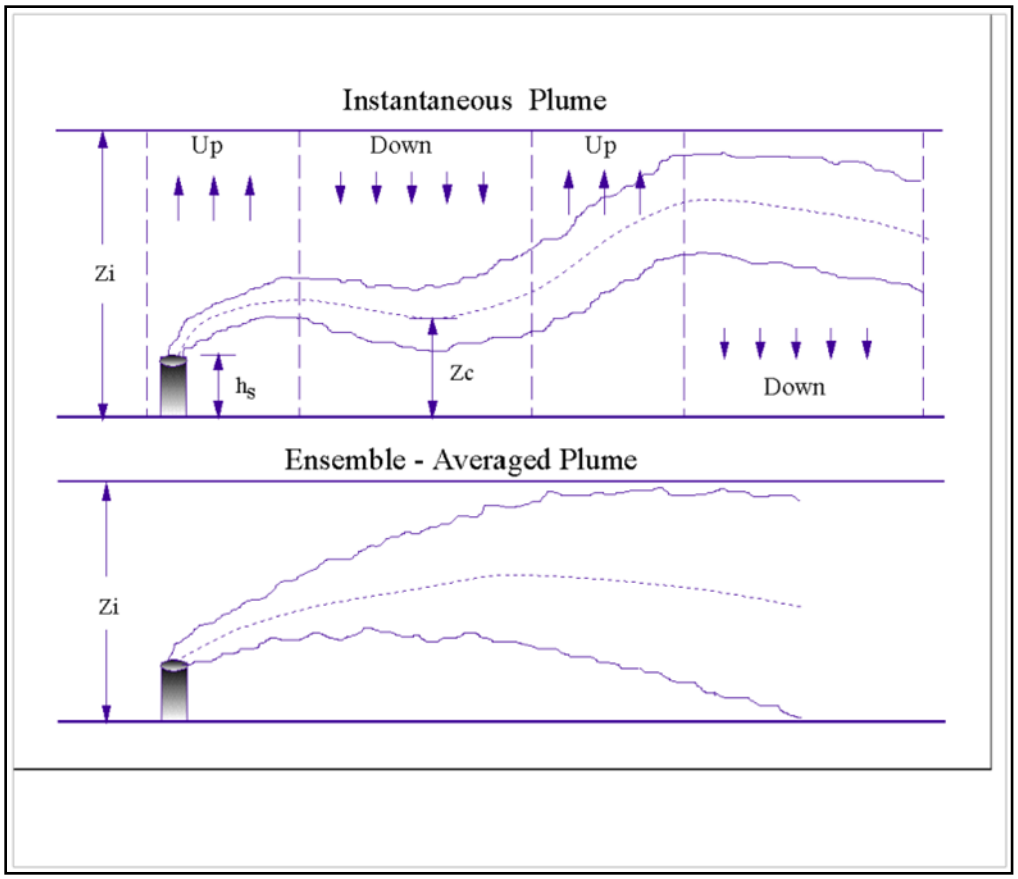

Figure 12. Instantaneous and corresponding ensemble-averaged plume in the CBL

In addition to the non-Gaussian F_z, AERMOD has the following features. For buoyant releases, there is no "final" plume rise assumed. Instead, the plume or particle trajectories are determined by the addition of a distance-dependent plume rise and the random vertical displacement caused by the vertical distribution of w. Ground level concentrations first appear when the negative or downdraft velocities are sufficiently large to overcome the plume rise velocity and carry plume sections to the surface. The direct transport of plume material to the ground is treated by the "direct" source located at the stack. That is, the direct source treats that portion of the plume's mass to first reach the ground, and all subsequent reflections of the mass at $z = z_i$ and 0 (where z_i is the mixed layer height in the CBL (Cimorelli et al., 2004). For plume segments or particles initially rising in updrafts, an "indirect" or modified-image source is included (above the mixed layer) to address the initial quasi-reflection of plume material at $z = z_i$,

i.e., for material that does not penetrate the elevated inversion. This source is labeled "indirect" because it is not a true image source (i.e., as is found in models such as ISC) - the plume is not perfectly reflected about z_i. Thus, the indirect source treats that portion of the plume's mass that first reaches z_i and all subsequent reflections of that particular mass at $z = 0$ and z_i. For the indirect source, a plume rise (Δh_i) is added to delay the downward dispersion of material from the CBL top (see Figure 13); this mimics the plume's lofting behavior, i.e., the tendency of buoyant plumes to remain temporarily near z_i and resist downward mixing. For non-buoyant sources the indirect source reduces to the first image source (as found in ISCST3) resulting from the first reflection at $z = z_i$. Additionally, a "penetrated" source or plume (above the CBL top) is included to account for material that initially penetrates the elevated inversion but is subsequently re-entrained by and disperses in the growing CBL.

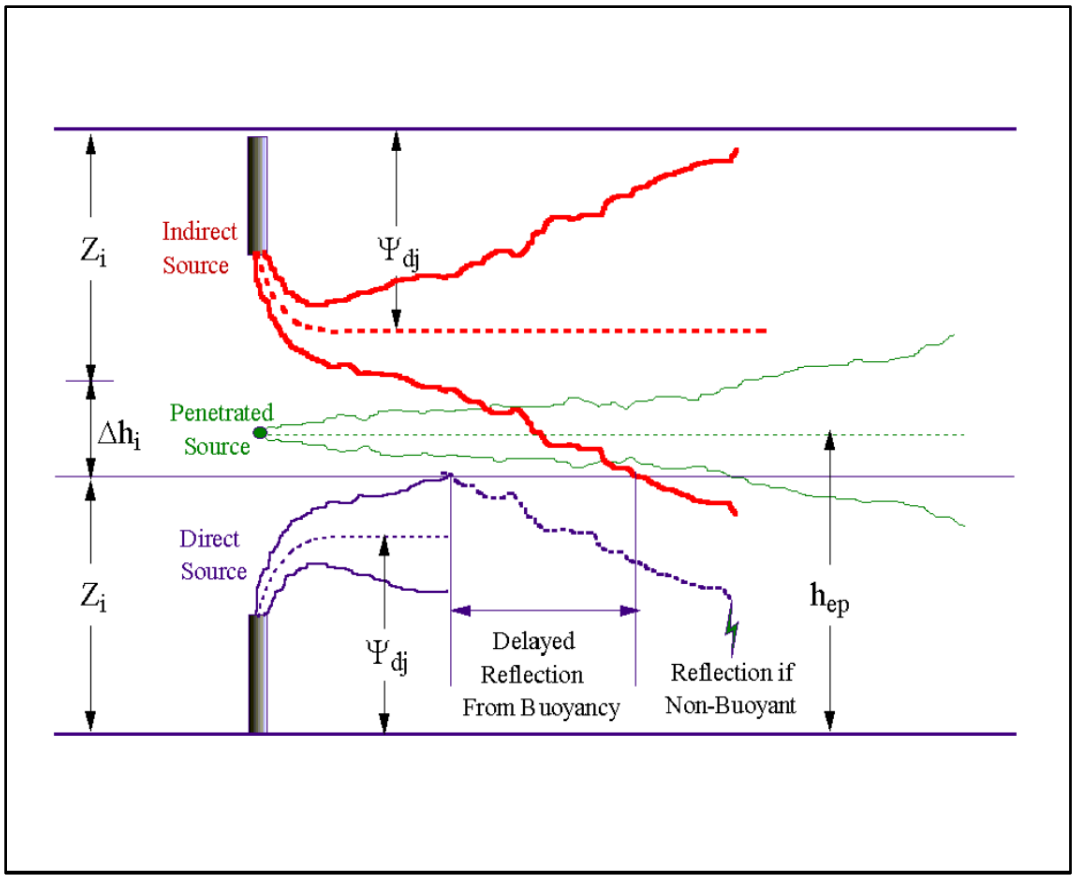

Figure 13. AERMOD's three plume treatment of the CBL

In line with the above concepts there are three main mathematical sources that contribute to the modeled concentration field: 1) the direct source (at the stack), 2) the indirect source, and 3) the penetrated source. The strength of the direct source is f_pQ, where Q is the source emission rate and f_p is the calculated fraction of the plume mass trapped in the CBL ($0 \leq f_p \leq 1$). Likewise, the indirect source strength is f_pQ since this (modified image) source is included to satisfy the no-flux boundary condition at $z = z_i$ for the trapped material. The strength of the penetrated source is $(1\text{-}f_p)Q$, which is the fraction of the source emission that initially penetrates into the elevated stable layer. In addition to the three main sources, other image sources are included to satisfy the no-flux conditions at $z = 0$ and z_i.

For material dispersing within a convective layer, the conceptual picture (see Figure 12) is a plume embedded within a field of updrafts and downdrafts that are sufficiently large to displace the plume section within it. The relationship between the particle (or air parcel) height, z_c and w is found by superposing the plume rise (Δh) and the vertical displacement due to w (i.e., wx/u), as

$$z_c = h_s + \Delta h + \frac{wx}{u}, \qquad \textbf{(52)}$$

where h_s is the stack height (corrected for stack tip downwash), u is the mean wind speed (a vertical average over the convective boundary layer) and x is the downwind distance. The Δh above includes source momentum and buoyancy effects as given by eq. **(91)** below (see Briggs (1984)). The F_z or pdf of z_c is found from the vertical velocity PDF p_w as described in Weil et al. (1997). In the CBL a good approximation to p_w is the superposition of two Gaussian distributions (Baerentsen and Berkowicz 1984; Weil 1988a) such that

$$p_w = \frac{\lambda_1}{\sqrt{2\pi}\sigma_{w1}} \exp\left(-\frac{\left(w - \overline{w_1}\right)^2}{2\sigma_{w1}^2} \right) + \frac{\lambda_2}{\sqrt{2\pi}\sigma_{w2}} \exp\left(-\frac{\left(w - \overline{w_2}\right)^2}{2\sigma_{w2}^2} \right), \qquad \textbf{(53)}$$

where λ_1 and λ_2 are weighting coefficients for the two distributions with $\lambda_1 + \lambda_2 = 1$(the subscripts 1 and 2 refer to the updraft and downdraft distributions, respectively). The parameters of the pdf (w_1, w_2, σ_{w1}, σ_{w2}, λ_1, λ_2) are functions of σ_w (the "total" or overall root mean square vertical turbulent velocity), the vertical velocity skewness $S = \overline{w}^3/\sigma_w^3$ (where $\overline{w}^3$ is the third moment of w), and a parameter $R = \sigma_{w1}/\overline{w_1} = -\sigma_{w2}/\overline{w_2} = 2$. An expanded discussion of the PDF parameters is given in Weil et al. (1997).

The instantaneous plume is assumed to have a Gaussian concentration distribution about its randomly varying centerline. The mean or average concentration is found by summing the concentrations due to all the random centerline displacements. This averaging process results in a skewed distribution which AERMOD represents as a bi-Gaussian pdf (i.e., one for updrafts and the other for downdrafts). Figure 14 illustrates the bi-Gaussian approach to approximate the skewed vertical concentration distribution in the CBL. The figure shows two mean trajectories, each representing the average of many individual trajectories of parcels (or particles) released into downdrafts (the downdraft plume) or updrafts (the updraft plume). The velocities determining these mean trajectories are: 1) the mean horizontal wind speed (u), 2) the vertical velocity due to plume buoyancy (v_{buoy}), and 3) the mean updraft ($\overline{w}_1$) or downdraft ($\overline{w}_2$) velocity. The mean height of each trajectory, $\overline{z}_{c1}$ or $\overline{z}_{c2}$, can be found by averaging eq. **(53)**. The parcel (or particle) height distributions are thus, related to concentration and are characterized by σ_{z1} ($= \sigma_{w1}x/u$) and σ_{z2} ($= \sigma_{w2}x/u$), the standard deviations of the two concentration distributions comprising the bi-Gaussian form as derived in Weil et al. (1997).

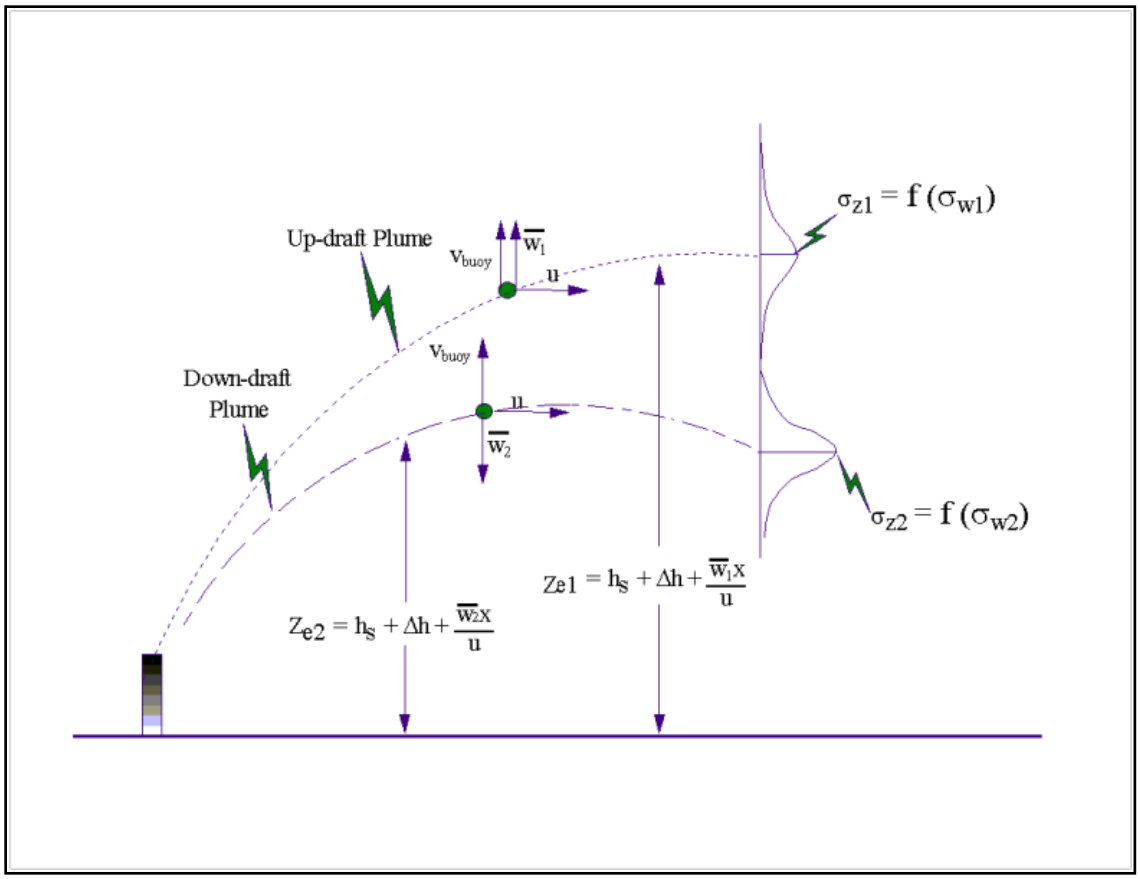

Figure 14. AERMOD's pdf approach for plume dispersion in the CBL. AERMOD approximates the skewed distribution by superimposing two Gaussian distributions, the updraft and downdraft distributions.

Figure 15 compares the bi-Gaussian pdf with the Gaussian form, which is symmetric about $w = 0$. As can be seen, for the negative and positive tails of the distributions, the bi-Gaussian pdf is biased towards smaller and larger p_w values, respectively, than the Gaussian. In addition, for the bi-Gaussian forms, approximately 60% of the area under the p_w curve is on the negative side of the w axis and approximately 40% on the positive side. This is consistent with the results of numerical simulations and field observations (Lamb 1982; Weil 1988a).

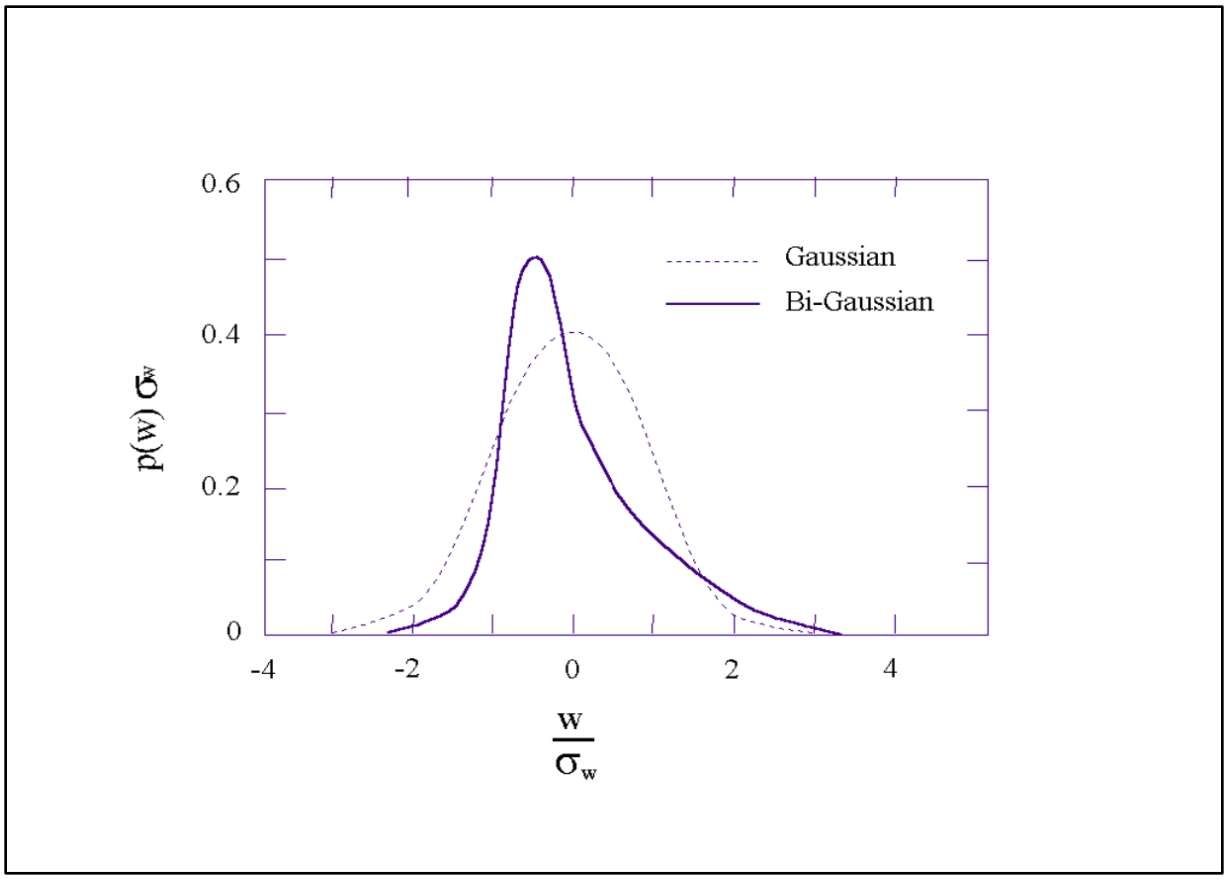

Figure 15. Probability density functon of the vertical velocity. While the Gaussian curve is unskewed, the bi-Gaussian curve has a skewness of S=1.

In the PDF approach used here (Weil et al. 1997), there are, as mentioned in the previous section, three primary sources that contribute to the modeled concentration field: 1) the "direct" or real source at the stack, 2) an "indirect" source that the model locates above the CBL top to account for the slow downward dispersion of buoyant plumes that "loft" or remain near, but below, z_i , and 3) a "penetrated source" that contains the portion of plume material that has penetrated into the stable layer above z_i. The direct source describes the dispersion of plume material that reaches the ground directly from the source via downdrafts. The indirect source is included to treat the first interaction of the "updraft" plume with the elevated inversion - that is, for plume sections that initially rise to the CBL top in updrafts and return to the ground via downdrafts. Image sources are added to treat the subsequent plume interactions with the ground

and inversion and to satisfy the zero-flux conditions at $z = 0$ and at $z = z_i$. This source plays the same role as the first image source above z_i in the standard Gaussian model but differs in the treatment of plume buoyancy. For the indirect source, a modified reflection approach is adopted in which the vertical velocity is reflected at $z = z_i$, but an "indirect" source plume rise Δh_i is added to delay the downward dispersion of plume material from the CBL top. This is intended to mimic the lofting behavior. The penetrated source is included to account for material that initially penetrates the elevated inversion but subsequently can reenter the CBL via turbulent mixing of the plume and eventual re-entrainment into the CBL. Figure 13 illustrates the three-plume approach - a fundamental feature of AERMOD's convective model. In AERMOD, the total concentration (C_c) in the CBL is found by summing the contribution from the three sources. For the horizontal plume state, the C_c is given by

$$C_c\{x_r, y_r, z_r\} = C_d\{x_r, y_r, z_r\} + C_r\{x_r, y_r, z_r\} + C_p\{x_r, y_r, z_r\}, \qquad \textbf{(54)}$$

where C_d, C_r, and C_p are the contributions from the direct, indirect and penetrated sources, respectively. The total concentration for the terrain-following state has the form of eq. **(54)** but with z_r replaced by z_p.

The fraction f_p of the source material that remains trapped in the CBL is found from

$$\begin{aligned} f_p &= 0 && \text{if} \quad \Delta h_h < 0.5\Delta h_{eq} \\ f_p &= 1 && \text{if} \quad \Delta h_h > 1.5\Delta h_{eq} \\ f_p &= \frac{\Delta h_h}{\Delta h_{eq}} - 0.5 && \text{if} \quad 0.5\Delta h_{eq} < \Delta h_h > 1.5\Delta h_{eq} \end{aligned} \qquad \textbf{(55)}$$

where $\Delta h_h = z_i - h_s$, and Δh_{eq} is the equilibrium plume rise in a stable environment. The Δh_{eq} has the form Berkowicz et al. (1986)

$$\Delta h_{eq} = \left(2.6^3 P_s + (2/3)^3\right)^{1/3} \Delta h_h \quad \textbf{(56)}$$

where $P_s = F_b / u N_h^2 \Delta h_h^3$ is the penetration parameter, and the stack buoyancy flux (F_b), and Brunt-Vaisala frequency (N_h) are given respectively by

$$F_b = g w_s r_s^2 \frac{\Delta T}{T_s} \quad \textbf{(57)}$$

and

$$N_h = \left[\frac{g}{\theta\{z_i\}} \frac{\partial \theta}{\partial z}\bigg|_{z>z_i} \right]^{1/2}. \quad \textbf{(58)}$$

Here, u is the wind speed at stack height; g is the gravitational acceleration; w_s, r_s, and T_s are the stack exit velocity, radius, and temperature, respectively; and θ is the ambient potential temperature. The N_h in eq. **(58)** is based on the potential temperature gradient in the elevated stable layer, provided by AERMET, capping the CBL. In general, this layer is within z_i and z_i + 500 m.

5.2.1 Direct Source contribution to concentration calculations in the CBL

Following Weil et al. (1997), the concentration due to the direct plume is given by:

$$C_d\{x_r, y_r, z\} = \frac{Q f_p}{\sqrt{2\pi}\tilde{u}} F_y \cdot \sum_{j=1}^{2} \sum_{m=0}^{\infty} \frac{\lambda_j}{\sigma_{zj}} \left[\exp\left(-\frac{\left(z - \Psi_{dj} - 2mz_i\right)^2}{2\sigma_{zj}^2} \right) + \exp\left(-\frac{\left(z + \Psi_{dj} + 2mz_i\right)^2}{2\sigma_{zj}^2} \right) \right], \quad \textbf{(59)}$$

where

$$\Psi_{dj} = h_s + \Delta h_d + \frac{\overline{w}_j x}{u}, \qquad \textbf{(60)}$$

u is the wind speed at stack top, $F_y \left(= \frac{1}{\sqrt{2\pi}\sigma_y} \exp\left(\frac{-y^2}{2\sigma_y^2}\right)\right)$ the lateral distribution function with meander (discussed in Section 5.4), $\overline{w_j} = a_j w_*$ (a_j is defined below in eq. **(62)**, Δh_d is the direct source plume rise calculated from eq. **(91)**, and $z = z_r$ and z_p in the horizontal and terrain-following states, respectively. Here, Ψ_{dj} and σ_{zj} are the effective source height and vertical dispersion parameter corresponding to each of the two distributions in eq. **(53)**. The subscript j is equal to 1 for updrafts and 2 for downdrafts. The lateral and vertical dispersion parameters (σ_y and σ_{zj}), resulting from the combined effects of ambient, buoyancy-induced, and building-induced turbulence are calculated as discussed in Sections 5.5.1.1 and 5.5.1.2 respectively. Here, σ_{zj} (with j = 1 or 2) is the vertical dispersion parameter corresponding to each of the Gaussian distributions used in the bi-Gaussian pdf, (see Section 5.5.1.2) and λ_j, the weighting coefficient for each distribution in eq. **(53)**, is calculated from Weil et al. (1997) as

$$\begin{aligned} \lambda_1 &= +\frac{\overline{w}_2}{\overline{w}_2 - \overline{w}_1} = +\frac{a_2}{a_2 - a_1} \\ \lambda_2 &= -\frac{\overline{w}_1}{\overline{w}_2 - \overline{w}_1} = -\frac{a_1}{a_2 - a_1} \end{aligned} \qquad \textbf{(61)}$$

where

$$\begin{aligned} a_1 &= \frac{\widetilde{\sigma}_{wT}}{w_*}\left(\frac{\alpha S}{2} + \frac{1}{2}\left(\alpha^2 S^2 + \frac{4}{\beta}\right)^{1/2}\right) \\ a_2 &= \frac{\widetilde{\sigma}_{wT}}{w_*}\left(\frac{\alpha S}{2} - \frac{1}{2}\left(\alpha^2 S^2 + \frac{4}{\beta}\right)^{1/2}\right) \end{aligned} \qquad \textbf{(62)}$$

.

Recall that $\widetilde{\sigma}_{wT}$ is the total effective vertical turbulence and is calculated from eq. **(34)**. The parameters appearing in eq. **(62)** are given by

$$\begin{aligned} \frac{\overline{w}^3}{w_*^3} &= 0.125 \qquad\qquad for \quad H_p\{x\} \geq 0.1 z_i \\ \frac{\overline{w}^3}{w_*^3} &= 1.25 \frac{H_p\{x\}}{z_i} \qquad for \quad H_p\{x\} < 0.1 z_i \end{aligned} \tag{63}$$

where,

$$\begin{aligned} \alpha &= \frac{1+R^2}{1+3R^2} \\ \beta &= 1+R^2 \\ S &= \frac{\overline{w}^3 / w_*^3}{\left(\widetilde{\sigma}_{wT}/w_*\right)^3} \equiv Skewness\ \ factor, \end{aligned} \tag{64}$$

and R is assumed to be 2.0 (Weil et al., 1997). Likewise, the term $\overline{w_j}\ x/u$ in eq. **(60)** follows from the F_z derivation and the w_j appearing in the bi-Gaussian form (see discussion of eq. **(53)**). The lateral dispersion parameter ($\sigma_{y,}$) is calculated from eq. **(75)** (Weil et al., 1997).

In eq. **(59)**, an image plume is used to satisfy the no-flux condition at the ground, i.e., an image plume from a source at $z = -h_s$, which results in the exponential terms containing $z + \Psi_{dj}$ on the right-hand side of eq. **(59)**. This image source results in a positive flux of material at $z = z_i$, and additional image sources are introduced at $z = 2\ z_i + h_s$, $-2\ z_i - h_s$, $4z_i + h_s$, $-4z_i - h_s$, etc. to satisfy all the subsequent no-flux conditions occurring at $z = 0$ and z_i.

5.2.2 Indirect Source contribution to concentration calculations in the CBL

The concentration due to the indirect source is calculated from:

$$C_r\{x_r, y_r, z\} = \frac{Qf_p}{\sqrt{2\pi}\,\tilde{u}} \cdot F_y \cdot \sum_{j=1}^{2} \sum_{m=1}^{\infty} \frac{\lambda_j}{\sigma_{zj}} \left[\exp\left(-\frac{\left(z + \Psi_{rj} - 2mz_i\right)^2}{2\sigma_{zj}^2} \right) + \exp\left(-\frac{\left(z - \Psi_{rj} + 2mz_i\right)^2}{2\sigma_{zj}^2} \right) \right] \quad \textbf{(65)}$$

where $\Psi_{rj} = \Psi_{dj} - \Delta h_i$, and z is either z_r (for the horizontal plume state) or z_p (for the terrain-following state). As shown in Figure 13, the indirect plume is modeled as a reflected version of the direct plume with an adjustment (Δh_i - calculated from eq. **(92)**) to the reflected plume height to account for the delay in vertical mixing due to plume lofting at the top of the boundary layer.

5.2.3 Penetrated source contribution to concentration calculations in the CBL

For the penetrated source the concentration expression has a Gaussian form in both the vertical and lateral directions. The concentration due to this source is given by:

$$C_p\{x_r, y_r, z\} = \frac{Q\left(1 - f_p\right)}{\sqrt{2\pi}\;\tilde{u}\,\sigma_{zp}} F_y \cdot \sum_{m=-\infty}^{\infty} \left[\exp\left(-\frac{\left(z - h_{ep} + 2mz_{ieff}\right)^2}{2\sigma_{zp}^2} \right) + \exp\left(-\frac{\left(z + h_{ep} + 2mz_{ieff}\right)^2}{2\sigma_{zp}^2} \right) \right] \quad \textbf{(66)}$$

where z_{ieff} is the height of the upper reflecting surface in a stable layer (see Section 5.3) and z is either z_r for the horizontal plume state or z_p for the terrain-following state. The vertical dispersion parameters (σ_{zp}) are calculated as described in Section 5.5.1.2.

The penetrated plume height, h_{ep}, is taken as the height of the plume centroid above the mixed layer and is calculated from eq. **(94)**.

5.3 Concentrations in the SBL

For stable conditions, the AERMOD concentration expression (C_s in eq. **(48)**) has the Gaussian form and is similar to that used in many other steady-state plume models (e.g., HPDM (Hanna and Paine 1989)). The C_s is given by

$$C_s\{x_r, y_r, z\} = \frac{Q}{\sqrt{2\pi}\tilde{u}\,\sigma_{zs}} \cdot F_y \cdot \sum_{m=-\infty}^{\infty} \left[\exp\left(-\frac{\left(z - h_{es} - 2mz_{ieff}\right)^2}{2\sigma_{zs}^2} \right) + \exp\left(-\frac{\left(z + h_{es} + 2mz_{ieff}\right)^2}{2\sigma_{zs}^2} \right) \right], \qquad \textbf{(67)}$$

where z_{ieff} is the effective mechanical mixed layer height, σ_{zs} is the total vertical dispersion in the SBL (see discussion in Section 5.5), and h_{es} is the plume height (i.e., stack height plus the plume rise - see Section 5.6.2).

Above the mechanical mixed layer height, z_{im} (eq. **(26)**), the turbulence level is generally expected to be small and thus supports little vertical mixing of the plume. AERMOD is designed (in the SBL) with an effective mixing lid, z_{ieff}, that retards but does not prevent plume material from spreading into the region above the estimated mechanical mixed layer. When the final plume height is well below z_{im}, the plume does not interact with z_{im}. When the plume is below z_{im} yet the "upper edge" (plume height plus 2.15 σ_{zs}) of the stabilized plume reaches z_{im}, the effective mixing lid is allowed to increase and remain at a level near the upper edge of the plume. In this way, AERMOD allows the plume to disperse downwards, but where the turbulence aloft is low, vertical plume growth is limited by an effective reflecting surface that is folding back only the extreme tail of the vertical plume distribution. There is no strong concentration doubling effect as occurs with reflections from an assumed hard lid. Downward dispersion is primarily a factor of σ_w averaged from the receptor to the plume height. If the plume height is above the mixed layer height, the calculation of the effective σ_w will include regions in which σ_w is likely to be small. This, in effect, retards plume growth by an amount dependent upon how much of the plume is above z_{im}. Therefore, whether the plume is above or

below z_{im}, the region of low turbulence above z_{im} will have an appropriate effect on the concentration distribution within the mixing layer.

When the plume buoyancy carries the rising plume into the relatively non-turbulent layer above z_{im}, the reflecting surface is still placed at 2.15 σ_{zs} above the effective plume height because there will be plume spread due to plume buoyancy and downward mixing is still important. Therefore, in the SBL, plume material is assumed to reflect off an elevated surface which is defined as:

$$z_{ieff} = MAX\left[\left(h_{es} + 2.15\sigma_{zs}\{h_{es}\};\ z_{im}\right)\right]. \qquad \textbf{(68)}$$

where σ_{zs} in eq. **(68)** is determined from equations found in Section 5.5.1.2 with σ_{wT} and u evaluated at h_{es}; not as an effective parameter. It is important to note that z_{ieff} depends on downwind distance since σ_{zs} is distance dependent. In fact, as eq. **(68)** suggests, this effective reflecting surface is only folding back the extreme tail of the upward distribution. Also, if the height of the receptor $z_r \geq z_{ieff}$ then the effective reflecting surface is not considered. This approach is also implemented for the penetrated source. For the penetrated and injected sources z_{ieff} is calculated using eq. **(68)** with σ_{zs} and h_{es} replaced by σ_{zp} and h_{ep} respectively.

5.4 Treatment of lateral plume meander

In AERMOD we include the effect that lower-frequency, non-diffusing eddies (i.e., meander) have on plume concentration. Meander (or the slow lateral back and forth shifting of the plume) decreases the likelihood of seeing a coherent plume after long travel times. This effect on plume concentration could best be modeled with a particle trajectory model, since these models estimate the concentration at a receptor by counting the number of times a particle is seen in the receptor volume. However, as a simple steady state model, AERMOD is not capable of producing such information. AERMOD accounts for meander by interpolating

between two concentration limits: the coherent plume limit (which assumes that the wind direction is distributed about a well-defined mean direction with variations due solely to lateral turbulence) and the random plume limit, (which assumes an equal probability of any wind direction).

For the coherent plume, the horizontal distribution function (F_{yC}) has the familiar Gaussian form:

$$F_{yC} = \frac{1}{\sqrt{2\pi}\sigma_y} \exp\left(\frac{-y^2}{2\sigma_y^2}\right), \quad \textbf{(69)}$$

where σ_y is the lateral dispersion parameter (see Section 5.5). For the random plume limit, the wind direction (and plume material) is uniformly distributed through an angle of 2π. Therefore, the horizontal distribution function F_{yR} takes the simple form:

$$F_{yR} = \frac{1}{2\pi x_r}, \quad \textbf{(70)}$$

where x_r is radial distance to the receptor. Although the form of the vertical distribution function remains unchanged for the two plumes, its magnitude is based on downwind distance for the coherent plume and radial distance for the random plume.

Once the two concentration limits (C_{Ch} - coherent plume; C_R - random plume) have been calculated, the total concentration for stable or convective conditions ($C_{c,s}$) is determined by interpolation. Interpolation between the coherent and random plume concentrations is accomplished by assuming that the total horizontal "energy" is distributed between the wind's mean and turbulent components. That is,

$$C_{c,s} = C_{Ch}\left(1 - \sigma_r^2 / \sigma_h^2\right) + C_R\left(\sigma_r^2 / \sigma_h^2\right), \qquad \textbf{(71)}$$

where σ_h^2 is a measure of the total horizontal wind energy and σ_r^2 is a measure of the random component of the wind energy. Therefore, the ratio σ_r^2/σ_h^2 is an indicator of the importance of the random component and can therefore be used to weight the two concentrations as done in eq. **(71)**.

The horizontal wind is composed of a mean component $\overline{u}$, and random components σ_u and σ_v. Thus, a measure of the total horizontal wind "energy" (given that the alongwind and crosswind fluctuations are assumed equal i.e., $\sigma_u = \sigma_v$), can be represented as

$$\sigma_h^{\ 2} = 2\widetilde{\sigma}_v^{\ 2} + \overline{u}^2, \qquad \textbf{(72)}$$

where $\overline{u} = (\tilde{u}^2 - 2\tilde{\sigma}_v^2)^{1/2}$. The random energy component is initially $2\tilde{\sigma}_v^2$ and becomes equal to σ_h^2 at large travel times from the source when information on the mean wind at the source becomes irrelevant to the predictions of the plume's position. The evolution of the random component of the horizontal wind energy can be expressed as

$$\sigma_r^2 = 2\tilde{\sigma}_v^2 + \overline{u}^2\left(1 - \exp\left({}^{-x_r}/_{\tilde{u}T_r}\right)\right), \qquad \textbf{(73)}$$

where T_r is a time scale (= 24 hrs) at which mean wind information at the source is no longer correlated with the location of plume material at a downwind receptor. Analyses involving autocorrelation of wind statistics (Brett and Tuller 1991) suggest that after a period of approximately one complete diurnal cycle, plume transport is "randomized." Equation **(73)** shows that at small travel times, $\sigma_r^2 = 2\tilde{\sigma}_v^2$, while at large times (or distances) $\sigma_r^2 = 2\tilde{\sigma}_v^2 + \overline{u}^2$, which is the total horizontal kinetic energy (σ_h^2) of the fluid. Therefore, the relative contributions of the coherent and random horizontal distribution functions (eq. **(71)**) are based on

the fraction of random energy contained in the system (i.e., σ_r^2/σ_h^2).

The application of eq. **(71)** is relatively straight forward in the SBL. Since concentrations in the SBL are represented as a single plume, C_s can be calculated directly from eq. **(71)**. By contrast, for convective conditions the situation is complicated by the inclusion of plume penetration. Since σ_r^2 depends on the effective parameters (eq. **(73)**), the concentration weighting factors found in eq. **(71)** will be different for the non-penetrated and penetrated plumes of the CBL. This is handled by combining the penetrated and non-penetrated weighting factors ($\sigma_r^2/\sigma_h^2|_P$ and $\sigma_r^2/\sigma_h^2|_{NP}$) into a single effective factor ($\sigma_r^2/\sigma_h^2|_{CBL}$). That is,

$$\left.\sigma_r^2/\sigma_h^2\right|_{CBL} = f_p \cdot \left.\sigma_r^2/\sigma_h^2\right|_P + \left(1-f_p\right)\cdot \left.\sigma_r^2/\sigma_h^2\right|_{NP}, \qquad \textbf{(74)}$$

where f_p (see eq. **(55)**) is the fraction of the source material that remains trapped in the CBL. Using eq. **(74)**, concentrations in the CBL (C_c) are calculated from eq. **(71)** with (σ_r^2/σ_h^2) replaced by $(\sigma_r^2/\sigma_h^2|_{CBL})$.

5.5 Estimation of dispersion coefficients

The overall standard deviations ($\sigma_{y,z}$) of the lateral and vertical concentration distributions are a combination of the dispersion (represented by σ_{ya}, σ_{za}) resulting from ambient turbulence, and dispersion (σ_b) from turbulence induced by plume buoyancy. Building induced dispersion is not included here since a separate approach (see Section 5.5.3) is taken for situations in which building wake effects contribute to the total dispersion. Dispersion induced by ambient turbulence is known to vary significantly with height, having its strongest variation near the earth's surface. Unlike present regulatory models, AERMOD has been designed to account for the effect of variations of turbulence with height on dispersion through its use of "effective parameters" (see Section 4.2), which are denoted by an overscript tilde, e.g., $\tilde{\sigma}_{wT}$.

AERMOD treats vertical dispersion from ambient turbulence (σ_{za}) as a combination of a specific treatment for surface dispersion and the more traditional approach based on Taylor (1921) for elevated dispersion. Using this approach, good agreement with observations was achieved in the SBL. However, the results in the CBL indicated that the treatment of lateral dispersion near the surface was problematic. This problem was corrected through the development of an empirical relationship for σ_{ya} near the surface using the full (CBL and SBL) Prairie Grass data set. A description of the resulting formulations for σ_{ya} and σ_{za} is presented in the next section.

The approach used to combine the above contributions to dispersion assumes that the effects are independent of one another. Thus, the total dispersion coefficients, for situations that do not include building downwash effects, are calculated from the following general expression (Pasquill and Smith 1983):

$$\sigma_{y,z}^2 = \sigma_{ya,za}^2 + \sigma_b^2, \qquad \textbf{(75)}$$

where the subscripts y and z are deleted from σ_b because σ_{yb} is assumed equal to σ_{zb}. With the exception of the CBL's penetrated source the form of eq. **(75)** applies to all source dispersion in both the CBL and SBL such that $\sigma_{y,z}$ becomes $\sigma_{ys,zs}$ and $\sigma_{yjs,zj}$ and $\sigma_{ya,za}$ becomes $\sigma_{yas,zas}$ and $\sigma_{yajs,zaj}$ for the SBL and CBL, respectively. For the penetrated source, the total dispersion is assumed to include ambient and buoyancy induced turbulence only; building wakes are assumed to have little influence. For the injected source, the total dispersion is calculated as if the source were in the SBL.

A comment on notation: eq. **(75)** applies for both lateral and vertical dispersion in the SBL and CBL. In references to the SBL, σ_z appears as σ_{zs} in the dispersion equation; σ_{za} appears as σ_{zas}. In reference to the CBL, σ_z appears as σ_{zj} for the dispersion expression applicable to the

direct and indirect sources and σ_{za} appears as σ_{aj}; for the penetrated source σ_z appears as σ_{zp} in the dispersion expression.

5.5.1 Dispersion from ambient turbulence

5.5.1.1 Lateral dispersion from ambient turbulence

In general terms, the ambient component of the lateral dispersion is based upon Taylor (1921) such that:

$$\sigma_{ya} = \frac{\tilde{\sigma}_v \, x}{\tilde{u}\left(1 + \frac{x/\tilde{u}}{2T_{Ly}}\right)^p}, \qquad \textbf{(76)}$$

where $p = 0.5$, u is the wind speed, σ_v is the root-mean-square lateral turbulence velocity, and T_{Ly} is the Lagrangian integral time for the lateral turbulence. Application of eq. **(76)** in a preliminary version of AERMOD yielded poor concentration estimates in comparison to those found in the Prairie Grass field experiments (Barad 1958). Specifically, the lateral spread was not well matched. Therefore, the lateral dispersion expression was reformulated to allow for an empirical fit to the Prairie Grass data.

Using an approach similar to that of Venkatram et al. (1984), T_{Ly} is found to be l/σ_v where l is an appropriate length scale for lateral turbulence. Equation **(76)** can be written in terms of the non-dimensional downwind distance X and a non-dimensional height scale α as:

$$\sigma_{ya} = \frac{\tilde{\sigma}_v x}{\tilde{u}\left(1 + \alpha X\right)^p} \qquad \textbf{(77)}$$

where $X(= \tilde{\sigma}_v \, x/\tilde{u}zi \,)$ is the non-dimensional distance with u and σ_v given by effective parameters, where $\alpha = z_i / l$, and z_i is the mixed layer height.

Based on a preliminary comparison of σ_{ya} (eq. **(77)**) with selected stable and convective cases from the Prairie Grass experiment (Barad 1958), α was found equal to 78 and p equal to 0.3. As such, α is treated as a fitting parameter. In later comparisons against the full Prairie Grass data set (Figure 16), eq. **(77)** tended towards the lower envelope of this widely scattered data (i.e., lateral dispersion estimates are on the lower end of the distribution of measurements). However, the preliminary values of α (= 78) and p (= 0.3) produced good agreement between AERMOD concentration predictions and observations (Brode 2002). Therefore, these preliminary values were retained in AERMOD, and eq. **(77)** applies for the calculation of σ_{ya} for all plumes in both the SBL and CBL.

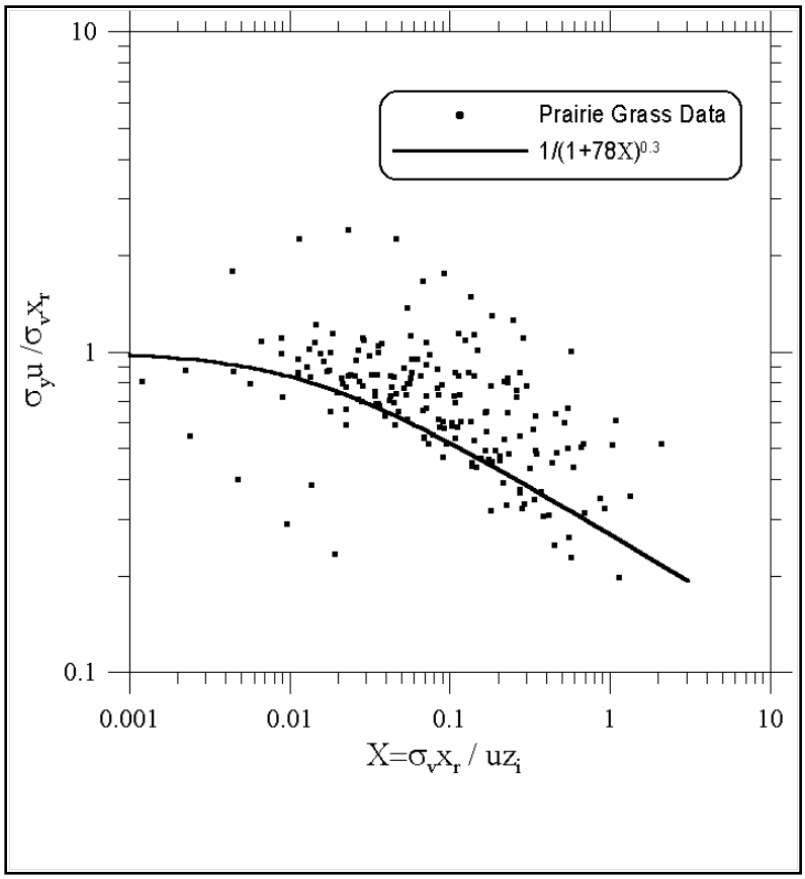

Figure 16. Lateral spread (Fy) as a function of non-dimensional distance (X). The data is taken from the Prairie Grass experiment (Barad, 1958).

The ambient component of the lateral dispersion for the penetrated source, i.e. a source which has been released below z_i, but penetrates above, is calculated using eq. **(77)** with h_{es} set equal to h_{ep} (the height of the penetrated source). However, for the injected source, i.e. source released above z_i, no substitution is needed since these sources are modeled as a stable source.

To account for the increase in the turbulence length scale and hence the Lagrangian time scale with release heights greater than that at Prairie Grass, α is scaled as follows:

$$\alpha = 78\left(z_{PG} \Big/ z_{\max}\right), \qquad \textbf{(78)}$$

where z_{PG} = 0.46 m (Prairie Grass release height), and $z_{max} = \max(z; z_{PG})$. To insure that α does not become unrealistically large for surface releases, z is not allowed below z_{PG} (i.e., 0.46 m). In the SBL, $z = h_{es}$; in the CBL $z = h_s$; for penetrated sources, $z = h_{ep}$. As α becomes small for large release heights, σ_{ya} would tend to grow linearly with downwind distance.

5.5.1.2 Vertical dispersion from ambient turbulence

For sources in the SBL (and for sources in the CBL that are emitted directly into the stable layer above the mixed layer), the ambient portion of the vertical dispersion (σ_{zas}) is composed of an elevated (σ_{zes}) and near-surface (σ_{zgs}) component. For $h_{es} < z_i$ simple interpolation provides a smooth transition between the two components.

$$\sigma_{zas} = \left(1 - \frac{h_{es}}{z_i}\right)\sigma_{zgs} + \left(\frac{h_{es}}{z_i}\right)\sigma_{zes}. \qquad \textbf{(79)}$$

For $h_{es} \geq z_i$ σ_{zas} is set equal to σ_{zes}. The expressions for calculating h_{es} are found in Section 5.6.2. It should be noted, for sources in the SBL, that σ_{zas} is the specific form of the ambient portion of the vertical dispersion (i.e., σ_{za} in eq. **(75)**).

In the SBL, the elevated portion of the vertical dispersion follows the form of eq. **(76)**:

$$\sigma_{zes} = \widetilde{\sigma}_{wT}\left(x/\widetilde{u}\right) \Bigg/ \left(1 + \frac{x/\widetilde{u}}{2T_{Lzs}}\right)^{1/2}, \qquad \textbf{(80)}$$

where σ_{wT} is the vertical turbulence due to the mechanical mixing (Cimorelli et al., 2004).

As with the lateral component, the Lagrangian time scale (T_{Lzs}) for the vertical turbulence can be written in the form (Venkatram et al. 1984)

$$T_{Lzs} = \frac{l}{\widetilde{\sigma}_{wT}} \quad . \tag{81}$$

The length scale l is an interpolation between the limiting length scales for neutral conditions and stable conditions

$$\frac{1}{l} = \frac{1}{l_n} + \frac{1}{l_s}. \tag{82}$$

where $l_n = 0.36\, h_{es}$ and $l_s = 0.27\ \tilde{\sigma}_{wT}/N$. Under very stable conditions or at large heights, l approaches l_s. When conditions are near neutral, N is very small and l approaches l_n.

By combining equations **(80)**, **(81)**, and **(82)** we find the following expression that is used by AERMOD to compute σ_{zes}, the elevated portion of the vertical dispersion for the stable source:

$$\sigma_{zes} = \frac{\widetilde{\sigma}_{wT}\, t}{\left[1 + \frac{\widetilde{\sigma}_{wT}\, t}{2}\left(\frac{1}{0.36 h_{es}} + \frac{N}{0.27\widetilde{\sigma}_{wT}}\right)\right]^{1/2}}. \tag{83}$$

Finally, to complete the description of eq. **(79)**, the surface portion of vertical dispersion (σ_{zgs}) in the SBL, is calculated from Venkatram (1992) as

$$\sigma_{zgs} = \sqrt{\frac{2}{\pi}}\left(\frac{u_* x}{\widetilde{u}}\right)\left(1 + 0.7\frac{x}{L}\right)^{-1/3} \quad . \tag{84}$$

For the direct and indirect sources in the CBL, the ambient portion of the vertical

dispersion (σ_{za} of eq. **(75)**) is denoted as σ_{zaj} (j = 1, 2) to distinguish between updrafts and downdrafts. σ_{zaj} is composed of an elevated (σ_{zej}) and surface (σ_{zg}) portion and is given by

$$\sigma_{zaj}^2 = \sigma_{zej}^2 + \sigma_{zg}^2, \qquad \textbf{(85)}$$

where the elevated portion (σ_{zej}) is obtained from Weil et al. (1997) as

$$\sigma_{zej} = \alpha_b \frac{\sigma_{wj}\, x}{\tilde{u}}, \qquad \textbf{(86)}$$

where σ_{wj} is a parameter in the bi-Gaussian pdf (eq. **(53)**).

The expression $\alpha_b = \min(0.6 + 4H_p/z_i, 10.0)$ designed to be 1.0 above the surface layer ($H_p > 0.1\ z_i$) and to otherwise match Venkatram's (1992) result for vertical dispersion from a surface source in a neutral boundary layer.

For the CBL, the vertical dispersion from a source within the surface layer ($H_p\{x\} < 0.1\ z_i$) is parameterized by

$$\sigma_{zg} = b_c\left(1 - 10\left(H_p / z_i\right)\right)\cdot\left(u_* / \tilde{u}\right)^2 \cdot\left(x^2 / |L|\right), \qquad \textbf{(87)}$$

where $b_c = 0.5$, u_* is the friction velocity, and L is the Monin-Obukhov length; above the surface layer ($H_p > 0.1 z_i$), σ_{zg} is assumed to equal zero. In the limit of a surface release ($H_p = 0$), the parameterization of eq. **(87)** follows the form suggested by Venkatram (1992) for vertical dispersion in the unstable surface layer; i.e., $\sigma_z \propto (u_*/\tilde{u})^2 x^2/|L|$. The parameterization is designed to: 1) agree with Venkatram's result in the limit of a surface release, 2) provide good agreement between the modeled and observed concentrations from the Prairie Grass experiment

(Perry et al., 2005), and 3) decrease with source height in the surface layer and ultimately vanish for above the surface layer. The constant b_c was chosen to satisfy the second design requirement. In the limit of a neutral boundary layer σ_{zg} is equal to zero.

The total vertical dispersion for the penetrated source σ_{zp} (= σ_z in eq. **(75)**) is a combination of both ambient and buoyancy effects. The ambient portion of the vertical dispersion for the penetrated source contains only an elevated component σ_{zes} (= σ_{zss}) since it is assumed to be decoupled from the ground surface by its location above z_i and therefore unaffected by the underlying surface. The ambient vertical dispersion for the penetrated source is computed as the elevated portion of a stable source (σ_{zes} of eq. **(83)**) with $N = 0$ and with no contribution from the surface component. The Brunt-Vaisala frequency, N, is set to zero because the penetrated plume passes through the well mixed layer (where $N \approx 0$) prior to dispersing to receptors within the mixed layer.

5.5.2 Buoyancy induced dispersion (BID) component of σ_y and σ_z

For all plumes, the buoyancy induced dispersion (BID) is calculated following Pasquill (Pasquill 1976) and Weil (1988b) as

$$\sigma_b = \frac{0.4\Delta h}{\sqrt{2}}, \qquad \textbf{(88)}$$

where Δh is the plume rise appropriate for each of the plume types (direct, indirect, penetrated, and stable plumes). The direct source plume rise is calculated from eq. **(91)**, stable plume rise (Δh_s) is calculated from eq. **(95)** and the plume rise for the penetrated source $\Delta h_p = h_{ep} - h_s$ where h_{ep} is calculated from eq. **(94)**).

5.5.3 Treatment of building downwash

AERMOD incorporates the Plume Rise Model Enhancements (PRIME) (Schulman et al. 2000) algorithms for estimating enhanced plume growth and restricted plume rise for plumes affected by building wakes (U.S. EPA, 1995). PRIME partitions plume mass between a cavity recirculation region and a dispersion enhanced wake region based upon the fraction of plume mass that is calculated to intercept the cavity boundaries. These boundaries are established from estimates of the locations of the lateral and vertical separation streamlines. Dispersion of the recirculated cavity mass is based on building geometry and is assumed to be uniformly mixed in the vertical. At the boundary of the cavity region, cavity mass is emitted into the wake region. Here, it is combined with plume mass that was not captured by the cavity and dispersed at an enhanced rate based on source location, release height and building geometry. The enhancement of turbulence within the wake decays gradually with distance, allowing for a smooth transition to ambient levels of turbulence in the far-field. A probability density function model and an eddy diffusivity model (Weil 1996) are used for dispersion estimates in the near-wake and far-wake regions, respectively. Plume rise, for sources influenced by a building, is estimated using a numerical model that includes effects from streamline deflection near the building, vertical wind speed shear, enhanced dilution from the turbulent wake and velocity deficit. In general, these building induced effects act to restrict the rise that the plume would have in the absence of the building.

PRIME was originally designed (Schulman et al., 2000) to enhance plume growth using Pasquill Gifford (PG) dispersion (Pasquill 1961; Gifford 1961). AERMOD's estimate of plume growth is based on dispersion parameters derived from profiles of turbulence (see Section 4), not from radiation base turbulence surrogates as is done in the PG approach. A basic design tenet for incorporating PRIME into AERMOD was to be as faithful as possible to the PRIME formulation while ensuring that 1) AERMOD's ambient dispersion was used in place of PG dispersion and 2) far beyond the wake region, where building influences should be insignificant, concentrations approach the AERMOD estimate. Therefore, within the wake, PRIME

algorithms are used exclusively to calculate concentration with AERMOD-derived ambient turbulent intensities as input. To ensure a smooth transition between concentrations estimated by PRIME, within the wake, and AERMOD estimates in the far field, concentrations beyond the wake are estimated as the weighted sum of the two calculations. That is, beyond the wake the total concentration (C_{total}) is calculated as follows:

$$C_{Total} = \gamma\, C_{\mathrm{Pr}\,ime} + \left(1-\gamma\right) C_{AERMOD} \qquad \textbf{(89)}$$

where C_{prime} is the concentration estimated using the PRIME algorithms with AERMOD-derived meteorological inputs, C_{AERMOD} is the concentration estimated using AERMOD without considering building wake effects, and γ the weighting parameter. The weighting parameter, γ, is designed such that the contribution from the PRIME calculation decreases exponentially with vertical, lateral and downwind distance from the wake. It is calculated as follows:

$$\gamma = \exp\left(\frac{-\left(x-\sigma_{xg}\right)^2}{2\sigma_{xg}^2}\right)\exp\left(\frac{-\left(y-\sigma_{yg}\right)^2}{2\sigma_{yg}^2}\right)\exp\left(\frac{-\left(z-\sigma_{zg}\right)^2}{2\sigma_{zg}^2}\right) \qquad \textbf{(90)}$$

where x is the downwind distance from the upwind edge of the building to the receptor, y is the lateral (crosswind) distance from the building centerline to the receptor, z is the receptor height above ground, σ_{xg} is longitudinal dimension of the wake, σ_{yg} is the distance from the building centerline to lateral edge of the wake, and σ_{zg} is the height of the wake at the receptor location.

5.6 Plume rise calculations in AERMOD

5.6.1 Plume rise in the CBL

The plume rise for the direct source is given by the superposition of source momentum and buoyancy effects following Briggs (1984).

$$\Delta h_d = \left(\frac{3F_m x}{\beta_1^2 u_p^2} + \frac{3}{2\beta_1^2} \cdot \frac{F_b x^2}{u_p^3} \right)^{1/3} \quad \textbf{(91)}$$

where $F_m = (T/T_s) w_s^2 r_s^2$ the stack momentum flux, $F_b = g w_s r_s^2 (\Delta T/T_s)$ is the stack buoyant flux, r_s is the stack radius corrected for stack tip downwash, and β_1 (= 0.6) is an entrainment parameter. It should be noted that u_p is the wind speed used for calculating plume rise. In the CBL u_p is set equal to $u\{h_s\}$.

As shown in Figure 13, the indirect plume, which is included to treat the no flux condition at $z = z_i$, is modeled as a reflected version of the direct plume with an adjustment (Δh_i) to the reflected plume height to account for the delay in vertical mixing due to plume lofting at the top of the boundary layer. That height adjustment is given by

$$\Delta h_i = \left(\frac{2F_b z_i}{\alpha_r u_p r_y r_z} \right)^{1/2} \frac{x}{u_p}, \quad \textbf{(92)}$$

where r_y and r_z are the lofting plume half-widths in the lateral and vertical directions, u_p is the wind speed used for plume rise, and α_r = 1.4. The product of crosswind dimensions of the assumed elliptical plume is calculated from Weil et al. (1997) as

$$r_y r_z = r_h^2 + \frac{a_e \lambda_y^{3/2}}{4} \cdot \frac{w_*^2 x^2}{u_p^2}, \quad \textbf{(93)}$$

where $r_h = \beta_2 (z_i - h_s)$, β_2 = 0.4, λ_y = 2.3, and a_e = 0.1 (dimensionless entrainment parameter). For a derivation and discussion of Δh_i see Weil et al. (1997).

The height that the penetrated source achieves above z_i is calculated as the equilibrium plume rise in a stratified environment and is determined by the source buoyancy flux, the stable stratification above z_i, and the mean wind speed. In line with Weil et al. (1997), the penetrated source plume height, h_{ep}, is taken as the centroid of plume material above the inversion. For complete penetration ($f_p = 0$) $h_{ep} = h_s + \Delta h_{eq}$. However, for partial penetration ($f_p > 0$), h_{ep} is chosen as the average of the heights of the upper plume edge $h_s + 1.5\ \Delta h_{eq}$ and z_i, or

$$h_{ep} = \frac{h_s + z_i}{2} + 0.75\Delta h_{eq}. \qquad \textbf{(94)}$$

where Δh_{eq} is defined in eq. **(56)**.

5.6.2 Plume rise in the SBL

Plume rise in the SBL is taken from Weil (1988b), which is modified by using an iterative approach which is similar to that found in Perry et al. (1989). When a plume rises in an atmosphere with a positive potential temperature gradient, plume buoyancy decreases because the ambient potential temperature increases as the plume rises; thus, plume buoyancy with respect to the surroundings decreases. To account for this, the plume rise equations have been modified. With this modification, AERMOD computes stable plume rise, Δh_s, from Weil et al. (1988b) as

$$\Delta h_s = 2.66\left(\frac{F_b}{N^2 u_p}\right)^{1/3}\cdot\left[\frac{N' F_m}{F_b}\sin\left(\frac{N' x}{u_p}\right)+1-\cos\left(\frac{N' x}{u_p}\right)\right]^{1/3}, \qquad \textbf{(95)}$$

where $N' = 0.7N$ with N given by eq. **(58)**. N and u are evaluated initially at stack height. Once plume rise has been computed, subsequent plume rise estimates are made (iteratively until convergence) by averaging the u and N values at stack top with those at $h_S + \Delta h_S/2$. Equation **(95)** is used for downwind distances that are less than the distance to final rise (x_f). Beyond x_f, Δh_s remains constant. The distance at which the stable plume reaches its maximum rise is given by

$$x_f = \frac{u_p}{N'}\arctan\left(\frac{-F_m N'}{F_b}\right). \qquad \textbf{(96)}$$

Upon substituting eq. **(95)** for x in eq. **(97)** the maximum final rise of the stable plume $\Delta h_s\{x_f\}$ reduces to:

$$\Delta h_s\{x_f\} = 2.66\left(\frac{F_b}{u_p N^2}\right)^{1/3}. \qquad \textbf{(97)}$$

As with eq. **(95)**, the velocity, u_p, and N in eq. **(97)** are evaluated initially at stack height and then iteratively.

When the atmosphere is close to neutral, the Brunt Vaisala frequency, N, is close to zero, and eq. **(95)** can predict an unrealistically large plume rise. Under, these circumstances, plume rise is limited by atmospheric turbulence. This happens when the rate of plume rise under neutral conditions is comparable to σ_w. Under these conditions, stable plume rise (eq. **(97)**) is limited by the neutral rise calculated from Weil (1985) as

$$\Delta h_s = 1.2\, L_n^{3/5}\left(h_s + 1.2\, L_n\right)^{2/5}, \qquad \textbf{(98)}$$

where the neutral length scale $L_n = F_b/(u_p u_*^2)$.

As the wind speed approaches zero, eq. **(95)** again predicts unrealistic values. In these near-calm conditions the stable plume rise (eq. **(97)**) is limited by the calm rise expression that is based on the work of Morton et al. (1956) and Briggs (1969) such that,

$$\Delta h_s = \frac{4 F_b^{1/4}}{N^{3/4}}. \qquad \textbf{(99)}$$

Finally, the stable plume rise is limited by a calculation of the unstable rise (see Section 5.6.1).

5.7 Source characterization

AERMOD gives the user the ability to characterize a source as either a point, a volume, an area, a roadway, or a buoyant line. Additionally, AERMOD has the capability of characterizing irregularly shaped area sources.

Point sources are characterized exactly as in the ISC3 model (U.S. EPA, 1995). The input to the model includes the location, elevation, emission rate, stack height, stack gas temperature, stack gas exit velocity, and stack inside diameter. The temperature, exit velocity, and diameter are required for plume rise calculations.

Similarly, volume sources require the same input as the ISC3 model. This includes the location, elevation height (optional), height of release, emission rate, the initial lateral plume size (σ_y) and initial vertical plume size (σ_z). AERMOD differs from ISC3 in the treatment of volume sources only in how the initial plume size is implemented. Where ISC3 uses the virtual source technique to account for initial plume size, AERMOD adds the square of the initial plume size to the square of the ambient plume size:

$$\sigma_y^2 = \sigma_{yl}^2 + \sigma_{yo}^2, \qquad \textbf{(100)}$$

where σ_{yo} is the initial horizontal plume size, σ_{yl} is the plume size before accounting for the initial size, and σ_y is the resultant plume size after accounting for the initial size.

The area source treatment is enhanced from that available in ISC3. In addition to being input as squares or rectangles, area sources may be input as circles or polygons. A polygon may be defined by up to 20 vertices. A circle is defined by inputting its center location and radius. The AERMOD code uses this information to create an equivalent, nearly circular polygon of 20 sides, with the same area as the circle. As with ISC3, AERMOD allows for the calculation of a simple half-life decay.

As was described in section 2.0, Model Overview, the buoyant line source algorithm from the Buoyant Line and Point Source (BLP) model (Schulman and Scire, 1980) was incorporated into AERMOD beginning with version 15181. The input to the model includes emission rate and average release height for individual lines, and average building length, average building height, average building width, average line source width, average building separation, and average buoyancy for the single source. Users should refer to the BLP User's Guide for a description of the formulation of the BUOYLINE source type in AERMOD.

The RLINE source type was added beginning with version 19191 to better characterize mobile source emissions (i.e., roadways). The RLINE source type is an adaptation of the Research Line (R-LINE) model (Snyder and Heist, 2013). The formulation of the RLINE source type was updated in version 23132 to harmonize the RLINE source type with other source types (POINT, AERA, and VOLUME) in AERMOD which also resulted in an update to the dispersion coefficients. For a complete description of the formulation of the RLINE source type in AERMOD, refer to Snyder and Heist (2013) and EPA (2023e).

5.8 Plume volume molar ration method (PVMRM)

PVMRM was first introduced in AERMOD in version 04300 as an option for modeling the conversion of NOx to NO2 in the presence of ozone. The implementation is based on the work of Hanrahan (1999) and adapted for AERMOD. Details regarding the formulation of the PVMRM option in AERMOD, and preliminary model evaluation results are available in U.S. EPA (2015).

5.8.1 Definition of plume volume

5.8.1.1 Total vs. relative dispersion

The PVMRM determines the conversion rate for NO_x to NO_2 based on a calculation of the NO_x moles emitted into the plume, and the amount of O_3 moles contained within the volume of the plume between the source and receptor. The dispersion algorithms in AERMOD and other steady-state plume models are based on the use of total dispersion coefficients, which are formulated to represent the time-averaged spread of the plume. A more appropriate definition of the volume of the plume for purposes of determining the ozone moles available for conversion of NOx is based on the instantaneous volume of the plume, which is represented using relative dispersion coefficients (Cole and Summerhays, 1979; Bange, 1991). The implementation of PVMRM in AERMOD is based on the use of relative dispersion coefficients to calculate the plume volume. Weil (1996 and 1998) has defined formulas for relative dispersion that are consistent with the AERMOD treatment of dispersion, and which can be calculated using meteorological parameters available within AERMOD.

5.8.1.2 Calculation of relative dispersion coefficients

The formula for relative dispersion combines the effects of buoyancy-induced turbulence, which should dominate close to the source, and ambient turbulence, which begins to dominate further downwind. Since the travel time from the source to the receptor is important for defining relative dispersion, the relative dispersion coefficients are calculated based on the radial distance from source to receptor. Weil (1996 and 1998) assumes relative dispersion (σ_r) to be isotropic, so that $\sigma_{rx} = \sigma_{ry} = \sigma_{rz} = \sigma_r$. The relative dispersion (σ_r) due to the combined effects of buoyancy- induced turbulence (σ_{rb}) and ambient turbulence (σ_{ra}) is parameterized as follows:

$$\sigma_r = (\sigma_{rb}^3 + \sigma_{ra}^3)^{1/3}. \quad \textbf{(101)}$$

The buoyancy-induced dispersion term, σ_{rb}, is calculated in AERMOD as

$$\sigma_{rb} = \frac{0.4\,\Delta h}{\sqrt{2}}, \quad \textbf{(102)}$$

where Δh is the plume rise. Relative dispersion due to ambient turbulence, σ_{ra}, is parameterized by

$$\sigma_{ra} = \frac{a_1 \varepsilon^{1/2} t^{3/2}}{1 + a_2 t / T_{Lr}}, \quad \textbf{(103)}$$

where a_1 is a constant (= 0.57), $a_2 = 0.62\ a_1$, t is the plume travel time (= x/U), and T_{Lr} is a Lagrangian time scale for relative dispersion defined as

$$T_{Lr} = a_{r1} \frac{z_i}{\sigma_w}, \quad \textbf{(104)}$$

where $a_{r1} = 0.46$, z_i is the mixing height, and σ_w is the vertical turbulence parameter. The turbulence dissipation rate, γ, is calculated as follows, based on Weil (1996):

$$\varepsilon = \frac{b\sigma_w^2}{T_{Lr}}, \quad \textbf{(105)}$$

where b is a constant (= 0.78). The values of wind speed (U) and σ_w used in eq. **(103)** through eq. **(105)** are the effective values, calculated as averages across the layer from the plume centroid height to the receptor height (up to $2.15\Phi_z$), following the procedure used in AERMOD to calculate effective values. Using the effective values of σ_w, AERMOD calculates effective values of the turbulence dissipation rate, γ.

Since the relative dispersion coefficients are source- and meteorology-dependent in AERMOD, the model generates a table of relative dispersion coefficients as a function of

distance for the dominant source for each receptor and each hour in order to complete the plume volume calculation.

The original PVMRM utilized the relative dispersion coefficients described above to define the plume volume. These relative dispersion coefficients are applicable to unstable/ convective conditions but are likely to overpredict the plume volume for stable conditions, resulting in overpredictions of NO_2 concentrations. The PVMRM algorithm was modified for version 15181 to use the "standard" total dispersion coefficients incorporated in AERMOD to define the plume volume during stable conditions.

5.8.1.3 Treatment of volume and area sources

If the dominant source is a volume source, then the initial lateral and vertical dimensions of the volume source are included in the calculation of the relative dispersion coefficients for purposes of calculating the plume volume, as follows:

$$\sigma_r = (\sigma_{rb}^3 + \sigma_{ra}^3 + \sigma_0)^{1/3}, \quad \textbf{(106)}$$

where σ_0 is the initial dispersion coefficient of the volume source calculated as $\sqrt{\sigma_{y0}\sigma_{z0}}$ based on the initial lateral (Φ_{y0}) and vertical (Φ_{z0}) dimensions input by the user. If a volume source is included among the major contributing sources, it is treated the same as a point source in defining the combined plume volume.

For application of PVMRM to area sources, the plume volume is extended laterally, if necessary, to include the projected width of the area source or sources that are included among the major contributing sources. The emissions from an area source are included in the calculation of the NO_x moles emitted into the plume if the centroid of the area source is within

the box defined by the along-wind and crosswind extent of major contributing sources. In addition, if an area source is the dominant source, then the relative dispersion coefficients are calculated based on the radial distance from the centroid of the area source to the receptor.

5.8.1.4 Defining extent of plume

The original implementation of PVMRM in AERMOD used four (4) times the relative dispersion coefficients to define the plume volume, which accounts for more than 99.99% of the plume. The original implementation also used a minimum value 5.0 m for the plume radius to account for near-source effects (e.g., downwash), which is consistent with the initial plume volume assumed by Hanrahan (1999). Given the fact that the PVMRM option in AERMOD assumes full and instantaneous mixing of the NO and O_3 within the plume, using such a large percentage of the plume volume may introduce a bias to overpredict ambient concentrations of NO_2. Beginning with version 16216, the PVMRM option uses 2.58 times the relative dispersion coefficients to define the plume volume for unstable conditions, which accounts for about 99% of the plume, and a minimum plume radius of 15.0 m. For stable conditions, the PVMRM option uses 1.282 times the total dispersion coefficients to define the plume volume, consistent with the original approach proposed by Hanrahan (1999), which accounts for about 80 percent of the plume volume, and minimum plume radius of 9.0 m. Since AERMOD incorporates a horizontal meander algorithm that increases lateral plume spread beyond that accounted for based on dispersion coefficients, the number of sigmas used to define the plume volume for stable conditions is adjusted to account for meander, i.e.,

$$NSUBZ = \min\left(2.15, 1{,}282 * \left(\frac{SYEFF}{SY}\right)\right),$$

where NSUBZ is the number of sigmas used to define the plume volume and SYEFF is the effective σ_y value that replicates the plume centerline associated with meander but based on a standard Gaussian plume calculation. An upper bound of 2.15 is applied, which corresponds with

the point at which the concentration is 10 percent of the centerline value and is used to define the extent of the plume in other contexts (e.g., initial dispersion coefficients for volume sources). The minimum value of the dispersion coefficient is also adjusted based on the ratio 1.282/NSUBZ, where NSUBZ is the adjusted value.

The original implementation of PVMRM used the radial distance from source to receptor to calculate the plume volume and the moles of NOx contained in the plume. Beginning with version 16216, the downwind distance is used to calculate these values. Use of the downwind distance provides a more realistic estimate of NOx conversion consistent with a straight-line, steady-state plume model, such as AERMOD.

5.8.1.5 Adaption for AERMOD terrain algorithm

The vertical dimension of the plume volume is based on the relative dispersion coefficient for the dominant source and the range in plume heights for the major contributing sources. Since the effective plume heights differ for the terrain following and terrain responding components, the vertical dimension was modified to calculate the range of plume heights separately for both the terrain following and terrain responding components, and then use a weighted value for the vertical dimension based on the terrain (plume state) weighting factor, f, defined in Section 5.1.

5.8.1.6 Treatment of penetrated plumes

For unstable conditions with partial or full plume penetration above the mixing height, z_i, separate relative dispersion coefficients are calculated for the penetrated portion of the dominant plume. For cases with partial penetration for the dominant plume, AERMOD calculates two plume volumes, one based on relative dispersion coefficients for the direct source and another based on the relative dispersion coefficients for the penetrated source. Since AERMOD uses the same dispersion coefficients for the direct and indirect sources, separate

values of relative dispersion coefficients for the indirect source are not needed. The effective plume volume used in the application of PVMRM is based on a weighted average of the direct and penetrated plume volumes using the Plume Penetration Factor (PPF) for the dominant source. The model stores the plume centroid heights for both the direct and penetrated plumes for all sources at each receptor, and these are used to incorporate the effect of the major contributing sources on the volumes for the direct and penetrated plumes.

5.8.2 Minimum ozone concentration for stable conditions

Based on the implementation of NO_2 conversion methods in ISCST3, AERMOD applies a limit to the minimum ozone. The AERMOD model first keeps track of the maximum ozone concentration over the previous 24 hours. If the Monin-Obukhov length is positive (i.e., stable), with a value of less than 50 meters (very stable), then the maximum ozone concentration over the previous 24 hours is used as the minimum value. If the Monin-Obukhov length is positive and the value is over 500 meters (nearly neutral), then no minimum ozone concentration is applied for that hour. If the Monin-Obukhov length is between 50 meters and 500 meters, then the minimum ozone concentration is determined by linear interpolation, i.e., the minimum value is calculated as O3MAX * (500 – L)/450, where O3MAX is the maximum ozone concentration over the previous 24 hours, and L is the Monin-Obukhov length in meters.

This approach is primarily applicable for tall stacks, where ozone concentrations aloft may be higher than surface measurements, as surface ozone will be titrated overnight by surface emissions of NO but can maintain daytime-high concentrations above the mixed layer. The option can be turned off via the NOMINO3 keyword, which will use the hourly measured ozone for NO conversion rather than the value computed as described above. The use of the NOMINO3 option may generally be applicable for surface releases and shorter stacks, where the plume heights are expected to be within the surface layer during typical nighttime conditions. As with all NO_2 conversion options, this option should be used in consultation with the appropriate reviewing authority.

5.9 Generic Reaction Set Method (GRSM)

The Generic Reaction Set Method (GRSM) was introduced into AERMOD as an ALPHA option in version 21112 and upgraded to a BETA option in version 22112 with additional updates in version 23132. Carruthers et al., 2017, document the development of a technique that accounts for the equilibrium between NO, NO_2, and ozone in the atmosphere called the Atmospheric Dispersion Model Method, ADMSM. The ADMSM uses similar calculations for plume entrainment as PVMRM but adds a "reaction rate" based on solar radiation and travel time from source to receptor. The reaction rate is based on the generic reaction set (GRS) chemistry scheme, which is a semi-empirical photochemical model developed originally by CSIRO in Australia (Azzi and Johnson, 1992; Venkatram et al., 1994) for multiple step conversions between NO, NO_2, and O_3 which limit NO conversion based on the available ozone.

Reaction rates are determined by three equations (see equations 4-8 in Carruthers et al., 2017):

$$d[NO2]/dt = k[NO][O3] - J[NO2] \quad \textit{(Equation B-1)}$$

$$d[NO]/dt = J[NO2] - k[NO][O3] \quad \textit{(Equation B-2)}$$

$$d[O3]/dt = J[NO2] - k[NO][O3] \quad \textit{(Equation B-3)}$$

Where the reaction rate coefficient *k* is defined as:

$$k = 4.405*\exp(-1370/Tamb) \quad \textit{(Equation B-4)}$$

And the photo-dissociation rate *J* are defined as:

$$J = 8*10\text{-}4*\exp(-10/Q) + 7.4*10\text{-}6*Q \quad \textit{(Equation B-5)}$$

Where Q is solar radiation in W/m2.

A fifth order Runge-Kutta scheme with adaptive time-stepping is used to solve the equations, to give 'post-chemistry' concentrations at each receptor. The post-chemistry NO and NO_2 values at each receptor are partitioned between the sources, based on the partitioning of the pre-chemistry NO_X, to give post-chemistry NO and NO_2 instantaneous plume concentrations for each receptor and source combination. The post-chemistry ensemble plume concentrations are then calculated from these post-chemistry instantaneous plume concentration values, again using the ratio of the plume cross sectional areas.

The GRSM method was further revised in AERMOD version 23132 with minor updates and re-evaluated as described in Stocker et al. (2023) and U.S. EPA (2024c).

5.10 Adjustments for the urban boundary layer

Although urban surface characteristics (roughness, albedo, etc.) influence the boundary layer parameters at all times, the effects of the urban sublayer on the structure of the boundary layer are largest at night and relatively absent during the day (Oke, 1998). An urban "convective-like" boundary layer forms during nighttime hours when stable rural air flows onto a warmer urban surface. Following sunset, the urban surface cools at a slower rate than the rural surface because buildings in the urban area trap the outgoing thermal radiation and the urban subsurface has a larger thermal capacity. AERMOD accounts for this by enhancing the turbulence above that found in the rural stable boundary layer (i.e., a convective-like urban contribution to the total turbulence in the urban SBL). The convective contribution is a function of the convective velocity scale, which in turn, depends on the surface heat flux and the urban mixed layer height. The upward heat flux is a function of the urban-rural temperature difference.

The urban-rural temperature difference depends on a large number of factors that cannot easily be included in applied models such as AERMOD. For simplicity, the data presented in Oke (1973; 1982) is used to construct an empirical model. Oke presents observed urban-rural

temperature differences for several Canadian cities with populations varying from about 1000 up to 2,000,000. These data represent the maximum urban effect for each city since they were collected during ideal conditions of clear skies, low winds, and low humidity. An empirical fit to the data yields the following relationship:

$$\Delta T_{u-r} = \Delta T_{\max}\left[0.1\,\ln\left(P/P_o\right) + 1.0\right], \qquad \textbf{(107)}$$

where ΔT_{max} = 12 ℃, P_o = 2,000,000 (the city population associated with the maximum temperature difference in Oke's data), and P is the population of the urban area being modeled.

Since the ambient nighttime temperature of an urban area is higher than its surrounding rural area, an upward surface heat flux must exist in the urban area. It is assumed that this upward surface heat flux is related to the urban-rural temperature difference through the following relationship:

$$H_u = \alpha\,\rho c_p\,\Delta T_{u-r} u_*, \qquad \textbf{(108)}$$

where α is an empirical constant, ρ is the density of air, and c_p is the specific heat at constant pressure. This expression is analogous to the bulk transfer parameterization of heat flux over a homogeneous surface (e.g., Businger (1973)), with α defined as the "bulk" transfer coefficient. We chose α to ensure that the upward heat flux is consistent with maximum measured values of the order of 0.1 m s^{-1} ºC . Because ΔT_{u-r} has a maximum value on the order of 10 ºC, and u_* is on the order of 0.1 m s^{-1}, α should have a maximum value on the order of 0.1. Although we assume that α has a maximum (city center) value of about 0.1, AERMOD uses an effective value of α that is averaged over the entire urban area. Assuming a linear variation of α from 0 at the edge of the urban area to about 0.1 at the center of the urban area results in an area average equal to one-third of that at the center (since the volume of cone is one-third of that of a right circular

cylinder of the same height). Therefore, AERMIC tested an area-averaged value of α equal to 0.03 against the Indianapolis data. This choice for α is consistent with measured values of the upward heat flux in Canadian cities reported by Oke (1973; 1982). The results of the developmental testing indicated that this choice for α resulted in an adequate fit between observations and AERMOD-predicted concentrations.

The mixing height in the nighttime urban boundary layer, z_{iu}, is based on empirical evidence presented in Oke (1973; 1982) that, in turn, suggests the following relationships:

$$z_{iu} \approx R^{1/2} \ \ and \ \ R \approx P^{1/2}, \qquad \textbf{(109)}$$

where R is a measure of the city size and P is the population of the city. The first relationship is based on the observed growth of the internal convective boundary layer next to shorelines (Venkatram 1978). The second relationship implicitly assumes that population densities do not vary substantially from city to city.

Equation **(109)** leads to the following equation for the nocturnal urban boundary layer height due to convective effects alone:

$$z_{iuc} = z_{iuo}\left(P/P_o\right)^{1/4}, \qquad \textbf{(110)}$$

where z_{iuo} is the boundary layer height corresponding to P_o. Based on lidar measurements taken in Indianapolis (1991) and estimates of z_{iu} found by Bornstein (1968) in a study conducted in New York city, z_{iuo} is set to 400 m in AERMOD.

In addition, since effects from urban heating should not cause z_{iu} to be less than the mechanical mixing height, z_{iu} is restricted from being less than z_{im}. Therefore, the mixed layer height for the nighttime urban boundary layer is computed as:

$$z_{iu} = Max\left[z_{iuc};\, z_{im}\right]. \qquad \textbf{(111)}$$

Once the urban mixing height has been estimated, a surrogate convective velocity scale (appropriate for the magnitude of convective turbulence present) is computed by substituting z_{iu} and H_u into the definitional equation for w_* (Deardorff 1970). That is,

$$w_{*u} = \left(\frac{g\, H_u\, z_{iuc}}{\rho c_p\, T} \right)^{1/3}, \qquad \textbf{(112)}$$

where w_{*u} is the urban nighttime convective velocity scale and T is the near-surface air temperature.

Having estimated w_{*u} the turbulence in the nighttime urban can be enhanced using the expressions found in Section 4.1.5. However, since for low level sources σ_{wT} depends primarily on u_* (see eq. **(34)** and eq. **(35)**) it is not possible to directly enhance σ_{wT} for these sources using w_{*u}. Therefore, an effective friction velocity (u_{*eff}) is developed as a surrogate for w_{*u} in the lower portion of urban PBL. We define u_{*eff} as the friction velocity that is consistent with $\sigma_{wm} = \sigma_{wc}$ at $z = 7z_o$. Assuming $z = 7z_o$ is always less $0.1z_{iuc}$, u_{*eff} is estimated by equating σ_{wc} (eq. **(35)**) with σ_{wm} (eq. **(37)**) and solving for u_*. Once u_{*eff} is found, the urban friction velocity for nighttime conditions (u_{*u}) is calculated as the maximum of u_{*eff} and u_* (the rural and daytime urban friction velocity).

Then using the enhanced velocity scales u_{*u} and w_{*u}, the nighttime convective portion of the turbulence in the urban boundary layer is computed using the expressions turbulence found in Section 4.1.5. That is, σ_{wc} and σ_{wm} are calculated from eq. **(35)** and eq. **(37)**, respectively, with w_{*u} used in place of the daytime convective velocity scale (w_*) and u_{*u} substituted for the rural u_*. Furthermore, for consistency purposes, an urban nighttime Monin-Obukhov length is calculated using eq. **(8)** with substitutions u_{*u} for u_* and H_u (eq. **(108)**) for H. This results in a

convective urban Monin-Obukhov length. For dispersion calculations, during stable hours, the absolute value of the urban Monin-Obukhov length is used, while daytime transition hours will use the original convective urban Monin-Obukhov length. To maintain consistency, during stable hours, the most neutral Monin-Obukhov length is selected between the urban nighttime Monin-Obukhov length and the rural Monin-Obukhov length, resulting in a stable-to-neutral atmosphere. Similarly, during daytime transition hours, the most convective Monin-Obukhov length value is selected between the urban Monin-Obukhov length and the rural Monin-Obukhov length, resulting in a neutral-to-convective atmosphere.

Finally, the total nighttime turbulence in the urban boundary layer is calculated as the sum (in quadrature) of the convective (urban) and mechanical (rural) portions. With these enhanced levels, vertical dispersion due to ambient turbulence (σ_{za}) in the urban boundary layer is calculated from eq. **(83)** (the SBL formulation for σ_{za}) with the urban PBL assumed to be neutral (i.e., $N = 0$). For the lateral dispersion in the urban boundary layer, σ_{ya} is calculated using the SBL formulation given by eq. **(76)**.

The potential temperature gradient in the night-time urban boundary layer is set equal to the upwind rural profile (Section 4.1.3) for all heights above z_{iu}, and is assumed to be equal to a small positive value below z_{iu}; i.e.,

$$\begin{aligned} \partial\theta/\partial z &= 10^{-5} && for \quad z \le z_{iu} \\ \partial\theta/\partial z &= rural\ value && for \quad z > z_{iu}. \end{aligned} \qquad \textbf{(113)}$$

For plumes below z_{iu} , the effective reflection surface is set equal to the height of the urban boundary layer (i.e., $z_{ieff} = z_{iu}$). Plumes that rise above z_{iu} ($h_{es} > z_{iu}$) are modeled with a z_{ieff} that is calculated from eq. **(68)** with z_{im} replaced by z_{iu}. Plume rise in the urban stable boundary layer is calculated from eq. **(95)-(99)** with $\partial\theta/\partial z$ taken from eq. **(113)**.

Use of this value for $\partial\theta/\partial z$ provides an appropriate near-neutral plume rise formulation that is expected within the nocturnal urban boundary layer. When AERMOD was originally promulgated, plume height in these conditions was not allowed to exceed 1.25 z_{iu}. This created potential issues for tall stacks with buoyant plumes in urban areas, as the limit of 1.25 z_{iu}, artificially limited the plume rise of these types of sources. With 15181, a change was made to the urban formulation to no longer limit the plume rise but treat such sources as pseudo penetrated plume sources to allow for the plumes to rise above the urban boundary layer when the stack height plus initial plume rise was greater than or equal to the urban mixing height. In version 22112, a further modification was made to calculate plume penetration parameters when the stack height plus plume rise is greater than or equal to the urban mixing height *and* the stack height is less than the urban mixing height. This change was made to avoid divide by zero in the plume penetration calculations. For more information about AERMOD's penetrated plume calculations, see Section 5.2.3.

For daytime conditions ($L < 0$) in urban areas, AERMOD uses the same formulations as in rural areas (i.e., no urban-related adjustments to boundary layer characteristics). However, beginning with AERMOD version 11059, the urban boundary layer options are still implemented for early daytime hours when the rural convective mixing height is less than the urban mixing height calculated by Equations 110 and 111. This change to continue the urban boundary layer options for early daytime hours was made because for early daytime hours, the lack of urban adjustments could result in an unrealistic drop in mixing heights for urban sources when the urban boundary layer height is still larger than the rural convective mixing height.

An analysis of the Indianapolis, IN urban SF6 study used as part of the AERMOD evaluation shows that the continued application of the urban adjustments for early morning or early evening hours increased model performance compared to observations. Observed Robust Highest Concentrations (RHC) for Indianapolis were 5.5 $\mu g/m^3$, while RHC values without the transition procedure were 4.3 $\mu g/m^3$ and RHC values with the transition procedure were 4.5 $\mu g/m^3$. Limiting the analysis to convective hours, which are the hours most affected by the

transition procedure, showed observed RHC values of 5.5 μg/m^3, 4.2 μg/m^3 with no transition procedure, and 4.7 μg/m^3 with the transition procedure.

Urban boundary layer adjustments were implemented in version 19191 for the RLINE and RLINEXT source types which require the BETA and ALPHA flag, respectively. Based on algorithms for the AERMOD area source, modification was introduced so when a RLINE or RLINEXT source is specified as an urban source, the u_* urban nighttime Monin-Obukhov length, z_{iu}, and z_o parameters are recalculated for morning transition and stable hours. As initial integration of the RLINE and RLINEXT source types in version 19191 is based on algorithms of version 1.2 of the Research LINE source (R-LINE) model (Snyder et al, 2013), the R-LINE methodology for calculation of w_*, is included. The methodology incorporates a check to set any negative w_* values to 0.0, associated with stable meteorological conditions, unlike other AERMOD source types that accept negative w_* values. The resultant w_* values are then used in the calculation of σ_v for RLINE and RLINEXT sources only.

Urban boundary layer adjustments were also implemented with the BUOYLINE source type as an ALPHA option in version 19191. The ALPHA requirement was removed for the BUOYLINE source type in version 22112 and the PG Stability class assignment was corrected for the BOUYLINE source when the urban option is used. PG stability class is set to 4 for stable hours when the urban boundary layer adjustments are applied.

6. List of symbols

B_o	Bowen ratio - ratio of the sensible to latent heat fluxes (dimensionless)
C_{AERMOD}	concentration estimated using AERMOD without considering building wake effects (g m^{-3})
$C_{c,s}\{x_r,y_r,z_r\}$	concentration contribution from the horizontal plume state - convective and stable (g m^{-3})
$C_{c,s}\{x_r,y_r,z_p\}$	concentration contribution from the terrain-following plume state - convective and stable (g m^{-3})
$C_c\{x_r,y_r,z_r\}$	total concentration (CBL) (g m^{-3})

$C_d\{x_r,y_r,z_r\}$		concentration contribution from the direct source (CBL) (g m^{-3})
$C_p\{x_r,y_r,z_r\}$		concentration contribution from the penetrated source (CBL) (g m^{-3})
$C_r\{x_r,y_r,z_r\}$		concentration contribution from the indirect source (CBL) (g m^{-3})
$C_s\{x_r,y_r,z_r\}$		total concentration (SBL) (g m^{-3})
$C_T\{x_r,y_r,z_r\}$		total concentration (CBL) (g m^{-3})
C_{ch}		concentration from the coherent plume used in meander calculations (gm^{-3})
C_R		concentration from the random plume used in meander calculations (g m^{-3})
C_D		neutral drag coefficient (cal g^{-1} $^{\circ}C^{-1}$)
C_{prime}		concentration estimated using the PRIME algorithms with AERMOD-derived meteorological inputs (g m^{-3})
c_p		specific heat at constant pressure (= 1004 J g^{-1} K^{-1})
	F_b	plume buoyancy flux (m^4 s^3)
F_y		total horizontal distribution function - with meander (m^{-1})
F_{yC}		horizontal distribution function for a coherent plume (m^{-1})
F_{yR}		horizontal distribution function for a random plume (m^{-1})
F_G		flux of heat into the ground (W m^{-2})
	F_m	plume momentum flux (m^4s^2)
F_z		total vertical distribution function (m^{-1})
f		plume state weighting function (dimensionless)
f_p		fraction of plume mass contained in CBL = (1 - penetration factor) dimensionless)
g		acceleration due to gravity (9.8 m s^{-2})
H		sensible heat flux (W m^{-2})
H_c		critical dividing streamline (m)
	H_p	plume centroid height (m)
H_u		heat flux in the nighttime boundary layer (W m^{-2})
h_c		receptor specific terrain height scale (m)
h_{ep}		penetrated source plume height above stack base (m)
h_s		stack height corrected for stack tip downwash (m)
Δh		general symbol for distance dependent plume rise (m)
Δh_d		plume rise for the direct source (m)
Δh_{eq}		equilibrium plume rise in a stable environment (m)
Δh_h		depth of the layer between z_i and the stack top (m)
Δh_p		plume rise for the penetrated source (m)
Δh_i		plume rise for the indirect source (m)
Δh_s		plume rise for the stable source (m)
i_z		vertical turbulence intensity

k	von Karman constant k = 0.4 (dimensionless)
l	length scale used in determining the Lagrangian time scale (m)
l_n	neutral length scale - a component of l (m)
l_s	stable length scale - a component of l (m)
L	Monin-Obukhov length (m)
N	Brunt-Vaisala frequency (s^{-1})
N_h	Brunt-Vaisala frequency above z_i (s^{-1})
n	cloud cover (fractional)
P	population of urban area
p_y	lateral probability density function
p_z	vertical probability density function
p_w	probability density function of the instantaneous vertical velocities
Q	source emission rate (g/s)
R	solar insolation (W m^{-2})
R_n	net radiation (W m^{-2})
R_o	*clear sky solar insolation (W m^{-2})*
$r(\varphi)$	Albedo {solar elevation} (dimensionless)
r'	noontime albedo (dimensionless)
r_s	stack radius - corrected for stack tip downwash (m)
r_y	lateral dimension of an elliptical plume
r_z	vertical dimension of an elliptical plume
S	skewness factor (dimensionless)
T	ambient temperature (K)
T_{Ly}	lateral lagrangian time scale (sec)
T_{Lzc}	vertical lagrangian time scale for the CBL (sec)
T_{Lzs}	vertical lagrangian time scale for the SBL (sec)
T_r	time scale used in the meander algorithm (sec)
T_{ref}	ambient temperature - at reference temperature height (K)
T_s	stack gas temperature (K)
T_u	urban surface temperature (K)
t	time (sec)
ΔT	difference between stack gas and ambient temperature (K)
ΔT_{u-r}	urban-rural temperature difference (K)
u	wind speed (m s^{-1})
u_{cr}	minimum speed for which the expression for u*, in the SBL, has a real valued solution (m s^{-1})
u_o	defined in eq. **(14)** and used in eq. **(15)**

u_p	wind speed that is used for plume rise (m s^{-1})
u_{ref}	wind speed at reference height (m s^{-1})
u_{th}	wind speed instrument threshold - separate value for each data set (offsite & onsite) (m s^{-1})
u_*	surface friction velocity (m s^{-1})
u_{*eff}	effective surface friction velocity - surrogate for w_{*u} (m s^{-1})
u_{*u}	surface friction velocity for nighttime urban conditions (m s^{-1})
w	random vertical velocity in the CBL (m s^{-1})
$\overline{w}_j$	mean vertical velocity for the updraft (j = 1) and the downdraft (j = 2) distributions (m-s^{-1})
w_s	stack exit gas velocity (m-s^{-1})
w_*	convective velocity scale (m-s^{-1})
w_{*u}	urban nighttime convective velocity scale (m-s^{-1})
X	non-dimensional downwind distance (dimensionless)
x_r	downwind distance to a receptor (m)
x_f	distance to final plume rise (m) - eq. **(44)** for the CBL; eq. **(96)** for the SBL
x_m	downwind distance at which plume material uniformly mixed throughout the boundary layer (m)
(x_r,y_r,z_r)	receptor location
(x_t,y_t,z_t)	terrain point location
z_{base}	user specified elevation for the base of the temperature profile (i.e., meteorological tower)
z_c	total height of the plume in the CBL considering both plume rise and effects from convective turbulence (m)
z_i	mixing height (m): z_i = MAX [z_{ic}; z_{im}] in the CBL and $z_i = z_{im}$ in the SBL
z_{ic}	convective mixing height (m)
z_{ie}	equilibrium height of stable boundary layer
z_{ieff}	height of the reflecting surface in the SBL or in the stable layer above the above the CBL (m)
z_{im}	mechanical mixing height (m)
z_{iu}	urban nighttime boundary layer mixing height (m)
z_{iuc}	urban nighttime boundary layer mixing height due to convective effects alone (m)
z_{msl}	height of stack base above mean sea level (m)
z_o	surface roughness length (m)
z_{PG}	release height used in the Prairie Grass experiment (m)

z_p	receptor "flagpole" height - height of a receptor above local terrain (m)
z_r	height of the receptor above local source base (m)
z_{ref}	reference height for wind (m)
z_{Tref}	reference height for temperature (m)
z_t	height of the terrain above mean sea level (m)
$\tilde{\alpha}$	general symbol used to represent the effective parameters in the treatment of the inhomogeneous boundary layer. In the text the effective values of the parameters u, σ_w, σ_v and TL are denoted by underscoring the character
γ	parameter used to weight C_{AERMOD} and C_{Prime} in estimating concentrations that are influenced by building downwash (dimensionless)
θ	potential temperature (K)
θ_*	temperature scale (K)
λ_j	weighting coefficient for the updraft (j = 1) and downdraft (j = 2) distributions of equations **(53)**,**(59)** and **(65)**
ρ	density of air (kg m^{-3})
σ_b	buoyancy induced dispersion for the direct & indirect sources (m)
σ_h^2	total horizontal wind "energy" used in the meander algorithm (m^2)
σ_r^2	random "energy" component of the total horizontal wind "energy" used in the meander algorithm (m^2)
σ_{SB}	Stephen Boltzman constant (5.67×10^{-8} $Wm^{-2}K^{-4}$)
σ_u	along-wind turbulence (m s^{-1})
σ_v	lateral turbulence (m s^{-1})
σ_{vc}	convective portion of the lateral turbulence (m s^{-1})
σ_{vo}	surface value of the lateral turbulence (m s^{-1})
σ_{vm}	mechanical portion of the lateral turbulence (m s^{-1})
σ_{vT}	total lateral turbulence (m s^{-1})
σ_w	vertical turbulence (m s^{-1})
σ_{wc}	convective portion of the vertical turbulence (m s^{-1})
σ_{wm}	mechanical portion of the vertical turbulence (m s^{-1})
σ_{wml}	mechanical portion of the vertical turbulence generated in the PBL (m s^{-1})
σ_{wmr}	mechanical portion of the vertical turbulence above the PBL (residual) (m s^{-1})
σ_{wT}	total vertical turbulence (m s^{-1})
σ_{xg}	longitudinal dimension of the building wake (m)
σ_y	total lateral dispersion for the direct & indirect sources (m)
$\sigma_{ya,zaj}$	ambient turbulence induced dispersion for the direct & indirect sources (m)
σ_{zas}	ambient dispersion for the stable source (m)
σ_{yg}	distance from the building centerline to lateral edge of the building wake (m)

σ_{yl}	lateral spread from combined effects of ambient turbulence and building downwash (m)
σ_{zp}	total dispersion for the penetrated source (m)
σ_{zs}	total dispersion for the stable source (m)
σ_{zaj}	ambient vertical dispersion for the updraft & downdrafts plumes (j = 1,2), respectively, for both the direct & indirect sources (m)
σ_{zej}	elevated portion of σ_{zaj} (m)
σ_{zes}	elevated portion of σ_{zas} (m)
σ_{zg}	height of the building wake at the receptor location (m)
σ_{zj}	total vertical dispersion for the updrafts and downdrafts (j = 1,2 respectively), for both the direct and indirect sources
σ_{zg}	surface portion of σ_{zaj} (m)
σ_{zgs}	surface portion of σ_{zas} (m)
τ	time constant controlling the temporal interpolation of z_{im} (sec)
φ	solar elevation angle
φ_p	fraction of plume mass below H_c (dimensionless)
Ψ_{dj}	total height of the direct source plume (i.e. release height + buoyancy + convection) (m)
Ψ_{rj}	total height of the indirect source plume (m)
ψ_m	similarity function for momentum (stability correction) - eq. **(7)** for the CBL and eq. **(29)** for the SBL (dimensionless)

Appendix A. Input / output needs and data usage

A.1 AERMET input data needs

Besides defining surface characteristics, the user provides several files of hourly meteorological data for processing by AERMET. At the present time AERMET is designed to accept data from any for the following sources: 1) standard hourly National Weather Service (NWS) data from the most representative site; 2) morning soundings of winds, temperature, and dew point from the nearest NWS upper air station; and 3) site-specific wind, temperature, turbulence, pressure, and radiation measurements (if available).

The minimum measured and/or derived data needed to run the AERMOD modeling system are as follows:

A.1.1 Meteorology

- wind speed (u);
- wind direction;
- cloud cover - opaque first then total (n);
- ambient temperature (t);
- morning sounding.

Cloud cover is also used in dry deposition calculations in the AERMOD model. Therefore, if cloud cover is missing and the Bulk Richardson Number Scheme is being used (see 3.3.1) then an equivalent could cover is calculated as follows, based on van Ulden and Holtslag (van Ulden and Holtslag 1985):

$$n_{eq} = \left(\frac{1 - \theta_* / 0.09}{0.5} \right)^{0.5}, \qquad \textbf{(114)}$$

where θ_* is the temperature scale as calculated from eq. **(18)**.

A.1.2 Directionally and/or Monthly Varying Surface Characteristics

- noon time albedo (r);
- Bowen ratio (B_o);
- roughness length (z_o) -

For AERMET, the user can specify monthly variations of three surface characteristics. These include: the albedo (r), which is the fraction of radiation reflected by the surface; the Bowen ratio (B_o), which is the ratio of the sensible heat flux to the evaporation heat flux; and the surface roughness length (z_o), which is the height above the ground at which the horizontal wind velocity is typically zero. Values for albedo and Bowen ratio should be based on a 10 km x 10 km area centered on the meteorological tower. Values for surface roughness should be based on a 1 km radius around the meteorological tower and can be differentiated for up 12 wind sectors. Surface characteristics should be determined with the aid of the AERSURFACE program (U.S. EPA, 2024f). Refer to the AERSURFACE and AERMET User's Guides (U.S. EPA, 2024d) for additional information on determining appropriate surface characteristic values.

A.1.3 Other

- Latitude;
- Longitude;
- Time zone;
- Wind speed instrument threshold for each data set (u_{th}).

A.1.4 Optional

- Solar radiation;
- Net radiation (R_n);
- Profile of vertical turbulence (σ_w);

- Profile of lateral turbulence (σ_v)

A.2 Selection and use of measured winds, temperature, and turbulence in AERMET

A.2.1 Threshold Wind Speed

The user is required to define a threshold wind speed (u_{th}) for site-specific data sets. Although the current version of AERMOD cannot accept a separate u_{th} for NWS data, a separate u_{th} should be selected for each on-site data set being used.

A.2.2 Reference Temperature and Height

The reference height for temperature (z_{Tref}), and thus the reference temperature, is selected as the lowest level of data which is available between z_o & 100 m.

A.2.3 Reference Wind Speed and Height

The reference height for winds (z_{ref}), and thus the reference wind speed (u_{ref}), is selected as the lowest level of data which is available between 7 z_o & 100m. Although the current version of AERMOD cannot accept a separate z_{ref} for offsite data, we believe that a separate z_{ref} should be selected for each data set being used.

If no valid observation of the reference wind speed or direction exists between these limits the hour is considered missing, and a message is written to the AERMET message file. For the wind speed to be valid its value must be greater than or equal to the threshold wind speed. AERMOD processes hours of invalid wind speed, e.g. calms, in the same manner as ISC (EPA calms policy).

All observed wind speeds in a measured profile that are less than u_{th} are set to missing and, therefore, not used in the construction of the wind speed profile (profiling of winds is accomplished in AERMOD).

A.2.4 Calculating the Potential Temperature Gradient above the Mixing Height from Sounding Data

AERMET calculates $d\theta/dz$ for the layer above z_i as follows:

- If the sounding extends at least 500 m above z_i the first 500 m above z_i is used to determine $d\theta/dz$ above z_i.
- If the sounding extends at least 250 m above z_i (but not 500 m) then the available sounding above z_i is used to determine $d\theta/dz$ above z_i.
- AERMET limits $d\theta/dz$ above z_i to a minimum of 0.005 K m^{-1}.
- If the sounding extends less than 250 m above z_i then set $d\theta/dz$ = 0.005 K m^{-1} (a default value).

A.2.5 Measured Turbulence

All measured turbulence values are passed to AERMOD if the hour is non-missing. This is true even for those levels where the wind speed is below u_{th}. Based on measurements with research grade instruments, reasonable minimum turbulence levels in non-calm conditions for vertical turbulence (σ_w) and lateral turbulence (σ_v) values are set by AERMOD to 0.02 m s^{-1} and 0.2 m s^{-1}, respectively. Although these lower limits are applied to the measured values of the turbulence the calculated profile values of σ_w and σ_v are not subjected to any lower limits. We do not restrict these estimated profiles because it would bias the calculation of the effective values of turbulence, which are averages through the layer between the receptor and the plume height, in determining the dispersion of the plume. However, as discussed in Section A.9, these limits are applied to the effective values of turbulence and wind speed.

A.2.6 Data Substitution for Missing On-Site Data

If on-site data are missing for an hour, the hour is considered missing unless the user specifies a substitute data set. AERMET does not default to NWS (or any other offsite) data.

A.3 Information passed by AERMET to AERMOD

The following information is passed from AERMET to AERMOD for each hour of the meteorological data record.

- All observations of wind speed (u); wind direction; ambient temperature (T); lateral turbulence (σ_v); & vertical turbulence (σ_w) with their associated measurement heights.
- Sensible heat flux (H), friction velocity (u_*), Monin Obukhov length L, z_{im} (for all hours), z_{ic} & w_* (for convective hours only), z_o , $r\{\varphi\}$, & B_o, $d\theta/dz$ (above z_i), u_{ref} , wind direction at the reference height, z_{ref}, ambient temperature at the reference height (T_{ref}) (not used in AERMOD), & the reference height for temperature (z_{Tref})

A.4 Restrictions on the growth of the PBL height

AERMET restricts the growth of z_i to a reasonable maximum of 4000 m. This restriction applies to both calculated and measured mixing heights. Although mixing heights in excess of 4000 m may occur on rare occasions, in desert climates, the additional effect on surface concentration is most likely insignificant.

A.5 Initializing the mechanical mixing height smoothing procedure

If $\{t + \Delta t\}$, in eq. **(26)**, is the first hour of the data set then no smoothing takes place. Furthermore, if a missing value occurs at time step t then smoothing is not performed at time step $\{t + \Delta t\}$ but is restarted for subsequent hours.

A.6 Determining the mixing height when the sounding is too shallow

The left-hand side of eq. **(22)** is determined from the morning temperature sounding and the right-hand side from the daytime history of surface heat flux. When the temperature sounding, obtained from the NWS, does not reach a height which is greater than the convective mixing height, we must assume a profile for the potential temperature gradient to estimate z_{ic}. This is accomplished as follows:

- Determine $d\theta/dz$ in the top 500 m layer of the sounding. However, if part of the 500 m layer is within the first 100 m of the PBL, the layer should be reduced (to a minimum thickness of 250 m) to avoid using the portion of the sounding that is below 100 m. If the above conditions cannot be satisfied, then z_{ic} is defined as missing.
- Extend the sounding by persisting $d\theta/dz$ up and recomputing z_{ic}.
- Provide warning messages which tell users
    - the height of the actual sounding top,
    - that $d\theta/dz$ has been extrapolated above the sounding z_{ic}, and
    - that z_{ic} has been recomputed.
- Allow the user to reject the "fixed-up" value for z_{ic} by defining it as missing.

A.7 Input data needs for AERMAP

The following data is required input for AERMAP

- DEM formatted terrain data (x_t, y_t, z_t).
- Design of receptor grid; AERMAP accepts either polar, Cartesian, or discrete receptors.

A.8 Information passed by AERMAP to AERMOD

AERMAP passes the following parameters to AERMOD: x_r, y_r, z_r, z_t, & the height scale (h_c) for each receptor.

A.9 Wind speed and turbulence limits used in model calculations

When calculating the effective parameters, limits are applied such that:

$$\begin{aligned} \sigma_w\{z\} &= Max\left[\sigma_w\{z\};\ 0.02\ m\,s^{-1}\right] \\ \sigma_v\{z\} &= Max\left[\sigma_v\{z\};\ 0.05\,u\{h_s\};\ 0.2\ m\,s^{-1}\right]. \end{aligned} \qquad \textbf{(115)}$$

These limits are also applied when selecting the turbulence for plume rise calculations.

Dilution of the plume is determined by the wind that corresponds to the average over the magnitudes of the wind vectors during a given time interval. But measurements only give the vector averaged wind, which can be zero, even though the dilution wind is not zero. We can estimate the dilution wind by assuming that the vector wind, u_v, can be expressed as

$$u_v = (\overline{u} + u',\ v'), \qquad \textbf{(116)}$$

where $\overline{u}$ is the mean measured wind, and the primed quantities refer to the turbulent fluctuations. The assumption being made is $\overline{u_v} = \overline{u}$. If we assume that the measured velocity fluctuations correspond only to the angular variations of a constant vector, u_v, we can write from eq. **(116)** that

$$u_v^2 = \overline{u}^2 + \sigma_v^2 + \sigma_u^2 . \qquad \textbf{(117)}$$

In this simple model, u_v , is the dilution wind. If we take $\sigma_u = \sigma_v$, the dilution wind can be written as

$$u\{h_s\} = \sqrt{u\{h_s\}^2 + 2\,\sigma_v^2} . \qquad \textbf{(118)}$$

This formulation assures that the dilution wind is not zero as long as either $\overline{u}$ or σ_v is not zero. Similarly, at the time of plume rise calculations, the effective turbulence and effective wind speed will be recalculated using equations **(115)** and **(118)**, where the turbulence and winds will be evaluated at stack top.

A.10 Using profiles for interpolating between observations

When observations are available AERMOD uses the similarity profile functions to interpolate adjacent measurements. Figure 17 illustrates how AERMOD's INTERFACE uses the expected shape of a meteorological profile to interpolate between observations.

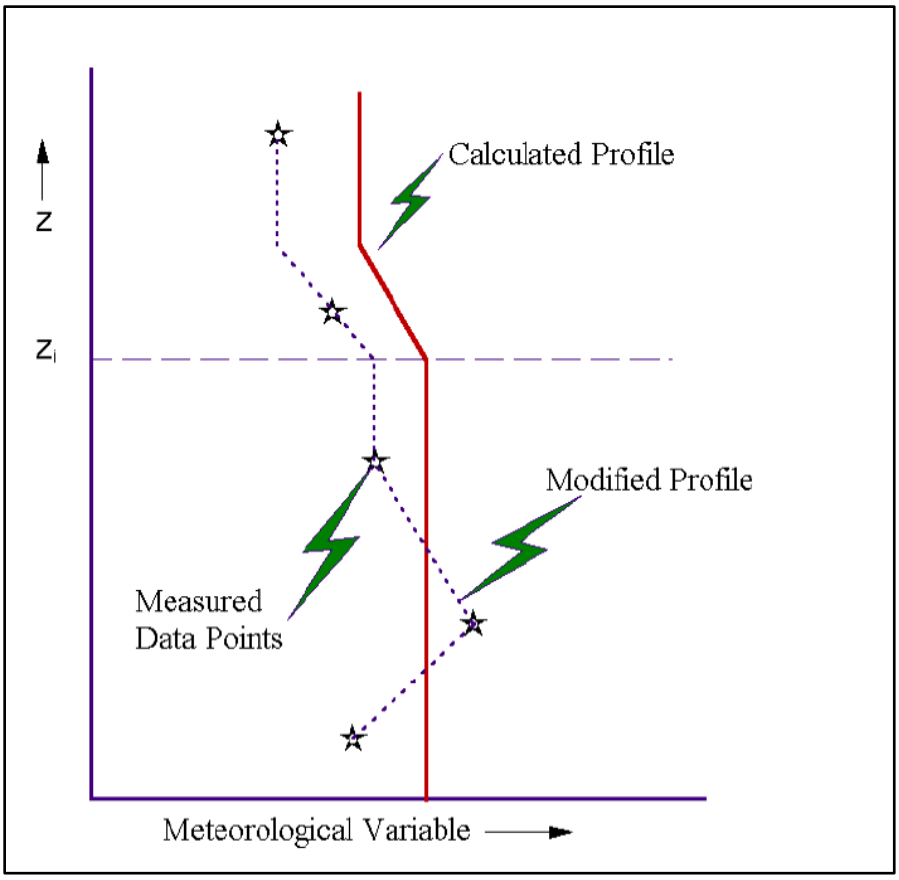

Figure 17. AERMOD's construction of a continuous meteorological profile by interpolating between observations.

For a gridded profile height between two observed profile heights, the observations are interpolated to the gridded height while maintaining the shape of the similarity profile. This is accomplished as follows:

1. the observations are linearly interpolated to the gridded profile height;
2. the similarity function is evaluated at the gridded profile height;
3. the similarity function is evaluated at the observed profile heights immediately above and below the grid height and linearly interpolated to the grid height;
4. the ratio of the value obtained in 2 to the value obtained in 3 is applied to the value obtained in 1.

For a gridded profile height above the highest observation, the procedure is modified slightly:

1. the observation at the highest observed profile height is extrapolated by persisting the value upward;
2. the similarity function is evaluated at the grid height;
3. the similarity function is evaluated at the highest height in the observed profile;
4. the ratio of the value obtained in 2 to the value obtained in 3 is applied to the value obtained in 1.

A similar procedure for extrapolating to heights above the observed profile is applied to heights below the lowest observed profile height.

A.11 Using measured mixing heights

If measured mixing heights are available, then they are treated in the following manner: If $L>0$ (SBL) the measured mixing height is defined as z_{ie} and it is treated the same as a calculated mechanical mixing height. If $L<0$ (CBL) the measured mixing height is defined as z_{ic}, and z_{ie} is calculated from eq. **(24)**, smoothed, then proceed as if both z_{ic} and the smoothed z_{im} had been calculated values.

If a user has "measured" mixing heights available (and chooses to use them), AERMET defaults to substituting calculated mixing heights for missing measurements and a message is

written that a substitution has occurred. If the user elects to substitute calculations for missing measurements, AERMET will print out a message to the message file for each hour that a substitution has occurred.

Appendix B. Description of ALPHA Options in AERMOD 24142

This appendix to the AERMOD Model Formulation document provides descriptions of the ALPHA options included in version 24142 of the AERMOD modeling system. Because these model options are not part of the promulgated regulatory formulation of AERMOD (U.S. EPA, 2024b), they are not included in the main text of the AERMOD Model Formulation document. It should be noted that there are no BETA options implemented within version 24142 of the AERMOD Modeling System. Refer to the AERMOD User's Guide (U.S. EPA, 2024g) for details on the required control file syntax to experiment with the ALPHA options described in this appendix.

B.1 Characterization of ALPHA and BETA Options

BETA options are more mature with respect to where they are along the path of development than ALPHA options. The scientific basis of BETA options is well established, implementation in the model is considered complete, and performance evaluations demonstrate their validity and justification for inclusion as a regulatory update to AERMOD. BETA options have generally met the criteria for justification as an alternative model (with appropriate approval from the EPA Regional Office with concurrence from the EPA Model Clearinghouse) and proposal as a regulatory formulation update to AERMOD.

In contrast to BETA options, ALPHA options are less mature in the development process than BETA options and can range anywhere from an idea or concept that EPA has identified to be explored as a priority development topic but is still in the initial research and experimental phases, to an option that is far along the development path but has not yet met all of the criteria necessary for justification as an alternative model and proposal as a regulatory update to the model formulation. In some cases, a new model option may be implemented as an ALPHA option that is not considered a change to the scientific formulation but needs to be more fully tested by the broader user community before it is implemented for use. ALPHA options that represent changes in the scientific formulation of the model may eventually reach maturity

in development and to be proposed and promulgated as scientific changes to the formulation of AERMOD while others may never develop that level of scientific maturity and eventually removed from the model. Each of the ALPHA options described below in version 24142 represent potential updates to the scientific formulation of AERMOD and must go through the regulatory update process which includes rulemaking to update the Guideline before they are considered part of the scientific formulation of the regulatory version of AERMOD.

B.2 ALPHA Options in AERMOD 24142

In contrast to BETA options, ALPHA options are less mature in the development process than BETA options and can range anywhere from an idea or concept that EPA has identified to be explored as a priority development topic but is still in the initial research and experimental phases, to an option that is far along the development path but has not yet met all of the criteria necessary for justification as an alternative model and proposal as a regulatory update to the model formulation. In some cases, a new model option may be implemented as an ALPHA option that is not considered a change to the scientific formulation but needs to be more fully tested by the broader user community before it is implemented for use. ALPHA options that represent changes in the scientific formulation of the model may eventually reach maturity in development and to be proposed and promulgated as scientific changes to the formulation of AERMOD while others may never develop that the level of scientific maturity and eventually removed from the model. Each of the ALPHA options described below in version 23132 represent potential updates to the scientific formulation of AERMOD and must go through the regulatory update process which includes rulemaking to update the Guideline before they are considered part of the scientific formulation of the regulatory version of AERMOD.

B.2.1 RLINE Extended (RLINEXT)

The RLINEXT source type refers to an extended version of the RLINE source type and was implemented in version 19191, concurrently with the RLINE source type, but as an ALPHA option. As an extension of the BETA RLINE source type, RLINEXT accepts

additional input parameters to represent depressed roadways (RDEPRESS), solid roadside barriers (RBARRIER), and perform wind profile calculations without a displacement height (RLINEFDH). Each of these are discussed separately below.

B.2.2 Solid Roadway Barrier (RBARRIER)

The RBARRIER option simulates the effects of solid roadside barriers on either or both sides of the roadway and can only be used concurrently with an RLINEXT source type. The development of the barrier algorithms is ongoing and are based on the work of Schulte et al, 2014; Ahangar, 2017; and Venkatram et al., 2021. Algorithm development has made use of measurements taken during several different experiments including studies conducted in EPA's wind tunnel (Heist et al., 2009) and field studies including the Idaho Falls experiment (Finn et al., 2010), the Raleigh near road study in 2006 (Baldauf et al., 2008), and the Phoenix, Arizona field study (Baldauf et al., 2016). Barrier input parameters are specified with the RBARRIER keyword on the SO pathway.

B.2.3 Depressed Roadways (RDEPRESS)

The RDEPRESS option accounts for dispersion associated with depressed roadways and can only be used concurrently with an RLINEXT source type. The development and refinement of the RDEPRESS option is ongoing by EPA's ORD, utilizing wind tunnel studies described in Heist et al, 2009. Road depression input parameters are specified with the RDEPRESS keyword on the SO pathway.

B.2.4 RLINE/RLINEXT Displacement Height (RLINEFDH)

The RLINEFDH option modifies the vertical wind profile calculations for the RLINE and RLINEXT source types without using a displacement height. This was added as an ALPHA option for the RLINE and RLINEXT source types to make the wind profile calculations more consistent with other AERMOD source types which do not consider a displacement height in the wind profile calculations. This option is enabled by including the

secondary keyword RLINEFDH on the CO pathway as a model option specified with the MODELOPT primary keyword.

B.2.5 Building Downwash Options

Analyses have shown AERMOD to both overpredict and underpredict ground-level concentrations in the building wake, depending on the building dimensions; stack height; stack location; and the orientation of the building relative to the wind direction. Overprediction and underprediction have been demonstrated in analyses of single, one-tiered rectangular buildings. Some examples in which AERMOD has been shown to be deficient with regard to building downwash include elongated buildings, buildings that are angled rather than perpendicular to the wind, and buildings with stacks located near a building corner (Perry et al., 2016; Petersen et al., 2017).

The building downwash algorithms in AERMOD are based on solid, square and rectangular ground-based buildings. Porous, streamlined, and lattice-type structures that are common at many sites have been shown to have a different influence on flow and dispersion than solid buildings. Currently, these types of structures can only be modeled in AERMOD as solid buildings which are not representative.

EPA's Air Quality Modeling Group (AQMG) has collaborated on multiple research initiatives to improve AERMOD's performance with respect to point emission sources that are subject to building downwash. These include initiatives lead by EPA's Office of Research and Development (ORD), the PRIME2 Advisory Subcommittee (PRIME2) within the Atmospheric Modeling and Meteorology (APM) Committee of the Air and Waste Management Association (A&WMA), the Sibley School of Mechanical and Aerospace Engineering at Cornell University, and the Bureau of Ocean Energy Management (BOEM).

ORD has performed wind tunnel experiments and embedded large eddy simulations (LES) to better understand how to parameterize buildings that are elongated and angled relative

to the wind flow and the parameterization of the plume in the cavity and far wake regions. The ORD studies are concentrated on single rectangular buildings, specifically investigating changes in plume parameters at discrete downwind distances from the building and source, longitudinal and lateral plume profiles, the lateral plume shift on the lee side of rotated buildings which resulted in recommended modifications to the current PRIME algorithm in AERMOD.

A&WMA involved the collaboration of technical experts, industry groups, and representatives from the regulatory agencies with the purpose of (1) providing a technical review forum to improve the PRIME building downwash algorithms in AERMOD; and (2) establishing a mechanism to review, approve, and implement new science into the model. A&WMA's research has included the reanalysis of existing wind tunnel data, as well as the completion of new wind tunnel experiments to investigate the decay of the building wake above the top of the building, appropriate height at which approach turbulence and wind speed are calculated, the reduction of wake effects for streamlined structures, and the effect of approach roughness on the wake. Their analyses have led to recommendations for new turbulence enhancement and velocity deficit equations that address these aspects, as well as an update to the degree of entrainment into the plume and the application of plume rise at the receptor when the plume is affected by downwash. Their analyses have led to recommendations for new turbulence enhancement and velocity deficit equations that address these aspects, as well as an update to the degree of entrainment into the plume and the application of plume rise at the receptor when the plume is affected by downwash.

Researchers at Cornell University have focused on the lateral plume shift on the lee side of rotated buildings which have prompted the addition of a new source type in AERMOD to further the research to better parameterize this phenomenon caused by building downwash.

BOEM sponsored the integration of the platform downwash algorithm in the Offshore Coastal Dispersion (OCD) model into AERMOD to further the research needed to enable

AERMOD to model to simulate dispersion from downwash effects caused by raised lattice and porous type structures such as offshore platforms.

The ALPHA options related to building downwash effects currently in AERMOD that have resulted from these different research initiatives are described in the sections that follow.

B.2.5.1 ORD_DWNW

Three ALPHA options have been implemented into AERMOD as a result of the research conducted by ORD and are enabled in the model control file with the use of the primary keyword ORD_DWNW on the CO pathway. These options attempt to address the following: (1) resolve a mismatch in plume width at the transition between the cavity and the far wake; (2) use an effective wind speed for the primary plume (instead of stack height wind speed); and (3) adjust the maximum ambient turbulence levels (Monbureau et al., 2018).

ORDCAV - Plume Spread Matching at Boundary Between Near-wake and Far-wake

The current implementation of PRIME in AERMOD creates a cavity plume and a re-emitted plume to simulate two distinct regions with a weighted distribution of mass between the two plumes. The cavity and re-emitted plumes initially have the same vertical dispersion on the leeward side of the building. The re-emitted plume is then allowed to grow with downwind distance while the vertical dispersion of the cavity plume remains unchanged throughout the cavity. This creates a discontinuity of the two plumes at the near-wake boundary that results in a reduction in ground level concentrations near cavity boundary. ORD has proposed eliminating this discontinuity such that the vertical dispersion of both plumes is equal at the cavity boundary. This change would result in an increase in the re-emitted plume concentration. Figure B-1 illustrates the mismatch at the cavity boundary (LR) in the vertical dispersion (σz) of the re-emitted plume (solid line) which grows from the lee wall through the cavity and the cavity plume (dotted line) which is constant through the cavity. This option was implemented as an

ALPHA option in AERMOD beginning with version 19191 and is specified in the AERMOD control file with the combination of the ORD_DWNW and ORDCAV keywords.

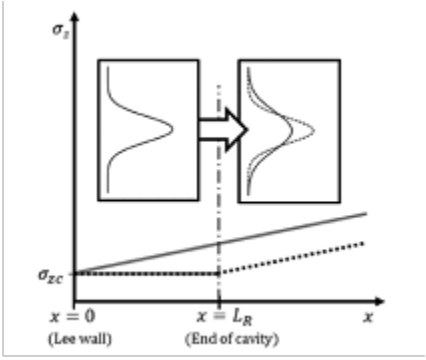

Figure B-1. Discontinuity in vertical dispersion (σ_z) between re-emitted plume (solid line) and the cavity plume (dotted line) at the cavity boundary (L_R). Inset: the vertical concentration profile within the cavity (left panel); the profile after plume is emitted from the cavity (solid line, original; dotted line, revised) (Monbureau et al., 2018).

ORDUEFF - Effective Wind Speed

The PRIME model currently uses the wind speed at stack height for the primary plume which likely under-estimates ground-level concentrations in the lee of the building. This is inconsistent with other source types in AERMOD where an effective wind speed (U_{eff}) is used. U_{eff} is defined as the averaged profiled wind speed between the receptor height and the plume centerline allowing the wind speed of the plume to change with a changing environment, such as the variability in surface roughness and stability. ORD has proposed the use of U_{eff} in PRIME which would result in a decrease in the wind speed toward the ground, i.e., the wind speed within the near wake, thus increasing cavity concentrations (Monbureau et al., 2018). This option was implemented as an ALPHA option in AERMOD beginning with version 19191 and is specified in the AERMOD control file with the combination of the ORD_DWNW and ORDUEFF keywords.

ORDUTURB - Maximum Turbulence

Vertical and lateral dispersion coefficients are based on the formulations of Weil (1996). When PRIME was implemented in AERMOD, the maximum value of the ambient turbulence intensity in the wake was reduced from Weil's published value of 0.07 to 0.06. ORD has proposed increasing this maximum turbulence value to Weil's original value of 0.07. Increased turbulence brings the plume down toward the ground more quickly and increases the dispersion. This will result in reduced concentrations for the primary source and a shorter downwind distance to the maximum ground-level concentrations (Monbureau et al., 2018). This option was implemented as an ALPHA option in AERMOD beginning with version 19191 and is specified in the AERMOD control file with the combination of the ORD_DWNW and ORDUTURB keywords.

B.2.5.2 AWMADWNW

As a result of the research performed by A&WMA, five ALPHA options have been implemented, two of which are variations of a single update. The updates are related to the effective wind speed of the primary plume, similar to ORD's proposal, new formulations for turbulence enhancement and velocity deficit which incorporate building shape (streamline versus rectangular) and approach turbulence intensity (surface roughness), which will subsequently affect the calculations of plume rise and the dispersion coefficients in PRIME (Petersen and Guerra, 2018), and the amount of entrainment into the plume affected by downwash.

AWMAUEFF - Effective Wind Speed

Similar to ORD, A&WMA also proposed to redefine how the wind speed is determined for the primary plume, which is currently defined at the stack height. A&WMA has proposed using the wind speed at the height of the plume centerline (Petersen and Guerra, 2018). This option was implemented as an ALPHA option in AERMOD beginning with version 19191 and

is specified in the AERMOD control file with the combination of the AWMADWNW and AWMAUEFF keywords.

AWMAUTURB/ AWMAUTURBHX - Turbulence Enhancement and Velocity Deficit

In their analyses of wind tunnel data, A&WMA has demonstrated that building wake effects decay rapidly back to ambient levels above the top of the building versus the current implementation in AERMOD in which wake effects can extend up to three building heights. In addition, the PRIME algorithm currently sets the lateral turbulence in the cavity equal to vertical turbulence, whereas the wind tunnel shows that lateral turbulence is less than the vertical turbulence. Finally, the current PRIME algorithm does not account for the effects of approach roughness on the wake. A&WMA has demonstrated that wake effects decrease as the approach roughness increases (Petersen et al., 2017).

Further, AERMOD is not able to properly characterize streamlined structures such as storage tanks and cooling towers. A wind tunnel study conducted by Petersen (2014) shows that dispersion is reduced in the wake of streamlined structures and that AERMOD may underpredict ground-level concentrations when these structures are modeled as rectangular buildings.

A&WMA has developed and proposed new formulations for turbulence enhancement and velocity deficit that address several of the limitations of PRIME previously mentioned, including rate of decay for building wake effects above the building, lateral turbulence enhancement in the wake, approach turbulence and wind speed, and wake effects for streamlined structures (Petersen and Guerra, 2018). Beginning with version 19191, two additional ALPHA options proposed by A&WMA were incorporated into AERMOD. The first enables A&WMA's new formulation and is specified with the keyword AWMAUTURB, along with the keyword AWMADWNW, as mentioned above. The AWMAUTURB option uses the minimum of the final momentum plume rise or a representative PRIME plume rise height for all

calculations. It also uses the final momentum plume rise height used to compute effective wind speed (UEFF), effective σ_w (SWEFF), effective σ_v (SVEFF), effective potential temperature gradient (TGEFF), and initial turbulence intensities (ambiy and ambiz) and computes mean wind speed, σw, and σv at 30 meters (U30, SW30 and SV30, respectively). The second option, STREAMLINE, when used in combination with the AWMAUTURB keyword, modifies the A&WMA equations for streamlined buildings.

Beginning with version 21112, the A&WMA's formulation was extended to use final momentum plume rise height to initially compute effective wind speed (UEFF), effective σ_w (SWEFF), effective σ_v (SVEFF), effective potential temperature gradient (TGEFF), and initial turbulence intensities (ambiy and ambiz) and then uses the PRIME computed plume rise at each downwind distance, and as with AWMAUTURB, computes mean wind speed, σ_w, and σ_v at 30 meters (U30, SW30 and SV30, respectively). This newer ALPHA option is enabled by using the keyword AWMAUTURBHX. The STREAMLINE option is available for use with AWMAUTURB and AWMAUTURBHX.

AWMAENTRAIN - Entrainment Constants

The AERMOD PRIME algorithm defines two entrainment constants, alpha (A) and beta (B), to solve equations for conservation of mass, energy, and momentum. These are not to be confused with the ALPHA and BETA option designations in AERMOD. The programmed constant values for alpha and beta constants used in the PRIME algorithm in AERMOD are 0.11 and 0.6, respectively. As discussed previously, AERMOD has been shown to overpredict in some cases. It has been proposed by A&WMA that this overprediction is due in part to an underprediction of plume rise, and the PRIME plume rise algorithm has not been tested against field or wind tunnel observations for building wake applications. A&WMA also suggests that the entrainment constants in the PRIME algorithm differ from those determined by other researchers. Based on wind tunnel observations and variation in the values of the alpha and beta entrainment constants (results to be published), A&WMA found that best performance was

based on a change in the beta entrainment constant value from 0.6 to 0.35. Beginning with version 21112, a new ALPHA option was included in AERMOD based on A&WMA's proposed change to the beta entrainment constant of a value of 0.35. The AERMOD programmed value of 0.6 can be overridden with the value 0.35 by specifying the keyword AWMAENTRAIN in combination with AWMADWNW.

B.2.5.3 PLATFORM

The platform downwash algorithm from OCD has been implemented in AERMOD as an ALPHA option to account for the treatment of building downwash effects from offshore platforms with the current AERMOD single boundary layer parameterization limitation. The platform downwash parameterization can be applied to the POINT, POINTHOR, and POINTCAP source types in AERMOD using the primary keyword PLATFORM in the SO pathway.

The OCD model was originally developed by the Mineral Management Service (MMS), now BOEM, in the 1980s for estimating plume transport and dispersion in marine and coastal environments (Hanna et al., 1985). OCD, like AERMOD, is a steady-state Gaussian dispersion model that simulates plume transport and dispersion based on boundary layer meteorological parameters. Like many of AERMOD's predecessors, boundary layer parameterization is based on the older P-G stability classes.

The original platform downwash algorithms were developed by Petersen (1986) and then slightly modified and incorporated in the OCD model (Hanna and Dicristofaro, 1988). These algorithms use the platform parameters to enhance the initial dispersion of the emission plume in a range of distances based on the distance from the emission source and the total height of the buildings and platform relative to the height of the emission release.

In Petersen's original formulation, additional initial dispersion added due to the presence of a platform in the lateral (y) and vertical (z) dimension is defined when $2.2 < x/H_b < 12.6$:

$$\sigma'_{y0} = [1.9 + 48.2(2x/W)^{-1.4}]^{0.5}$$
$$\sigma'_{z0} = [3.0 + 40.2(x/H_b)^{-1.4}]^{0.5}$$

where W is the platform width, H_b is the total height of the platform which is defined as the height above the sea surface of the top of highest influential building, and x is the distance downwind from the source. When x/H_b is outside this range, use x/H_b = 2.2 or x/H_b = 12.6 to determine the initial dispersion.

Modifications to Petersen's original platform downwash formulation were needed to make them applicable in all conditions for which the OCD model may be applied. The additional initial dispersion added due to the presence of a platform in the lateral (y) and vertical (z) dimension is defined when $2.2 < x/H_b < 12.6$:

$$\sigma'_{y0} = 0.071x[1.9 + 48.2(2x/W)^{-1.4} - 1]^{0.5}$$
$$\sigma'_{z0} = 0.11x^{0.81}[3.0 + 40.2(x/H_b)^{-1.4} - 1]^{0.5}$$

The additional initial dispersion due to the platform was added in quadrature to the lateral and vertical dispersion calculated without the platform.

AERMOD considers multiple plumes to derive a total solution for pollutant impacts under certain conditions. In a convective environment, AERMOD will define as few as one plume when the release is injected above the mixed layer or as many as three distinct plumes when the release is below the mixed layer which include the direct plume, the indirect plume, and the penetrated plume. In addition, the direct and indirect plumes each have distinct updraft and downdraft components. Separate lateral dispersion coefficients (σ_y) are computed for each

of the three plumes. Separate vertical dispersion coefficients (σ_z) are computed for each of the updraft and downdraft components of the direct and indirect plumes and the penetrated plume when defined. In a stable environment, a single plume is also defined.

In AERMOD σ_y and σ_z are computed as the root mean square of multiple components, commonly referred to addition in quadrature, including ambient turbulence and Buoyancy Induced Dispersion (BID). For sources subject to platform downwash, lateral and vertical dispersion components due to downwash have been incorporated into the appropriate root mean square equations. The downwash component was added to the solution for σ_y for a plume in a stable environment as well as the direct and penetrated plumes in an unstable environment. The downwash component was added to the solution for σ_z for a plume in a stable environment, the updraft and downdraft components of the direct plume in a convective environment, and a penetrated plume in a convective environment when defined.

The integration of the OCD platform downwash algorithm into AERMOD requires only three additional inputs beyond those required for POINT, POINTHOR, and POINTCAP source types to define the platform. These inputs generally mimic those required by the OCD model with some modification to their definitions, for adaption to AERMOD. These inputs, as well as stack height, as assumed and interpreted by AERMOD, are described below:

Stack height: Height of the release point above the sea surface. NOTE: This is input with the POINT, POINTCAP, or POINTHOR keyword on the SO card.

Building height (H_b): Height above the sea surface of the top of the tallest structure that could influence downwash. NOTE: This is input with the PLATFORM keyword on the SO card.

Platform width (W): Assuming a rectangular platform, the shorter of the two sides when comparing the lateral distance across the left most and right most buildings or structures

on the platform that can contribute to downwash. NOTE: This is input with the PLATFORM keyword on the SO card.

Platform base height (Zelp): The height of the bottom of the platform above the sea surface. NOTE: This is input with the PLATFORM keyword on the SO card.

There are several differences between the OCD and AERMOD models with respect to default model behaviors. AERMOD, by default and part of the regulatory formulation of AERMOD, applies stack-tip downwash, gradual plume rise, and buoyancy induced dispersion while OCD while none of these are part of the regulatory formulation of OCD. Thus, by default, AERMOD will apply stack-tip downwash, gradual plume rise, and buoyancy induced dispersion for a platform source consistent with all other POINT, POINTHOR, and POINTCAP source types.

B.2.5.4 SWPOINT

Based on studies performed by researchers at Cornell University, a new source type, SWPOINT, was added beginning with AERMOD version 21112 to further study the phenomenon researchers have coined as "sidewash" which is a lateral shift of the building wake cavity that forms on the lee side a building that occurs when the wind is oblique to one of the longer sides of an elongated building. Yang et al. (2020) investigated the flow structures and concentration fields under oblique wind conditions. A key finding was that the flow is not only entrained downward (downwash) but also directed by the oblique wind along the building leeward surface (sidewash), which creates a sidewash-downwash (S-D) vortex. This S-D vortex causes the plume to shift in the lateral direction.

As a research tool, the SWPOINT source has several limitations that need to be highlighted for the user who uses the SWPOINT source type to investigate and study the sidewash effect. These limitations include the following:

- Produces downwind concentrations from short stacks assumed to be centered along the leeward side of elongated buildings. Refer to Figure X below for an illustration of the assumed stack location with respect to the building and wind flow orientation.
- Model concentrations are limited to the building wake cavity. Impacts at receptors outside or in the transition zone from the building wake cavity are not calculated.
- Terrain impacts are not considered.
- Plume rise due to mechanical and thermal buoyancy is not considered.
- Building representation is assumed to be rectangular.
- PRIME downwash is not applied.
- SWPOINT sources have not been configured for use with EVENT processing, NO_X-to-NO_2 conversion methods, or the MAXDCONT source culpability processing.
- Stack top wind speeds below approximately 2 m/s have been shown to cause anomalously high concentrations. This parameter is quite sensitive and currently can shift from reasonable predicted concentrations to values several orders of magnitude with the adjustment of a few tenths of a meter per second.

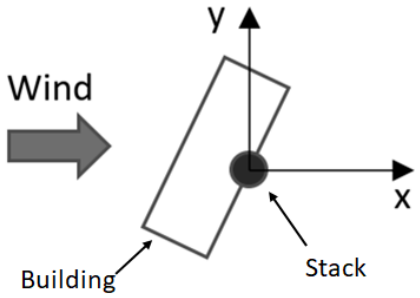

Figure B – 2. Fixed Stack location with respect to Building and Wind Flow Orientation

B.2.6 Low Wind Conditions (LOW_WIND)

To further explore the performance of AERMOD during low wind conditions and investigate possible improvements to AERMOD performance, the primary keyword LOW_WIND is available on the CO pathway to override default values for several variables and

default behavior. The EPA has identified two areas of model improvements to address these low wind issues:

1. Plume meander: adjustments to the treatment of plume meander within AERMOD and the modifications to the meander components, and

2. Meteorology and turbulence: adjustments to the minimum turbulence values, specifically the minimum sigma-v value and the sigma-w value, which are components of the turbulence, as well as the minimum wind speed, which is closely tied to the minimum turbulence values.

Using the LOW_WIND primary keyword, users can override the following:

- Adjustments to met
    - Minimum sigma-v - standard deviation of horizontal velocity, a turbulence parameter that impacts the horizontal size of the plume. Estimates of sigma-v in low wind conditions are often too small (approaching zero), requiring a minimum value to be set. During these low wind conditions, plume volumes are inherently small, generally resulting in higher concentrations. Increasing the minimum sigma-v will result in lowering the maximum concentrations estimated for surface releases.

    - Minimum wind speed – limits the calculated wind speed computed in the wind profile.
        - The model formulation has the minimum wind speed correlated to the minimum sigma-v.

        - AERMET uses the 2*sigma-v to reset low winds, this is applied more broadly in AERMOD as a check against effective wind speeds (i.e., the AERMET restriction is applied at the meteorology measurement height, but applied at different heights on the profile in AERMOD)

$$u_{min} = \sqrt[2]{2 * \sigma_v^2}$$

- Minimum sigma-w - standard deviation of vertical velocity, a turbulence parameter that impacts the vertical size of the plume. Estimates of sigma-w in low wind conditions are often too small (approaching zero), requiring a minimum value to be set. During these low wind conditions, plume volumes are inherently small, generally resulting in higher concentrations. Increasing the minimum sigma-w will result in lowering the maximum concentrations estimated for surface releases.

- Adjustments to dispersion

  - Plume meander/Lower and upper limit of FRAN – The Fraction of the Random plume, or FRAN, is the weighting factor used to average the direct or coherent plume and the random or pancake plume. The default range of FRAN in AERMOD is 0.0 - 1.0. These user-defined adjustments were added to off-set other adjustments to the meteorology result from the low wind options. Lowering the value of FRAN in general will increase concentrations.

$$C_{c,s} = C_{Ch}(1 - \sigma_r^2/\sigma_h^2) + C_R(\sigma_r^2/\sigma_h^2)$$

  - Big T – The random plume time scale, of Big T, is a scaling parameter that indicates the time lapse for which mean wind information at the source is no longer correlated with the location of plume material at a downwind receptor. Changing this term will increase the FRAN for any particular situation, but the impact is also distance-dependent, so the computed value will be larger at greater distances (i.e., the random portion of the plume will be larger at greater distances).

    - RLINE does not account for this distance dependence and in general, the meander computation is slightly different in RLINE.

$$\sigma_r^2 = 2\tilde{\sigma}_v^2 + \bar{u}^2(1 - \exp(-x_r/\tilde{u}T_r))$$

  - Momentum Balance FRAN Method - Alternate momentum balance (PBAL) approach to determine plume meander which overrides the default energy balance approach.

B.2.6.1 More on FRAN Momentum Balance Method

AERMOD accounts for plume meander by interpolating between two concentration limits: the coherent plume limit (assumes that the wind direction is distributed about a well-defined mean direction with variations due solely to lateral turbulence) and the random plume limit (assumes an equal probability of any wind direction).

Once these two concentration limits (C_{Ch} - coherent plume; C_R - random plume) have been calculated, the total concentration for stable or convective conditions ($C_{c,s}$) is determined by interpolation. Interpolation between the coherent and random plume concentrations is accomplished by assuming that the total horizontal "energy" is distributed between the wind's mean and turbulent components. That is,

$$C_{c,s} = C_{Ch}(1 - \sigma_r^2/\sigma_h^2) + C_R(\sigma_r^2/\sigma_h^2) \qquad \text{(Equation B-6)}$$

where σ_{h^2} is a measure of the total horizontal wind energy and σ_{r^2} is a measure of the random component of the wind energy. Therefore, the ratio $\sigma_{r^2}/\sigma_{h^2}$ is an indicator of the importance of the random component and can be used to weight the two concentrations as done in Equation B-8.

The horizontal wind is composed of a mean component $\bar{u}$, and random components σ_u and σ_v. Thus, a measure of the total horizontal wind "energy" (given that the along-wind and crosswind fluctuations are assumed equal i.e., $\sigma_u = \sigma_v$), can be represented as:

$$\sigma_h^2 = 2\tilde{\sigma}_v^2 + \bar{u}^2 \qquad \text{(Equation B-7)}$$

where $\bar{u} = (\tilde{u}^2 - 2\tilde{\sigma}_{v^2})^{1/2}$, where u is the mean component of the wind. The random energy component is initially $2\tilde{\sigma}_{v^2}$ and becomes equal to σ_{h^2} at large travel times from the source when information on the mean wind at the source becomes irrelevant to the predictions of the plume's

position. The evolution of the random component of the horizontal wind energy can be expressed as:

$$\sigma_r^2 = 2\tilde{\sigma}_v^2 + \bar{u}^2(1 - \exp(-x_r/\tilde{u}T_r)) \qquad \text{(Equation B-8)}$$

where T_r is a time scale (= 24 hours) at which mean wind information at the source is no longer correlated with the location of plume material at a downwind receptor.

The current blending between the coherent and random plume in AERMOD is based on the relative amount of energy indicated by the mean horizontal wind versus the energy indicated by the standard deviation in the horizontal winds. Recall that the formula for kinetic energy (KE) is:

$$KE = \frac{1}{2}m * v^2 \qquad \text{(Equation B-9)}$$

where *m* is mass and *v* is velocity.

Normally, the wind speed is a vector quantity. However, similarity theory, which is used to compute the AERMOD wind profile, treats the wind speed and wind direction separately, such that the wind speed is considered a scalar base-quantity. That is, a composite wind speed and wind direction are used rather than explicit values of the horizontal wind components (i.e., a north-south component and an east-west component). Accounting for wind speeds in the manner could result in an average wind speed of zero simply because the winds were from opposite directions in each part of the hour. The energy equation takes the dot-product of the wind speeds, resulting a scalar quantity as well. The result of using an energy-based balancing of the two wind speed values is that differences between the two are emphasized, particularly when one value is greater than one and the other is less than one. Under lower wind speeds, the horizontal fluctuations are typically larger (low winds are often characterized by frequent and wind changes in the wind direction, even though the wind speeds may be low). As wind speeds

increase, the horizontal fluctuations typically decrease. While the horizontal fluctuations are all generally less than 1 m/s (in fact, horizontal fluctuations are typically less than 0.5 m/s), the wind speed is typically greater than 1 m/s. When the winds increase, the use of an energy balance, which is a quadratic function of the wind speeds, will rapidly decreases the fraction of the random plume.

An alternative to using an energy balance would be to use a momentum balance. Recall that the equation for momentum (P) is:

$$P = m * v \qquad \text{(Equation B-10)}$$

The use of a momentum also differs from the energy approach in several ways:

- The momentum will vary linearly rather than a quadratic function of the wind speeds. As a result, divergence in the values will be less emphasized than in the current formulation. The result will be that fraction of the random plume will generally be larger at higher wind speeds.

- In contrast to the energy balance, a momentum balance would be a vector-based quantity, which is in some ways is more consistent with the concept of transport of a pollutant via winds, which will have a direction dependency (i.e., a vector dependency).

The momentum-based approach is applied as the square root of the random plume fraction.

B.2.7 PSD Credit (PSDCREDIT)

Due to the ozone limiting effects of the PVMRM option, the predicted concentrations of NO2 are not linearly proportional to the emission rate. Therefore, the approach of modeling NO2 increment consumption with PSD credits through the use of a negative emission rate for credit sources cannot be used with the PVMRM option.

Increment is the maximum allowable increase in concentration of a pollutant above a baseline concentration for an area defined under the Prevention of Significant Deterioration (PSD) regulations. The PSD baseline area can be an entire State or a subregion of a State such as a county or group of counties. Increment consumption is the additional air quality impact above a baseline concentration.

The baseline concentration is the ambient concentration of the pollutant that existed in the area at the time of the submittal of the first complete permit application by any source in that area subject to PSD regulations. A baseline source is any source that existed prior to that first application and the baseline date is the date of the PSD application. This baseline date is referred to as the minor source baseline date in PSD regulations. By definition, baseline sources do not consume increment. However, any baseline source that retires from service after the baseline date expands the increment available to new sources. Therefore, a PSD modeling analysis performed for a new source may need to account for this increment expansion. Such an analysis may therefore involve identification of three groups of sources: 1) increment-consuming sources; 2) retired (increment-expanding) baseline sources; and 3) existing, non-retired, baseline sources.

Calculating increment consumption under the PSDCREDIT option in AERMOD is not a simple arithmetic exercise involving the three groups of sources defined above. Since the amount of ozone available in the atmosphere limits the conversion of NO to NO2, interactions of plumes from the existing and retired baseline sources with those from the increment consuming sources must be considered as part of the calculation of net increment consumption.

Without the PSDCREDIT option, properly accounting for the potential interaction of plumes among the different source categories would require post-processing of results from multiple model runs. Internal processing algorithms have been incorporated in AERMOD under the PSDCREDIT option to account for the apportioning of the three groups of sources to properly calculate increment consumption from a single model run.

Defining the following three source groupings for the discussion that follows:

A = increment-consuming sources;

B = non-retired baseline sources; and

C = retired baseline, increment-expanding sources.

The calculation of the amount of increment consumption by the A sources cannot simply be estimated by modeling the **A** sources alone because of the possible interaction of those plumes with the plumes from **B** sources. The PVMRM algorithm is designed to account for such plume interactions and calculate the total NO to NO_2 conversion in the combined plumes based on the amount of ozone available. Therefore, the total increment consumption by the **A** sources is given by the difference between (1) the total future impact of increment consuming sources and non-retired baseline sources (**A**+**B**) and (2) the total current impact (**B**), which can be expressed as (**A**+**B**) – (**B**). Here (**A**+**B**) represents the value that would be compared against the National Ambient Air Quality Standard (NAAQS) for NO_2 during PSD review of the **A** sources.

In a case where some of the baseline sources have been retired from service (**C** sources), the PSD regulations allow the consideration of increment expansion when assessing compliance with the PSD increment. However, the amount of increment expansion cannot be estimated by simply modeling the **C** sources alone because of the possible interaction of those plumes with the plumes from **B** sources. Therefore, the total increment expansion, i.e., PSD credit, is calculated as the difference between (1) the total impact prior to the retirement of **C** sources, i.e.

(**B**+**C**), and (2) the total impact from existing (non-retired) baseline sources (**B**), which can be expressed as (**B**+**C**) – (**B**).

Finally, the net increment consumption is given by the difference between total increment consumption and the total increment expansion, or

$$[(\mathbf{A}+\mathbf{B}) - (\mathbf{B})] - [(\mathbf{B}+\mathbf{C}) - (\mathbf{B})] \qquad \text{(Equation B-11)}$$

Note that in the absence of any increment expansion, the net increment consumption is equal to the total increment consumption [(**A**+**B**) – (**B**)], as described above.

These expressions of net increment consumption and expansion cannot be interpreted as algebraic equations. Instead, the terms within parentheses represent the results of separate model runs that account for the combined effects of NOx conversion chemistry on specific groups of sources. The expression shown in Equation B-11 above represents four model simulations: (**A**+**B**), (**B**), (**B**+**C**), and (**B**) again. In this case, the two (**B**) terms do cancel each other, and we are left with:

$$[(\mathbf{A}+\mathbf{B})] - [(\mathbf{B}+\mathbf{C})] \qquad \text{(Equation B-12)}$$

The expression presented in Equation B-12 summarizes how the net increment consumption calculation is performed under the PSDCREDIT option. Under this option, AERMOD first models the **A** and **B** groups together, then models the **B** and **C** groups together, and finally computes the difference to obtain the desired result, i.e., the value to compare to the PSD increment standard. For AERMOD to perform the special processing associated with this option, the user must define which sources belong to each of the groupings defined above.

B.2.8 Deposition Options

The AERMOD model includes algorithms for both dry and wet deposition of both particulate and gaseous emissions. The deposition algorithms incorporated into AERMOD are based on the draft Argonne National Laboratory (ANL) report (Wesely et al., 2002), with modifications based on peer review. Treatment of wet deposition was revised from Wesely et al. (2002) based on recommendations by peer review panel members (Walcek et al., 2001). A full technical description of the deposition algorithms implemented in AERMOD is provided in an EPA report specific to these algorithms (U.S. EPA, 2003b).

Based on the guidance provided for application of the AERMOD model in the Guideline (U.S. EPA, 2024b), and the history of the deposition algorithms in the AERMOD and ISC models, the particle deposition algorithms with a user-specified particle size distribution (referred to below as "Method 1") can be applied simultaneously with the regulatory DFAULT keyword. Method 1 is comparable to the particle deposition algorithm in the ISCST3 model (EPA, 1995a). The gas deposition algorithms and the "Method 2" option for particle deposition based on the ANL draft report (Wesely, et al, 2002) are non-regulatory ALPHA options in AERMOD, and beginning with version 19191, the model will issue a fatal error message and abort processing if the ALPHA keyword is not specified with the gas deposition or Method 2 particle deposition options.

Table B - 1. Summary of Deposition Options

Pollutant Type	Model Output Type	Required Keywords	Allowed under DFAULT?
Gaseous	CONC w/dry depletion DDEP	CO GASDEPVD or CO GDSEASON, CO GDLANUSE, and SO GASDEPOS	No[1]
Gaseous	CONC w/wet depletion WDEP	SO GASDEPOS	No[1]
Gaseous	CONC w/dry & wet depletion DEPOS	CO GDSEASON, CO GDLANUSE, and SO GASDEPOS	No[1]
Particulate ("Method 1")	CONC w/dry and/or wet depletion DEPOS DDEP WDEP	SO PARTDIAM, SO PARTDENS, and SO MASSFRAX	Yes[2]
Particulate ("Method 2")	CONC w/dry and/or wet depletion DEPOS DDEP WDEP	SO METHOD_2	No[1]

[1]The ALPHA option must be included.

[2]While "Method 1" is allowed under the regulatory "DFAULT" option within AERMOD, the use of "Method 1" for particulate emissions in regulatory modeling applications should follow the guidance provided in Section 7.2.1.3 of the Guideline (U.S. EPA, 2024b).

The user should be aware that one or more of the following meteorological parameters are needed for deposition: precipitation code, precipitation rate, relative humidity, surface pressure, and cloud cover.

B.2.9 Time Travel Reaction Method (TTRM/TTRM2)

Beginning with version 21112, the Travel Time Reaction Method (TTRM) was added as an ALPHA option for NO_2 conversion that considers the distance and the travel time from the emission source to each receptor. In general, much of the conversion of NO to NO_2 occurs within the first minute of travel which limits the effectiveness of this method to the near field receptors. PVMRM, OLM, and ARM2 assume the reaction involving NO and available O_3 to form NO_2 occurs instantaneously. Although this chemical reaction is relatively rapid, it is not actually instantaneous and depends on the transport time to the downwind receptor of interest. TTRM, was initially implemented as a stand-alone ALPHA option which can determine the initial fraction of NO to NO_2 conversion in the travel time of each source emissions to each receptor. The conversion is capped at an upper limit, which is typically reached after a few tens of seconds of plume travel. Beyond the distance the fraction reaches the upper limit of the equilibrium fraction (generally 0.9), TTRM is no longer effective, and another method is needed for receptors beyond that distance.

Beginning with version 22112, TTRM was integrated more fully into AERMOD to be used simultaneously with PVMRM, OLM, or ARM2. This integration was also added as the ALPHA option, TTRM2, separate from TTRM which was retained as a stand-alone option. When TTRM2 is specified along with PVMRM, OLM, or ARM2, TTRM will be implemented for near field receptors where the fraction of conversion has not reached the upper limit, and the other specified method will be used for all other receptors.

Though the NO_X chemistry regime can involve a larger number of reactions, it is fairly well understood and can be parameterized to include a wide range of the relevant reactions. However, in the near-field (i.e., time scales on the order of minutes), the dominant reactions during the daytime are between NO, NO_2, and O_3 include:

$O_3 + NO \rightarrow NO_2 + O_2$ (k1) (Reaction 1)

$O_2 + NO_2 + h\nu \rightarrow NO + O_3$ (k2) (Reaction 2)

where k1 and k2 are the reaction rate constants for each reaction and hv is the incident solar radiation.[3]

These reactions (i.e., Reactions 1 and 2) are often summarized to emphasize the main reaction pathways commonly described as the pseudo-steady state (PSS) approximation. The steady-state assumption is based on the fact that both reactions are relatively and equally fast so equilibrium is reached quickly such that the reaction rate is the product of the reaction rate constant (i.e., k1 or k2) and the concentration of the reactants. So, when steady state is assumed, the reaction rates are equal and can be expressed as:

$$k1[O_3][NO] = k2[NO_2] \qquad \text{(Equation B-13)}$$

where $k1 = (15.33/T) \exp(-1450/T)$ ppb^{-1} sec^{-1}, $k2 = 0.0167\exp(-0.575/\cos(\theta))$ sec^{-1}, θ = zenith angle of sun (function of location latitude and time of day), and T is the ambient temperature in Kelvin (see equations 10 and 11 in Hanrahan, 1999). In the context of modeling with AERMOD, where NO is released and NO_X is conserved, NO can be removed from Equation B-13 by using the following relationship:

$$NO = NO_X - NO_2 \qquad \text{(Equation B-14)}$$

Substituting Equation B-14 into Equation B-13 and solving for NO_2/NO_X gives the following relationship:

$$[NO_2] / [NO_X] = (k1[O_3]) / (k2 + k1[O_3]) \qquad \text{(Equation B-15)}$$

Based on Equation B-15, the PSS ratio of NO_2/NO_X is a function of O_3, temperature, and sunlight. It should be noted that this solution assumes O_3 has reached PSS and thus, the reaction is not O_3 limited. The solution of this equation can provide a theoretical maximum for the NO_2/NO_X ratio.

The time-component (t) of this reaction can be computed based on reaction 1 and the value of k1, giving the expression:

$$d[NO]/dt = k1[NO][O_3] \qquad \text{(Equation B-16)}$$

Following the rearrangement and integration of Equation B-16, the relationship becomes:

$$\ln [NO] = - k1[O_3]t + C \qquad \text{(Equation B-17)}$$

where C is some constant. The constant, C, can be determined with the boundary conditions, when t = 0 and [NO] equals the starting NO concentration, $[NO]_o$. In this case, C = ln $[NO]_o$ and the integrated form for [NO] as a function of time can be expressed as:

$$\ln [NO] = - k1[O_3]t + \ln [NO]_o \qquad \text{(Equation B-18)}$$

Following the rearrangement of Equation B-18, the fraction of NO remaining can be expressed as:

$$[NO]/[NO]_o = \exp (-k1[O_3]*t) \qquad \text{(Equation B-19)}$$

Then the difference of the remaining NO converted to create NO_2 can be expressed as the fraction of NO converted to create NO_2 or NO_{frac}:

$$NO_{frac} = 1 – \exp(-k1[O_3]*t). \qquad \text{(Equation B-20)}$$

As shown by Hanrahan (1999) and detailed above, the reaction rate, k1, can be modified by the ambient temperature (T_{amb}, degree Kelvin). Equation B-20 provides an expression for calculating the travel time reaction of the NO-to-NO_2 conversion by O_3 in modeling systems.

Figure B-3 illustrates the fractional conversion of emitted NO to NO_2 (i.e., NO_{frac}) as a function of O_3 and travel time for three examples of ambient O_3 levels, assuming that the ambient temperature is 298 K in equation 9 and then substituting k into Equation B-20. Note that the fraction of NO converted NO_2 in the atmosphere needs to account for the in-stack NO_2 as well. For example, if the in-stack NO_2 is 10% of the emissions and 50% of the remaining NO is converted to NO_2, then the total NO_2 fraction is 0.10 + 0.5*0.9 = 0.55.

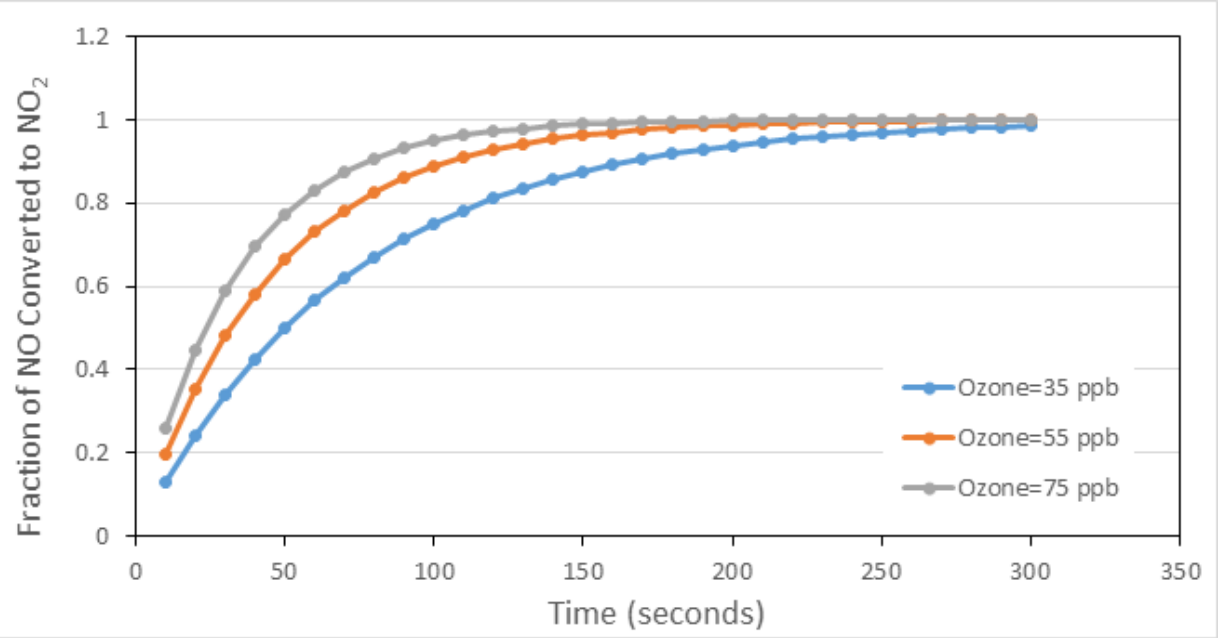

Figure B - 3. Conversion fraction of NO-to-NO2 as a function of O3 and travel time.

It is evident from Figure B-3 that after one minute of travel, much of the NO (for which there is available ozone) has been converted to NO_2, except for cases with low ambient ozone levels where much of the NO has been converted to NO_2 after two minutes of travel. However, there could be cases with well under a minute or two of travel time for which the reaction time conversion fraction is an important consideration. It is to be noted that this forward reaction (to convert NO to NO_2) is complemented later by an equilibrium state with another photochemical reaction that converts NO_2 to NO in the opposite direction in the presence of sunlight.

Therefore, the converted NO_2 fraction noted above is not an equilibrium result, but it can act as a lower limit to the conversion in the first minute after fresh NO is emitting from a source.

The TTRM option determines the initial fraction of NO-to-NO_2 conversion (i.e., NO_{frac}) in the travel time of each source emissions to each receptor. As shown in Figure B-3 and Table B-2, this option is most important for refining NO_2 modeled impacts under short travel times and within minutes of emission. Further, the effect of this option is most evident at near-field receptors or at distances within a kilometer of the emission source (see Table B-2). The method used in TTRM also assumes that the conversion is capped at an upper limit, which is typically reached within minutes of plume travel. Once the fraction reaches the upper limit of the equilibrium fraction (generally 0.9) with the calculation noted above, this reaction for further travel times is no longer an issue. Beyond these distances, other factors would play a greater role in NO conversion. Therefore, the implementation of this method could be considered as a refinement for Tier 3 options, rather than a stand-alone option in AERMOD, with the TTRM method providing the approach for NO_2 concentrations in the near-field and the Tier 3 options dominant elsewhere in the modeling domain.

Table B - 2. Conversion Fraction of NO to NO2 as a function of Ozone Concentration, Transport Time, and Wind Speed

Travel Time (seconds)	Conversion Fraction of NO to NO_2			Distance from Source [m]		
	Ozone = 35 ppb	Ozone = 55 ppb	Ozone = 75 ppb	Wind Speed = 1 m/s	Wind Speed = 5 m/s	Wind Speed = 10 m/s
10	0.130	0.196	0.257	10	50	100
20	0.242	0.353	0.448	20	100	200
30	0.340	0.480	0.590	30	150	300
40	0.426	0.582	0.696	40	200	400
50	0.500	0.664	0.774	50	250	500
60	0.565	0.730	0.832	60	300	600
120	0.811	0.927	0.972	120	600	1200
180	0.918	0.98	0.995	180	900	1800
240	0.964	0.995	0.999	240	1200	2400
300	0.984	0.999	1.000	300	1500	3000

The information needed to use this method and calculate the travel time reaction of the NO-to-NO_2 conversion in AERMOD is already available in the model, including the hourly ambient temperature provided in the meteorological inputs and ambient O_3 data when Tier 3 NO_2 conversion options are used in AERMOD. The method also involves some assumptions to calculate the travel time reaction, where the travel time reaction is dependent on which plume type (i.e., coherent or meander plume) has the larger weighting fraction and the hourly effective wind speed at plume height. Plume type is important for determining the algorithm that will be used for calculating the distance relative to the emission source and receptor location and wind direction. The distance algorithm can be based on a downwind, radial, or crosswind distance in AERMOD (see Figure B-4). For point and volume sources, the downwind distance is used with coherent dominant plumes at a receptor and radial distance is used with meander dominant plumes. The radial distance from the center of the emission source is used for all area sources. The crosswind distance does not factor in the TTRM calculations. AERMOD also calculates effective wind speeds based on plume type, where calculations may use the standard effective wind speed, penetrated effective wind speed, or direct effective wind speed.

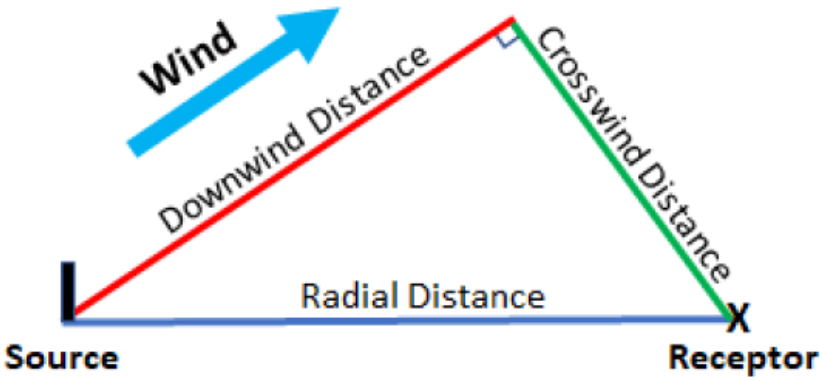

Figure B - 4. Distance Terms in AERMOD Relative to Source and Receptor Location and Wind Direction.

Once the most appropriate distance and effective wind speeds are determined, the reaction rate can be calculated and used to determine the NO_{frac}. As noted above, this fractional value is capped at the NO_2 Equilibrium level that by default in AERMOD is set to 90 percent. As with the Tier 3 methods, an in-stack NO_2 contribution is calculated from the hourly NO value and the remaining available NO is then scaled by NO_{frac} and added to the in-stack contribution to obtain the total NO_2 from each source at each receptor. The next step involves selecting the lower predicted NO_2 impact for each source and receptor. Thus, for receptors beyond the distance needed for the TTRM method to achieve a 90 percent conversion of NO to NO_2, the standard Tier 2 or 3 method would dictate the result. At closer distances, the lower fraction between the TTRM method and the Tier 2 or 3 method would dictate the result.

B.2.10 Highly Buoyant Plume (HBP)

Beginning with AERMOD version 23132, the highly buoyant plume (HBP) option was added as an ALPHA option. The HBP option was developed to refine AERMOD's treatment of hot buoyant plumes that penetrate the top of the convective mixed layer into the stable layer above. The formulation is based on the work of Weil (2020) and further refined by Warren et al. (2022) who have demonstrated an overprediction of concentrations at the surface for some hours due to what the authors describe as a premature mixing of the penetrated plume back into the mixed layer and down to the surface. Observations show that the penetrated plume resides in the stable layer until, through surface heating, the depth of the mixed layer grows until the top of the mixed layer intercepts the plume (Moore, 1988; Weil, 1997).

In short, Warren et al. (2022) state that the current formulation of AERMOD overstates vertical plume depth by overestimating sigma-z of the penetrated plume which represents the vertical dispersion of the plume. This assumes that a portion of the penetrated plume extends down into the mixed layer prior to when the mixed layer would reach a height to intersect the plume, resulting in premature mixing of the plume to the ground. The revised approach, implemented as the HBP alpha option, compares the convective mixing height of the current hour and next hour to determine how much the convective layer has grown over the hour and

the amount of the plume that has been mixed into the convective layer by the end of the current hour which determines the amount of plume allowed to mix down to the ground (Warren et al., 2022).

B.2.11 Area Meander (AREAMNDR)

Beginning with AERMOD version 23132, plume meander has been added as an ALPHA option for area sources (AREAMNDR), including AREA, AREAPOLY, AREACIRC, and LINE source types. This option applies the plume meander algorithms used with POINT and VOLUME source types to the area source types listed above, but with limitations.

Generally, model runtimes associated with area sources (without meander applied), can be significantly longer than those of POINT and VOLUME, because of the double integral formulation and numerical integration computations coded for resolving area source plume dimensions in the alongwind and crosswind directions. Activating plume meander for area sources, therefore, doubles the number of calculations and computational demands needed to resolve area source dimensions for both the coherent and meander plumes. As such, processing time is increased by approximately 30-50% when meander is applied to area sources.

The current implementation of area meander as an ALPHA option limits the receptors for which meander is applied. Moreover, meander is not being calculated for upwind receptors which affects both upwind and downwind concentrations; this is inconsistent with point and volume source meander. In addition, there remain scientific concerns with applying the meander algorithms developed for POINT and VOLUME source types to area source types. Additional research is required.

B.2.12 Aircraft Plume Rise (ARCFTOPT)

An ALPHA option to treat plume rise from aircraft emissions, sponsored by the Federal Aviation Administration (FAA), was added to AERMOD beginning with version 23132. Aircraft emissions from jet engines experience plume rise from both momentum and buoyancy but are commonly modeled as AREA and VOLUME source types in AERMOD which do not account for either momentum or buoyancy. The aircraft plume rise ALPHA option extends the formulation of AREA and VOLUME sources with additional input parameters based on the work of Pandey, et. al. (2023). AREA and VOLUME sources that include hourly varying aircraft input parameters can be identified through the source block keyword ARCFTSRC. The current implementation of aircraft plume rise requires that an additional seven aircraft parameters be supplied to AERMOD using an hourly varying emissions input file.

References

AECOM, 2010: AERMOD Low Wind Speed Evaluation Study Results. Prepared for the American Petroleum Institute and Utility Air Regulatory Group. Prepared by AECOM, Westford, MA. March 22, 2010.

Ahangar, F.E., Heist, D.K., Perry, S.G., and Venkatram, A. (2017). Reduction of air pollution levels downwind of a road with an upwind noise barrier. Atmospheric Environment, 155, pp. 1-10.

Andre, J. C. and L. Mahrt, 1982: The nocturnal surface inversion and influence of clean-air radiative cooling. *J.Atmos.Sci.,* **39,** 864-878.

Azzi M. and Johnson G (1992). An Introduction to the Generic Reaction Set Photochemical Smog Mechanism. Proc. 11th Clean Air Conf. 4th Regional IUAPPA Conf., Brisbane, Australia.

Baerentsen, J. H. and R. Berkowicz, 1984: Monte Carlo simulation of plume dispersion in the convective boundary layer. *Atmos.Environ.,* **18,** 701-712.

Baldauf, R., Thoma, E., Hays, M., Shores, R., Kinsey, J., Gullett, B., Kimbrough, S., Isakov, V., Long, T., Snow, R. and Khlystov, A. (2008). Traffic and meteorological impacts on near-road air quality: Summary of methods and trends from the Raleigh near-road study. Journal of the Air & Waste Management Association, 58(7), pp.865-878.

Baldauf, R.W., Heist, D., Isakov, V., Perry, S., Hagler, G.S., Kimbrough, S., Shores, R., Black, K. and Brixey, L. (2013). Air quality variability near a highway in a complex urban environment. Atmospheric environment, 64, pp.169-178.

Baldauf, R.W., Isakov, V., Deshmukh, P., Venkatram, A., Yang, B. and Zhang, K.M. (2016). Influence of solid noise barriers on near-road and on-road air quality. Atmospheric Environment, 129, pp.265-276.

Bange, P., L. Jannsen, F. Nieuwstadt, H. Visser, and J. Erbrink, 1991. "Improvement of the modeling of daytime nitrogen oxidation in plumes by using instantaneous plume dispersion parameters," *Atmos. Environ.*, **25A** (10), 2321-2328.

Barad, M. L., 1958: Project Prairie Grass, A Field Program in Diffusion. Geophysical Research Papers, No. 59, Vols. I and II, AFCRC-TR-58-235, Air Force Cambridge Research Center, 439pp.

Benson, P.E. (1992). A review of the development and application of the CALINE3 and 4 models. Atmospheric Environment. Part B. Urban Atmosphere, 26(3), pp.379-390.

Berkowicz, R., Olesen, J. R., and Torp, U., 1986: The Danish Gaussian air pollution model (OLM): Description, test and sensitivity analysis, in view of regulatory applications. *Air Pollution Modeling and Its Application.* De Wispelaire, V. C., Schiermeier, F. A., and

Grillani, N. V, Plemum, 453-481pp.

Bornstein, R. D., 1968: Observations of urban heat island effects in New York City. *J.Appl.Meteor.,* **7,** 575-582.

Bowne, N. E., R. J. Londergan, D. R. Murray, and H. S. Borenstein, 1983: Overview, Results, and Conclusions for the EPRI Plume Model Validation and Development Project: Plains Site. EPRI Report EA-3074, Project 1616-1, Electric Power Research Institute, Palo Alto, CA, 234 pp. 1983.

Brett, A. C. and S. E. Tuller, 1991: Autocorrelation of hourly wind speed observations. *J.Appl.Meteor.,* **30,** 823-833.

Briggs, G. A., 1969: Plume rise. USAEC Critical Review Series, TID-25075, NTIS, 81pp.

Briggs, G. A., 1971: Some recent analyses of plume rise observations. *Proceedings of the Second International Clean Air Congress.* Englund, H. M. and Berry, W. T., Academic Press, 1029-1032.

Briggs, G. A., 1973: Diffusion Estimation for Small Emissions. 1973 Annual Report, ATDL-106, Air Resources Atmospheric Turbulence and Diffusion Laboratory, Environmental Res. Lab., NOAA, Oak Ridge, TN.

Briggs, G. A., 1975: Plume rise predictions. *Lectures on Air Pollution and Environmental Impact Analysis.* Haugen, D. A., American Meteorological Society, 59-111pp.

Briggs, G. A., 1984: Plume rise and buoyancy effects. *Atmospheric Science and Power Production.* Randerson, D., U.S. Dept. of Energy, 327-366pp.

Briggs, G. A., 1988: Analysis of diffusion field experiments. *Lectures on Air Pollution Modeling.* Venkatram, A. and Wyngaard, J. C., American Meteorological Society, 63-117.

Briggs, G. A., 1993: Plume dispersion in the convective boundary layer. Part II: Analysis of CONDORS field experiment data. *J.Appl.Meteor.,* **32,** 1388-1425.

Brode, R. W., 2002: Evaluation of the AERMOD Dispersion Model.

Brost, R. A., J. C. Wyngaard, and D. H. Lenschow, 1982: Marine stratocumulus layers: Part II: Turbulence budgets. *J.Atmos.Sci.,* **39,** 818-836.

Businger, J. A., 1973: Turbulent transfer in the atmospheric surface layer. *Workshop on Micrometeorology.* Haugen, D. A., American Meteorological Society.

Businger, J. A., J. C. Wyngaard, Y. Izumi, and E. F. Bradley, 1971: Flux-profile relationships in the atmospheric surface layer. *J.Atmos.Sci.,* **28,** 181-189.

Carruthers, D. J., and Coauthors, 1992: UK atmospheric dispersion modelling system. Air Pollution Modeling and Its Application. Plenum Press, New York.

Carruthers, D.J., Stocker, J.R., Ellis, A., Seaton, M.D. and Smith, S.E. (2017). Evaluation of an explicit NOX chemistry method in AERMOD. Journal of the Air & Waste Management Association, 67(6), pp.702-712.

Carson, D. J., 1973: The development of a dry inversion-capped convectively unstable boundary layer. *Quart.J.Roy.Meteor.Soc.,* **99,** 450-467.

Caughey, S. J. and S. G. Palmer, 1979: Some aspects of turbulence structure through the depth of the convective boundary layer. *Quart.J.Roy.Meteor.Soc.,* **105,** 811-827.

Cimorelli, A. J., S. G. Perry, R. F. Lee, R. J. Paine, A. Venkatram, J. C. Weil, and R. B. Wilson, 1996: Current Progress in the AERMIC Model Development Program. Preprints, *89th Annual Meeting Air and Waste Management Association,* Air and Waste Management Association, Pittsburgh, PA.

Cimorelli, A. J., S. G. Perry, A. Venkatram, J. C. Weil, R. J. Paine, R. B. Wilson, R. F. Lee, W. D. Peters, R. W. Brode, and J. O. Paumier, 2002: AERMOD: Description of Model Formulation (Version 02222). EPA 454/R-02-002d. U. S. Environmental Protection Agency, Research Triangle Park, NC.

Cimorelli, A. J., S. G. Perry, A. Venkatram, J. C. Weil, R. J. Paine, R. B. Wilson, R. F. Lee, W. D. Peters, and R. W. Brode, 2005: AERMOD: A dispersion model for industrial source applications Part I: General model formulation and boundary layer characterization. *J.Appl.Meteor.* **44**, 682-693

Clarke, R. H., A. J. Dyer, R. R. Brook, D. G. Reid, and A. J. Troop, 1971: The Wangara experiment: boundary layer data. Technical Report No. 19, Division of Meteorological Physics CSIRO, Australia.

Cole, H.S. and J.E. Summerhays, 1979. "A review of techniques available for estimating short-term NO_2 concentrations," *J. Air Pollut. Control Assoc.*, **29**(8), 812-817.

Collier, L. R. and J. G. Lockwood, 1975: Reply to comment. *Quart.J.Roy.Meteor.Soc.,* **101,** 390-392.

Deardorff, J. W., 1970: Convective velocity and temperature scales for the unstable boundary layer for Rayleigh convection. *J.Atmos.Sci.,* **27,** 1211-1213.

Deardorff, J. W., 1972: Numerical investigation of neutral and unstable planetary boundary layers. *J.Atmos.Sci.,* **29,** 91-115.

Deardorff, J. W., 1979: Prediction of convective mixed-layer entrainment for realistic capping inversion structure. *J.Atmos.Sci.,* **36,** 424-436.

Deardorff, J. W., 1980: Progress in Understanding Entrainment at the Top of a Mixed Layer. Preprints, *Workshop on the Planetary Boundary Layer,* American Meteorological Society, Boston, MA.

DiCristofaro, D. C. *et al.*, 1985: EPA Complex Terrain Model Development: Fifth Milestone Report - 1985. EPA-600/3-85-069, U. S. Environmental Protection Agency, Research Triangle Park, North Carolina.

Dyer, A. J., 1974: A review of flux-profile relationships. *Bound.Layer Meteor.,* **7,** 363-372.

Fairall, C.W., E.F. Bradley, J.E. Hare, A.A. Grachev, and J.B. Edson, 2003: Bulk Parameterization of Air-Sea Fluxes: Updates and Verification for the COARE Algorithm. *J. Climate*, **16**, 571-591.

Finn, D., Clawson, K.L., Carter, R.G., Rich, J.D., Eckman, R.M., Perry, S.G., Isakov, V. and Heist, D.K. (2010). Tracer studies to characterize the effects of roadside noise barriers on near-road pollutant dispersion under varying atmospheric stability conditions. Atmospheric Environment, 44(2), pp.204-214.

Garratt, F. R., 1992: *The Atmospheric Boundary Layer.* Cambridge University Press, New York, New York, 334pp.

Gifford, F. A., 1961: Uses of routine meteorological observations for estimating atmospheric dispersion. *Nuclear Safety,* **2,** 47-51.

Hanna, S. R., 1983: Lateral turbulence intensity and plume meandering during stable conditions. *J.Appl.Meteor.,* **22,** 1424-1430.

Hanna, S.R., Schulman, L.L., Paine, R.J., Pleim, J.E., Baer, M., 1985. Development and evaluation of the offshore and coastal dispersion model. J. Air Pollut. Control Assoc. 35, 1039–1047. https://doi.org/10.1080/00022470.1985.10466003

Hanna, S. R., J. C. Weil, and R. J. Paine, 1986: Plume Model Development and Evaluation - Hybrid Approach. EPRI Contract No. RP-1616-27, Electric Power Research Institute, Palo Alto, CA.

Hanna, S.R., Dicristofaro, D.C., 1988. Development and Evaluation of the OCD/API (Offshore and Coastal Dispersion / American Petroleum Institute) Model.

Hanna, S. R. and R. J. Paine, 1989: Hybrid Plume Dispersion Model (HPDM) development and evaluation. *J.Appl.Meteor.,* **28,** 206-224.

Hanna, S. R. and J. S. Chang, 1991: Modification of the Hybrid Plume Dispersion Model (HPDM) for urban conditions and its evaluation using the Indianapolis data set, Volume III: Analysis of urban boundary layer data. EPRI Project No. RP-02736-1, Electric Power Research Institute, Palo Alto, CA.

Hanna, S. R. and J. S. Chang, 1993: Hybrid Plume Dispersion Model (HPDM), improvements and testing at three field sites. *Atmos.Environ.,* **27A,** 1491-1508.

Hanrahan, P.L., 1999. "The plume volume molar ratio method for determining NO_2/NO_x ratios in modeling. Part I: Methodology," *J. Air & Waste Manage. Assoc.*, **49**, 1324-1331.

Haugen, D. A. (Editor), 1959: Project Prairie Grass, A field program in diffusion. Geophysical Research Paper, No. 59, Vol. III. Report AFCRC-TR-58-235, Air Force Cambridge Research Center, 439 pp.

Hayes, S. R. and G. E. Moore, 1986: Air quality model performance: a comparative analysis of 15 model evaluation studies. *Atmos.Environ.,* **20,** 1897-1911.

Heist, D.K., Perry, S.G. and Brixey, L.A. (2009). A wind tunnel study of the effect of roadway configurations on the dispersion of traffic-related pollution. Atmospheric Environment, 43(32), pp.5101-5111.

Heist, D., Isakov, V., Perry, S., Snyder, M., Venkatram, A., Hood, C., Stocker, J., Carruthers, D., Arunachalam, S. and Owen, R.C. (2013). Estimating near-road pollutant dispersion: A model inter-comparison. Transportation Research Part D: Transport and Environment, 25, pp.93-105.

Hicks, B. B., 1985: Behavior of turbulent statistics in the convective boundary layer. *J.Appl.Meteor.,* **24,** 607-614.

Holtslag, A. A. M., 1984: Estimates of diabatic wind speed profiles from near-surface weather observations. *Bound.Layer Meteor.,* **29,** 225-250.

Holtslag, A. A. M. and A. P. van Ulden, 1983: A simple scheme for daytime estimates for the surface fluxes from routine weather data. *J.Climate Appl.Meteor.,* **22,** 517-529.

Irwin, J. S., J. O. Paumier, and R. W. Brode, 1988: Meteorological Processor for Regulatory Models (MPRM) User's Guide. EPA-600/3-88-043, U.S. Environmental Protection Agency, RTP, NC.

Izumi, Y., 1971: Kansas 1968 Field Program Data Report. No. 379, AFCRL-72-0041, Air Force Cambridge Research Laboratory, Bedford, MA, 79pp.

Kaimal, J. C., J. C. Wyngaard, D. A. Haugen, O. R. Cote', Y. Izumi, S. J. Caughey, and C. J. Readings, 1976: Turbulence structure in the convective boundary layer. *J.Atmos.Sci.,* **33,** 2152-2169.

Kasten, F. and G. Czeplak, 1980: Solar and terrestial radiation dependent on the amount and type of cloud. *Solar Energy,* **24,** 177-189.

Lamb, R. G., 1982: Diffusion in the convective boundary layer. *Atmospheric Turbulence and Air Pollution Modelling.* Nieuwstadt, F. T. M. and van Dop, H., Reidel, 159-229pp.

Lee, R. F., R. J. Paine, S. G. Perry, A. J. Cimorelli, J. C. Weil, A. Venkatram, and R. B. Wilson, 1998: Developmental Evaluation of the AERMOD Dispersion Model. Preprints, *10th Joint AMS/AWMA Conference on Application of Air Pollution Meteorology,* American Meteorological Society, Boston.

Lee, R. F., S. G. Perry, A. J. Cimorelli, R. J. Paine, A. Venkatram, J. C. Weil, and R. B. Wilson, 1995: AERMOD - the developmental evaluation. Preprints, *Tewnty-First NATO/CCMS*

International Technical Meeting on Air Pollution Modeling and Its Application, Baltimore, MD, U.S.A.

Liu, M. K., and G. E. Moore: 1984: Diagnostic validation of plume models at a plains site. EPRI Report No. EA-3077, Research Project 1616-9, Electric Power Research Institute, Palo Alto, CA. (1984)

Luhar, A.K., and K. N. Rayner, 2009: "Methods to Estimate Surface Fluxes of Momentum and Heat from Routine Weather Observations for Dispersion Applications under Stable Stratification", *Boundary-Layer Meteorology*, **132**, 437–454.

Misra, P. K., 1982: Dispersion of non-buoyant particles inside a convective boundary layer. *Atmos.Environ.,* **16,** 239-243.

Monbureau, E. M., Heist, D. K., Perry, S. G., Brouwer, L. H., Foroutan, H., Tang, W. (2018). Enhancements of AERMOD's building downwash algorithms based on wind tunnel and Embedded-LES modeling. Atmospheric Environment, 179, 321-330.

Moore, G. E., L. B. Milich, and M. K. Liu. 1988. Plume behaviors observed using lidar and SF6 tracer at a flat and hilly site. Atmos. Environ 22 (8):1673–88. 0004-6981. doi:10.1016/0004-6981(88)90396-4.

Morton, B. R., G. I. Taylor, and J. S. Turner, 1956: Turbulent gravitational convection from maintained and instantaneous sources. *Proc.Roy.Soc.London,* **A234,** 1-23.

Nieuwstadt, F. T. M. and H. van Dop, 1982: *Atmospheric Turbulence and Air Pollution Modelling.* Reidel, 358pp.

NOAA, 1974: Technical Memorandum ERL ARL-52, 1974. "Diffusion under Low Wind Speed, Inversion Conditions." Sagendorf, J. F., C. Dickson. Air Resources Laboratory, Idaho Falls, Idaho.

NOAA, 1976: Technical Memorandum ERL ARL-61, 1976. "Diffusion under Low Wind Speed Conditions near Oak Ridge, Tennessee." Wilson, R. B., G. Start, C. Dickson, N. Ricks. Air Resources Laboratory, Idaho Falls, Idaho.

Oke, T. R., 1973: City size and the urban heat island. *Atmos.Environ.,* **7,** 769-779.

Oke, T. R., 1978: *Boundary Layer Climates.* John Wiley and Sons, New York, New York, 372pp.

Oke, T. R., 1982: The energetic basis of the urban heat island. *Quart.J.Roy.Meteor.Soc.,* **108,** 1-24.

Oke, T. R., 1998: An algorithmic scheme to estimate hourly heat island magnitude. Preprints, *2nd Urban Environment Symposium,* American Meteorological Society, Boston, MA, 80-83.

Paine, R. J. and B. A. Egan, 1987: User's guide to the Rough Terrain Diffusion Model (RTDM) - Rev. 3.20. ERT Document PD-535-585, ENSR, Acton, MA, 260pp.

Paine, R. J. and S. B. Kendall, 1993: Comparison of observed profiles of winds, temperature, and turbulence with theoretical results. Preprints, *Joint conference of the American Meteorological Society and Air & Waste Management Association Specialty Conference: The Role of Meteorology in Managing the Environment in the 90s, Scottsdale, AZ. Publication VIP-29,* Air & Waste Management Association, Pittsburgh, PA.

Pandey, G., A Venkatram, and S. Arunachalam, 2023: "Accounting for plume rise of aircraft emissions in AERMOD." *Atmospheric Environment*, 314. https://doi.org/10.1016/j.atmosenv.2023.120106.

Panofsky, H. A. and J. A. Dutton, 1984: *Atmospheric Turbulence: Models and Methods for Engineering Applications.* John Wiley and Sons, New York, 417pp.

Panofsky, H. A., H. Tennekes, D. H. Lenschow, and J. C. Wyngaard, 1977: The characteristics of turbulent velocity components in the surface layer under convective conditions. *Bound.Layer Meteor.,* **11,** 355-361.

Pasquill, F., 1961: The estimation of the dispersion of windborne material. *Meteorol.Mag.,* **90,** 33-49.

Pasquill, F., 1976: Atmospheric dispersion parameters in Gaussian plume modeling - Part III: possible requirements for change in the Turner's Workbook values. EPA-600/4-76-030B, U. S. Environmental Protection Agency, Research Triangle Park, NC.

Pasquill, F. and F. R. Smith, 1983: *Atmospheric Diffusion.* John Wiley and Sons Inc., New York, 440pp.

Paumier, J. O., S. G. Perry, and D. J. Burns, 1992: CTDMPLUS: A dispersion model for sources near complex topography. Part II: Performance characteristics. *J. Appl. Meteor.*, 31, 646–660.

Perry, S. G., 1992: CTDMPLUS: A dispersion model for sources in complex topography. Part I: Technical formulations. *J.Appl.Meteor.,* **31,** 633-645.

Perry, S. G., D. J. Burns, R. J. Adams, R. J. Paine, M. G. Dennis, M. T. Mills, D. G. Strimaitis, R. J. Yamartino, and E. M. Insley, 1989: User's Guide to the Complex Terrain Dispersion Model Plus Algorithms for Unstable Situations (CTDMPLUS) Volume 1: Model Description and User Instructions. EPA/600/8-89/041, U.S. Environmental Protection Agency, RTP, NC, 196pp.

Perry, S. G., A. J. Cimorelli, R. F. Lee, R. J. Paine, A. Venkatram, J. C. Weil, and R. B. Wilson, 1994: AERMOD: A dispersion model for industrial source applications. Preprints, *87th Annual Meeting Air and Waste Management Association,* Air and Waste Management Association, Pittsburgh, PA.

Perry, S. G., A. J. Cimorelli, R. J. Paine, R. W. Brode, J. C. Weil, A. Venkatram, R. B. Wilson, R. F. Lee, and W. D. Peters, 2005: AERMOD: A dispersion model for industrial source applications Part II: Model performance against seventeen field-study databases. *J.Appl.Meteor*. **44**, 694-708.

Perry, S.G., Heist, D.K., Brouwer, L.H., Monbureau, E.M., and L.A. Brixley (2016). Characterization of pollutant dispersion near elongated buildings based on wind tunnel simulations, Atmospheric Environment, Vol. 42, 286-295.

Petersen, R.L., 1986. Wind tunnel investigation of the effect of platform-type structures on dispersion of effluents from short stacks. J. Air Pollut. Control Assoc. 36, 1347–1352. https://doi.org/10.1080/00022470.1986.10466185

Petersen, R.L., A. Kolesnikov, and A. Beyer-Lout. 2014. Evaluation of new wind tunnel, AERMOD and CFD methodologies to determine EBD/BPIPPRM in light of the 2011 EPA Memorandum. Technical Paper 33263. Presented at the 107th Annual A&WMA Conference & Exhibition, Long Beach, CA, June 24 27.

Petersen, R. L., Sergio A. Guerra & Anthony S. Bova. (2017). Critical Review of the Building Downwash Algorithms in AERMOD. J. Air Waste Management Association Vol. 67, Issue 8.

Petersen, R. L. and Guerra, S. A., (2018). PRIME2: Development and evaluation of improved building downwash algorithms for rectangular and streamlined structures. Atmospheric Environment, 173, 67-78.

Qian, W., and A. Venkatram, 2011: "Performance of Steady-State Dispersion Models UnderLow Wind-Speed Conditions", *Boundary Layer Meteorology*, **138**, 475-491.

Readings, C. J., D. A. Haugen, and J. C. Kaimal, 1974: The 1973 Minnesota atmospheric boundary layer experiment. *Weather,* **29,** 309-312.

Schulman, L.L., and J.S. Scire, 1980: Boyant Line and Point Source (BLP) Dispersion Model User's Guide. Final Report. Environmental Research & Technology, Inc. P-7304B. July 1980.

Schulman, L. L., D. G. Strimaitis, and J. S. Scire, 2000: Development and evaluation of the PRIME plume rise and building downwash model. *Journal of the Air & Waste Management Association,* **50,** 378-390.

Schulte, N., Snyder, M., Isakov, V., Heist, D. and Venkatram, A. (2014). Effects of solid barriers on dispersion of roadway emissions. Atmospheric environment, 97, pp.286-295.

Sheppard, P. A., 1956: Airflow over mountains. *Quart.J.Roy.Meteor.Soc.,* **82,** 528-529.

Smith, M. E., 1984: Review of the attributes and performance of 10 rural diffusion models. *Bull.Amer.Meteor.Soc.,* **65,** 554-558.

Snyder, W. H., R. S. Thompson, R. E. Eskridge, R. E. Lawson, I. P. Castro, J. T. Lee, J. C. R.

Hunt, and Y. Ogawa, 1985: The structure of the strongly stratified flow over hills: Dividing streamline concept. *J.Fluid Mech.,* **152,** 249-288.

Snyder, M. G., A. Venkatram, D. K. Heist, S. G. Perry, W. B. Petersen, and V. Isakov, 2013: RLINE: A Line source dispersion model for near-surface releases. *Atmos.Environ*., **77(0)**, 748-756.

Stocker, J., M. Seaton, S. Smith, J. O'Neill, K. Johnson, R. Jackson, and D. Carruthers (CERC). Evaluation of the Generic Reaction Set Method for NO2 conversion in AERMOD. The modification of AERMOD to include ADMS chemistry. Cambridge Environmental Research Consultants (CERC) Technical Report. August 8, 2023.

Stull, R. B., 1983: A heat flux history length scale for the nocturnal boundary layer. *Tulles,* **35A,** 219-230.

Sykes, R. I., D. S. Henn, and S. F. Parker, 1996: SCIPUFF - A generalized hazard dispersion model. Preprints, *9th Joint Conference on Applications of Air Pollution Meteorology with AWMA, Amer. Meteor. Soc.,* American Meteorological Society, Boston, 184-188.

Taylor, G. I., 1921: Diffusion by continuous movements. *Proc.London Math.Soc.,* **Ser. 2(20),** 196-211.

Turner, D. B., T. Chico, and J. Catalano, 1986: TUPOS - A Multiple Source Gaussian Dispersion Algorithm Using On-site Turbulence Data. EPA/600/8-86/010, U.S. Environmental Protection Agency, RTP, NC, 39pp.

U.S. EPA, 1992: Protocol for Determining the Best Performing Model. EPA-454/R-92-025, U.S. Environmental Protection Agency, RTP, NC.

U.S. EPA, 1995a: User's Guide for the Industrial Source Complex (ISC3) Dispersion Models (revised) Volume I - User Instructions. EPA-454/b-95-003a, U.S. Environmental Protection Agency, Research Triangle Park, NC.

U.S. EPA, 1995b: *Modeling Fugitive Dust Impacts from Surface Coal Mining Operations – Phase III.* U.S. Environmental Protection Agency, Office of Air Quality Planning and Standards, EPA-454/R-96-002. December 1995.

U.S. EPA, 2002: Compendium of Reports from the Peer Review Process for AERMOD. U.S. Environmental Protection Agency, RTP, NC. *http://www.epa.gov/scram001/7thconf/aermod/dockrpt.pdf*.

U.S. EPA, 2003a: AERMOD: Latest Features and Evaluation Results. EPA-454/R-03-003, U.S. Environmental Protection Agency, Research Triangle Park, North Carolina.

U.S. EPA, 2003b: AERMOD Deposition Algorithms Science Document (Revised Draft). U.S. Environmental Protection Agency, Research Triangle Park, North Carolina 27711.

U.S. EPA, 2012: User's Manual AERCOARE Version 1.0. EPA-910-R-12-008. U.S. EPA, Region 10, Seattle, WA.

U.S. EPA, 2015: Technical Support Document (TSD) for NO2-related AERMOD modifications. EPA-454/B-15-004. U.S. Environmental Protection Agency, Research Triangle Park, North Carolina. July 2015.

U.S. EPA, 2016: Technical Support Document (TSD) for AERMOD/BLP Development and Testing. EPA-454/B-16-009. U.S. Environmental Protection Agency, Research Triangle Park, North Carolina. December 2016.

U.S. EPA, 2017: Guideline on Air Quality Models, Appendix W to 40 CFR Part 51. U.S. Environmental Protection Agency, Research Triangle Park, North Carolina 27711.

U.S. EPA, 2023a: Evaluation of Addition of Terrain Treatment to the RLINE Source Type in AERMOD. EPA-454/R-23-012. U.S. Environmental Protection Agency, Research Triangle Park, North Carolina. October 2023.

U.S. EPA, 2023b: Evaluation of the Implementation of the Coupled Ocean Atmosphere Response Experiment (COARE) Algorithms into AERMET for Marine Boundary Layer Environments. EPA-454/R-23-008. U.S. Environmental Protection Agency, Research Triangle Park, North Carolina. October 2023.

U.S. EPA, 2023c: Evaluation of Prognostic Meteorological Data in AERMOD Overwater Applications. EPA-454/R-23-012. U.S. Environmental Protection Agency, Research Triangle Park, North Carolina. October 2023.

U.S. EPA, 2023d: Incorporation and Evaluation of the RLINE source type in AERMOD for mobile source applications. EPA-454/R-23-011. U.S. Environmental Protection Agency, Research Triangle Park, North Carolina. October 2023.

U.S. EPA, 2024a: Guidance on the Use of the Mesoscale Model Interface Program (MMIF) for AERMOD Applications. EPA-454/B-24-005. U.S. Environmental Protection Agency, Research Triangle Park, North Carolina. October 2024.

EPA, 2024b. Guideline on Air Quality Models: Ehancements to the AERMOD Dispersion Modeling System; Final Rule. 40 CFR Part 51, Appendix W.

U.S. EPA, 2024c: Technical Support Document (TSD) for Adoption of the Generic Reaction Set Method (GRSM) as a Regulatory Non-Default Tier-3 NO2 Screening Option. EPA-454/R-24-005. U.S. Environmental Protection Agency, Research Triangle Park, North Carolina. October 2024.

U.S. EPA, 2024d User's Guide for the AERMOD Meteorological Preprocessor (AERMET). EPA-454/B-24-004. U.S. Environmental Protection Agency, Research Triangle Park, North Carolina. October 2023.

U.S. EPA, 2024e: User's Guide for the AERMOD Terrain Preprocessor (AERMAP). EPA-454/B-24-008. U.S. Environmental Protection Agency, Research Triangle Park, NC.

U.S. EPA, 2024f: User's Guide for AERSURFACE Tool. EPA-454/B-24-003. U.S.

Environmental Protection Agency, Research Triangle Park, North Carolina. October 2024.

U.S. EPA, 2024g: User's Guide for the AMS/EPA Regulatory Model (AERMOD). EPA-454/B-24-007. U.S. Environmental Protection Agency, Research Triangle Park, North Carolina. October 2024.

USGS, 1994: The 1994 plan for the National Spatial Data Infrastructure - Building the foundation of an information-based society. Federal Geographic Data Committee Report. U.S. Geological Survey, Reston, VA.

van Ulden, A. P. and A. A. M. Holtslag, 1983: The stability of the atmospheric surface layer during nightime. Preprints, *Sixth Symposium on Turbulence and Diffusion,* American Meteorological Society, Boston, 257-260.

van Ulden, A. P. and A. A. M. Holtslag, 1985: Estimation of atmospheric boundary layer parameters for diffusion applications. *J.Climate Appl.Meteor.,* **24,** 1196-1207.

Venkatram, A., 1978: Estimating the convective velocity scale for diffusion applications. *Bound.Layer Meteor.,* **15,** 447-452.

Venkatram, A., 1980: Estimating the Monin-Obukhov length in the stable boundary layer for dispersion calculations. *Bound.Layer Meteor.,* **19,** 481-485.

Venkatram, A., 1982: A semi-empirical method to compute concentration associated with surface releases in the stable boundary layer. *Atmos.Environ.,* **16,** 245-248.

Venkatram, A., 1983: On dispersion in the convective boundary layer. *Atmos.Environ.,* 529-533.

Venkatram, A., 1988: Dispersion in the stable boundary layer. *Lectures on Air Pollution Modeling.* Venkatram, A. and Wyngaard, J. C., American Meteorological Society, 229-265pp.

Venkatram, A., 1992: Vertical dispersion of ground-level releases in the surface boundary layer. *Atmos.Environ.,* **26A,** 947-949.

Venkatram, A., R. Brode, A. Cimorelli, R. Lee, R. Paine, S. Perry, W. Peters, J. Weil, and R. Wilson, 2001: A complex terrain dispersion model for regulatory applications. *Atmospheric Environment,* **35,** 4211-4221.

Venkatram, A., D. G. Strimaitis, and D. Dicristofaro, 1984: A semiemperical model to estimate vertical dispersion of elevated releases in the stable boundary layer. *Atmos.Environ.,* **18,** 923-928.

Venkatram, A. and J. C. Wyngaard, 1988: *Lectures on Air Pollution Modeling.* American Meteorological Society, Boston, 390pp.

Venkatram A., Karamchandani P., Pai P. & Goldstein R. (1994). The Development and Application of a Simplified Ozone Modelling System (SOMS). Atmos. Environ. 28 (22),

pp 3365-3678. doi:10.1016/1352-2310(94)00190-V

Venkatram, A., Snyder, M.G., Heist, D.K., Perry, S.G., Petersen, W.B. and Isakov, V. (2013). Re-formulation of plume spread for near-surface dispersion. Atmospheric environment, 77, pp.846-855.

Venkatram, A., Heist, D.K., Perry, S.G., and Brouwer, L. (2021). Dispersion at the edges of near road noise barriers. Atmospheric Pollution Research, 12, pp. 367–374.

Walcek, C., G. Stensland, L. Zhang, H. Huang, J. Hales, C. Sweet, W. Massman, A. Williams, J, Dicke, 2001: Scientific Peer Review of the Report "Deposition Parameterization for the Industrial Source Complex (ISC3) Model." The KEVRIC Company, Durham, North Carolina.

Warren, J. C., Robert J. Paine, Jeffrey A. Connors, Carlos Szembek & Eladio Knipping: 2022. Evaluation of a revised AERMOD treatment of plume dispersion in the daytime elevated stable layer, Journal of the Air & Waste Management Association, 72:9, 1040-1052, DOI: 10.1080/10962247.2022.2094031

Weil, J. C., 1985: Updating applied diffusion models. *J.Climate Appl.Meteor.,* **24(11),** 1111-1130.

Weil, J. C., 1988a: Dispersion in the convective boundary layer. *Lectures on Air Pollution Modeling.* Venkatram, A. and Wyngaard, J. C., American Meteorological Society, 167-227pp.

Weil, J. C., 1988b: Plume rise. *Lectures in Air Pollution Modeling.* Venkatram, A. and Wyngaard, J. C., American Meteorological Society, 119-162pp.

Weil, J. C., 1992: Updating the ISC model through AERMIC. Preprints, *85th Annual Meeting of Air and Waste Management Association,* Air and Waste Management Association, Pittsburgh, PA.

Weil, J. C., 1996: A new dispersion model for stack sources in building wakes. Preprints, *Ninth Joint Conference on Applications of Air Pollution Meteorology with the Air & Waste Management Association,* American Meteorological Society, Boston, MA, 333-337.

Weil, J.C., 1998. The SERDP Open Burn/Open Detonation Dispersion Model (SOBODM), Volume IIa – Technical Description, and Volume IIb – Meteorological Inputs (DRAFT), CIRES, University of Colorado, Boulder, CO.

Weil, J. C. and R. P. Brower, 1983: Estimating convective boundary layer parameters for diffusion applications. PPSP-MD-48, Maryland Power Plant Siting Program, Maryland Department of Natural Resources, Baltimore, MD, 45pp.

Weil, J. C. and R. P. Brower, 1984: An updated Gaussian plume model for tall stacks. *J.Air Poll.Control Assoc.,* **34,** 818-827.

Weil, J.C., B. Templeman, R. Banta, R. Weber, and W. Mitchell, 1996. “Dispersion model

development for open burn/open detonation sources," *Preprints 9th Joint Conference on Applications of Air Pollution Meteorology*, American Meteorological Society, Boston, MA, 610-616.

Weil, J. C., L. A. Corio, and R. P. Brower, 1997: A PDF dispersion model for buoyant plumes in the convective boundary layer. *J.Appl.Meteor.,* **36,** 982-1003.

Weil, J. C.: 2020. New dispersion model for highly-buoyant plumes in the convective boundary layer. Modeling report to the Western Australia department of environmental conservation. January 2020.

Wesely, M.L, P.V. Doskey, and J.D. Shannon, 2002: Deposition Parameterizations for the Industrial Source Complex (ISC3) Model. Draft ANL report ANL/ER/TRB01/003, DOE/xx-nnnn, Argonne National Laboratory, Argonne, Illinois 60439.

Willis, G. E. and J. W. Deardorff, 1981: A laboratory study of dispersion in the middle of the convectively mixed layer. *Atmos.Environ.,* **15,** 109-117.

Wyngaard, J. C., 1988: Structure of the PBL. *Lectures on Air Pollution Modeling.* Venkatram, A., and Wyngaard, J. C., *eds.*, American Meteorological Society, 9-57pp.

Yang, B., Gu, J., & Zhang, K. M., 2020. Parameterization of the building downwash and sidewash effect using a mixture model. Building and Environment, 172, 106694.

Zilitinkevich, S. S., 1972: On the determination of the height of the Ekman boundary layer. *Bound.Layer Meteor.,* **3,** 141-145.

United States Environmental Protection Agency	Office of Air Quality Planning and Standards Air Quality Assessment Division Research Triangle Park, NC	Publication No. EPA-454/B-24-010 November 2024